A Study on the Design, Analysis and Development of an Electro-mechanical Hydropower Harnessing Model by Vortex Induced Vibration

Thesis Submitted by

BIPRODIP MUKHERJEE

Doctor of Philosophy (Engineering)

School of Water Resources Engineering
Faculty Council of Engineering & Technology
Jadavpur University
Kolkata, India

2018

Dedicated to

My grandmother

Late Bani Mukherjee

JADAVPUR UNIVERSITY
KOLKATA – 700 032, INDIA

INDEX NO. 160/17/E

Title of Thesis

A Study on the Design, Analysis and Development of an Electro-mechanical Hydropower Harnessing Model by Vortex Induced Vibration

Name, Designation & Institution of the Supervisor

Dr. Asis Mazumdar
Professor and Director
School of Water Resources Engineering
Jadavpur University
Kolkata, 700 032

Dr. Subhasish Das
Assistant Professor
School of Water Resources Engineering
Jadavpur University
Kolkata, 700 032

List of Journal Publication:

1. **Biprodip Mukherjee, Subhasish Das and Asis Mazumdar**. (2017). Complex flow phenomena of horizontally placed underwater cylinder above water bed. *Water and Energy International*. Volume: 60, Number: 8, Pages: 57 – 64. (Scopus Indexed)

List of Presentation in National/International/Conferences/ Workshops:

1. **Biprodip Mukherjee, Subhasish Das and Asis Mazumdar**. (2016). Electrical Energy Generation by Enhancing Flow Induced Vibration. *2nd International Conference on Control, Instrumentation, Energy & Communication, **IEEE**, Calcutta, India*. Pages: 368-371. 28th – 30th January, 2016.

2. **Biprodip Mukherjee, Subhasish Das and Asis Mazumdar**. (2016). Electrical Energy Generation by Enhancing Flow Induced Vibration. Sustainable Electrical Energy Generation Technique in Shallow Water Channels. ***IEEE** Students' Technology Symposium, Kharagpur, India*. Pages: 147-151. 30th September – 2nd October, 2016.

CERTIFICATE FROM THE SUPERVISORS

This is to certify that the thesis entitled "**A Study on the Design, Analysis and Development of an Electro-mechanical Hydropower Harnessing Model by Vortex Induced Vibration**" submitted by Shri **Biprodip Mukherjee,** who got his name registered on **15th January, 2015** for the award of Ph.D. (Engineering) degree of Jadavpur University is absolutely based upon his own work under the supervision of **Prof. Dr. Asis Mazumdar** and **Dr. Subhasish Das** and that neither his thesis nor any part of the thesis has been submitted for any degree or any other academic award anywhere before.

THESIS ADVISOR

Dr. Asis Mazumdar
Professor & Director
School of Water Resources Engineering
Jadavpur University

THESIS ADVISOR

Dr. Subhasish Das
Assistant Professor
School of Water Resources Engineering
Jadavpur University

Acknowledgements

I express my profound regards, sincere gratitude and gratefulness to *Prof. Dr. Asis Mazumdar* and *Dr. Subhasish Das* for being guide in the truest sense. It was their initiation, constant encouragement and help rendered in developing the experimental facilities in the Fluvial Hydraulics Laboratory of School of Water Resources Engineering, Jadavpur University which enabled me to carry out a major part of the present thesis work. It would also be very difficult to inculcate this work in pen and paper without their valuable advises.

I am also indebted to my supervisors for helping financially in the building up experimental facilities and providing moral support during tenure of my Ph.D. work.

I also convey my sincere gratitude to *Dr. Rajib Das*, Assistant Professor, School of Water Resources Engineering, Jadavpur University for his constant encouragement throughout.

My hearty thanks are to post graduate students Mr. Abhilash Jana, Mr. Rathin Biswas and Ms. Sudisha Kar. It was while helping their Master of Engineering thesis that the shape of the present work took its final form.

I will always remain indebted to my colleague Mr. Asim Kuila for providing direct and indirect help during my thesis work.

Finally, I give my deepest gratitude to my parents, my wife and my younger sister for giving me support during entire execution of my thesis.

BIPRODIP MUKHERJEE
Research Scholar
School of Water Resources Engineering
Jadavpur University
Kolkata – 700 032, West Bengal, India

Abstract

Electrical energy plays a key role in a country's growth. A country's growth mainly depends upon the capacity of the electrical energy that it can afford to run the wheels of technology. Natural energy in the whole world is found in a discrete manner. As a result it becomes typical to harness electricity from every energy points. Today most challenging problem that developing nations face is low-cost sustainable energy generation that can be solved by finding out ways to harness electricity amongst the scattered energy points. Development is also required for every technology that can generate energy at a competitive cost. Around 1500 A.D. Leonardo da Vinci first observed the vortex induced vibration (VIV) in the form of "Aeolian Tones". Then the studies of vortex induced vibration came into light when von Karman at California Institute of Technology proved that the Tacoma Narrows bridge collapse in 1940 was due to VIV. The vortex induced vibration also had detrimental effects on the high tension electric wires those runs for more than 100 km. Since then the engineers tried to suppress the vortex induced vibration while designing high rise buildings and towers of the electric wires. VIV manifests itself on many different branches of engineering, from cables to heat exchanger tube arrays. It is also a major consideration in the design of marine structures. Thus study of VIV is a part of a number of disciplines, incorporating fluid mechanics, structural mechanics, vibrations, computational fluid dynamics (CFD), acoustics, statistics, and smart materials. From the study of Bernitsas *et al.* (2005) it came to light that the vortex induced vibration could also be used in the process of energy generation. In this research a hydraulic structure consists of a movable cylinder with floating appendages and supporting structures were developed. This fluid-structure interaction phenomenon occurs due to the nonlinear resonance of cylinders (or spheres) through vortex shedding lock-in. The VIV is also called synchronization between vortex shedding and cylinder (or sphere) oscillations. It was also tested that this converter was capable of harnessing useful amount of electricity in the river flow of about 0.25 m/s. The device had been named as Vortex Induced Vibration Aquatic Clean Energy (VIVACE). But most importantly the device was tested in the ocean and Detroit River of North America. The water depth considered was above 5 m for a small energy converter. But in India there are many shallow water channels where water depth is about one m with flow velocity of about 0.25 m/s. In those water channels the micro-

hydro power plant may not be able to function. In this juncture the VIVACE has been modified at Fluvial Hydraulics Laboratory of School of Water Resources Engineering, Jadavpur University. The device had been designed in such a way that it might harness electricity from very shallow streams. Research has been carried to visualize in shallow depth of water flow how much power it is capable of harnessing. In view to the Design, Analysis and Development of an Electromechanical Hydropower Harnessing Model by Vortex Induced Vibration, the study in the thesis was divided into three parts. Since the modification as made in the study consist of the use of a hydraulic structure at the downstream of the movable cylinder. The study of the flow field analysis at the upstream of the hydraulic structure, over here it is also termed as fixed vertical plate were carried out. Basically it was proved from this research the horseshoe vortex generated from the plate aids to the vortex induced vibration of the cylinder. The vortex strength of the plate provides the extra lift force that the cylinder requires near the flume bed in a shallow water channel. Aim of this chapter is to find out the flow fields between a vertical plate and a submerged horizontal cylinder. Numerous experiments had been carried out by altering the plate sizes to 2, 3, 4 and 5 cm at the downstream of the submerged cylinder. From the nature of the flow fields as generated from the experiments and analysis perfect combination of the plate and submerged moving cylinder could be found that would enhance effective power generations. Moreover the same characteristics of the vortices could be visualized at every instant of the depth of the water flow where the moving cylinder would traverse. Along-with the knowledge of flow fields it also becomes important to understand the electrical aspects of the hydrokinetic energy device that is to be developed. Taking the view of the results coming out from the above hydraulics aspects, the electric aspects are to be developed. Then after developing the hydrokinetic generator the electrical parameters like voltage, current and power where recorded for various types of conditions like with or without modifications. As a whole it can be said that this device can be more useful in the shallow water courses and the results observed in the research suggest that with proper selection of cylinder diameter and hydraulic structure sizes, a sustainable power could be generated. In contemporary the device was found capable to grab the water energy at its maximum, though amount of power generation in laboratory may be miniscule. After modification, same prototype in real life condition can be a very handy weapon to supply few lighting loads at remote places.

Table of Contents

List of Figures

List of Tables

1.1 A beginning knowhow about vortex induced vibration

Vortex Induced Vibration (VIV) is a phenomenon where the motion induced on bluff bodies interacting with an external fluid flow produced by periodical irregularities. The classical example is the VIV of an underwater laying cylinder. VIV occurs when the vortex shedding frequency becomes same as the natural frequency of the body.

When the vortices donot seem to be shaped symmetrically round the body (with relevancy to its middle plane), totally different lift forces develop on upper and lower side of the body, therefore resulting in motion crosswise to the flow. This motion changes the characteristics of the vortex formation in such, the simplest way on because of restricted motion amplitude (differently from what would be expected during a typical case of resonance). The Strouhal number range relates the frequency of shedding to the rate of the flow and a characteristic dimension of the body, i.e. diameter in the case of a cylinder. It can be visualized how this happens by putting a cylinder into the water (a swimming-pool or even a bucket) and moving it in in the direction perpendicular to its axis. Since in real fluids there is always a presence of viscosity, the flow around the cylinder will be slowed down while in contact with its surface, forming the so-called boundary layer. At some point the boundary layer can separate from the body due to its excessive curvature.

VIV manifests itself on many different branches of engineering, from cables to heat exchanger tube arrays. It is also a major consideration in the design of marine structures now-a-days clean energy. Thus study of VIV is a part of a number of disciplines, incorporating fluid mechanics, structural mechanics, vibrations, computational fluid dynamics (CFD), acoustics, statistics and smart materials.

They occur in several engineering things, like bridges, stacks, transmission lines, craft management surfaces, offshore structures, thermo wells, engines, heat exchangers, marine cables, towed cables, drilling and production risers in oil production, mooring cables, moored structures, bound structures, buoyancy and spar hulls, pipelines, cable-laying and hydrodynamic structures and hydro acoustic application.

The most recent interest in long cylindrical members in water ensues from the event of organic compound resources in depths of a 1000 m. VIV is additionally a crucial source of fatigue injury of offshore oil exploration and production risers. These lean structures knowledge of each current flow and top-end motions of the ship vessel, that creates to the flow-structure relative motion and cause VIV.

The top-end vessel motion causes the riser to oscillate and the corresponding flow profile appears unsteady. One of the classical open channel flow problems in fluid mechanics concerns the flow around a circular cylinder, or more generally, a bluff body. At very low Reynolds number (based on the diameter of the circular member) the streamlines of the resulting flow is perfectly symmetric as expected from potential theory. However with the increase of Reynolds number the flow becomes asymmetric and the so-called Karman vortex street occurs. Much progress has been created throughout the past decade, each numerically and by experimentation, toward the understanding of the mechanics (dynamics) of VIV, albeit within the low-

Reynolds range regime. The elemental reason for this is often that VIV isn't a little perturbation superimposed on a mean steady motion. It is an inherently nonlinear, self-governed or self-regulated, with phenomenon multi-degree-of-freedom.

There is much that is known and understood plus much that remains in the empirical/descriptive realm of knowledge: what is the dominant response frequency, the range of normalized velocity, the variation of the phase angle (by which the force leads the displacement), and the response amplitude in the synchronization range as a function of the controlling and influencing parameters? Industrial applications highlight our inability to predict the dynamic response of fluid–structure interactions.

They still need the input of the in-phase and out-of-phase parts of the lift coefficients (or the cross force), in-line drag coefficients, correlation lengths, damping coefficients, relative roughness, shear stresses among alternative governing and influencing parameters, and therefore additionally need the input of comparatively massive safety factors. Fundamental studies as well as large-scale experiments (when these results are disseminated in the open literature) may provide the necessary understanding for the quantification of the relationships between the responses of a structure and subsequent governing and influencing parameters. It cannot be emphasized strongly enough that the current state of the laboratory art concerns the interaction of a rigid body (mostly and most importantly for a circular cylinder) whose degrees of freedom have been reduced from six to often one (that is transverse motion) with a three-dimensional separated flow, dominated by large-scale vertical structures. For velocities exceeding streamline flow, the inertia of the fluid starts to become important and, because the fluid stream passes the top a part of the cylinder, thanks to the presence of stagnation purpose the streamlines are unable to barter with the rear side of the cylinder. Therefore the fluid tends to become independent from the highest surface and peel off in a very dextral motion because it approaches the posterior of the cylinder, ending up as a shed vortex (it can peel off in a very counter dextral motion with relevancy flow direction from the lowest surface).

For a given water depth, length and width of the water channel, velocity of flow, this model with a horizontal cylinder placed transverse to the flow suggests the time of vortex formation will be proportional to the distance around the cylinder (or its diameter) and thus the frequency of vortex formation will be inversely proportional to the diameter. Furthermore, with the increase of flow velocity the vortex formation frequency also increases. This is what Strouhal found experimentally in 1878. The proportionality constant is called the Strouhal number and is a function of the Reynolds number. For that reason it is now known as the Strouhal-Reynolds number. It is almost equal to 0.2 for a wide range of Reynolds number. One can see the vortex shedding by shadow projection. Similar to a ripple tank, if a point light source is set up over the tank, then shadow patterns of the movement of water can be observed on the bottom of the water channel. Thus, not only one can demonstrate resonance oscillations of the cylinder, but can also see that the eddy vortices and the cylinder move in opposite directions. Vortex-induced vibrations are quite complicated—even in two dimensions. For example, various wake vortex modes are created with fluid flow shifting from one

mode to another. Additionally, the transverse direction motion of the object in the fluid effects the formation and/or shedding of vortices and can have a positive or negative feedback effect. Also, depending on the phase created in between object and streamline along with their frequency difference, a lock-in or synchronization effect may or may not occur. Furthermore, the ratio of the object-to-fluid mass as well as damping forces have a significant effect, leading to parameters described in the literature as effective mass, critical mass, high-mass ratio, etc. is also an excellent resource for those that wish to go deeper into the subject matter and it can be quite deep indeed.

For instance, the tallest building within the world, the Burj Khalifa in urban centre, UAE, incorporates a variation in cross section with height to assist make sure that vortices aren't shed coherently on the complete height of the building. Collapsing of the Tacoma Narrows Bridge in 1940 has been practically in various types of fluid mechanics studies as a spectacular example of resonance. Although vortex shedding is often cited as being the reason, Billah and Scanlan (1991) say that this is oversimplified physics and posit that the real culprit was flutter—a non-linear phenomenon in which the bridge was in motion due to self induced periodic impulses.

1.2 Literature review

Two basic areas of the literature are relevant to this dissertation: hydro energy conversion and the Vortex Induced Vibrations. Notably concepts taken from both the areas are basically two parts of the dissertation.

1.2.1 Hydro energy conversion

Natural energy in the whole world is found in a discrete manner. As a result it becomes emblematic to exploit power from every energy points. Today most challenging crisis that a developing nation faces is economical sustainable energy generation. This problem can be solved by finding out ways to harness electricity amongst the scattered energy points. Development is also required for every technology that can generate energy at a competitive cost. If the total part of renewable energy is rewind: (1) have high energy density, (2) be un-obstructive to navigation, (3) not diminish the value of expensive coastal real estate, (4) be friendly to marine life and the environment, (5) have low maintenance, (6) be robust, (7) meet life cycle cost targets, and (8) have a minimum life of 20 years. The challenge of meeting all of these requirements has been the focus of more than 40 years of worldwide efforts – particularly in Europe and Japan and to a lesser extent in the USA (Pontes and Falcao, 2001; Thorpe, 1998; WaveNet, 2003). Numerous devices have been designed and patented and several pilot devices have been launched (Pontes and Falcao, 2001; Technomare, 1996; WMCE, 2003). A universally acceptable converter, however, has not yet been developed (WaveNet, 2003). There are five sources of ocean energy: waves, currents, tides, thermal gradient, and salinity gradient. Some examples of how ocean energy converters fail to satisfy some of the Department of Energy or Commission of the European communities (DOE /CEC) criteria follow: (i) Converters based on surface oscillation, such as water

column, buoy, flap, or pendulum (Pontes and Falcao, 2001; WaveNet, 2003; WMCE, 2003), have high energy output only in a very narrow band of wave frequencies near resonance. At any particular location, waves are random allowing for a small window of optimal performance. In addition, waves occasionally apply extreme loads to structures, (ii) Converters of wind or tidal current energy (turbines, watermills) can extract energy proportionally to their projected surface at efficiency of 25% (Technomare, 1996) and only for currents stronger that 2 m/sec (~4 knots), below which they do not function efficiently, (iii) Tidal energy converters require at least a 5 m head, and are very large and as obtrusive as water dams. They also require a 5-7 years of construction period and significant initial capital cost, (iv) Most of the converters operate on the surface and near shore and occupy valuable coastal real estate, (v) Converters such as watermills, turbines, or tidal dams disturb marine life. The VIVACE (Vortex Induced Vibration Aquatic Clean Energy) Converter was then patented by (Bernitsas and Raghavan, 2005) to convert ocean/river current energy to electricity.

In coming to process of development of the rural areas small turbine operated hydropower systems can be very much helpful Jia-kun (2012) and such conventional turbine operated hydro power devices also tried to meet the above challenges. The solving of the immigration problem due to such hydropower power projects lies in two points, first step to be taken is, to organize planning and consummate system, put the river basin planning and the unified dispatch of watershed into effect, and focus on the ecological environment, the returns of investment, and the public participation; secondly, hydropower development is able to push forward in the immigration issue by transferring the simple way of financial compensation, promoting the reformation of changing the land rights into capital investment, and protecting the rights of immigrants. If the water could be re-used will be account for 40% of the reserves of workable conventional energy sources as stated by Boting (2010). By studying the prospects and problems of the hydropower development, it is believed that the people oriented principle should be followed, up-gradation of hydropower development concepts and innovative hydropower development model; seriously treat and properly handle the hydropower development issues to promote sustainable development of economic and social; develop water resource with the harmony of nature and human, put the construction of power plant and ecological environment in the same important role.

In view to the earlier researches a new type of hydrokinetic energy converter was designed at Fluvial Hydraulics Laboratory of School of Water Resources Engineering, Jadavpur University. The hydrokinetic energy converter can also be termed as modified VIVACE as developed by (Bernitsas and Raghavan, 2005; Raghavan, 2007). This type of modified modulo can help to generate electricity from shallow depth of water flow. Keeping in view to the rural scenario where electricity is scarce there this type of hydrokinetic energy device would be a benefit.

1.2.2 Vortex induced vibration energy conversion

The literature on Vortex Induced Vibrations of circular cylinders is very extensive and new knowledge is developed continuously using experiments (Carberry, 2002; Gharib, 1999; Govardhan, 2000; Khalak and Williamson, 1996; Klamo, 2006; Sumer and Fredsoe, 1997), field tests (Sumer and Fredsoe, 1997), and numerical simulations (Sumer and Fredsoe, 1997; Williamson and Govardhan, 2004). At this point in time, many of the aspects of VIV are understood well or the next research steps are well defined. Some new phenomena still are being revealed as more research is conducted. Separate reviews of literatures on different aspects of VIV of circular cylinders and vortex shedding around circular cylinders that are pertinent to each chapter in this dissertation presented more extensively in those. A quick introductory overview of some aspects of VIV, which pertains to all the forthcoming chapters and to performance of the VIVACE converter, is presented next. Accordingly, literature related to free vibrations of elastically supported rigid cylinders; forced vibrations of such structures; with cylinders having one or two degrees of freedom (Govardhan, 2000; Khalak and Williamson, 1996; Triantafyllou *et al.*, 2006; Williamson and Govardhan, 2004; Williamson and Jauvtis, 2004) is relevant. Ever since Leonardo da Vinci first observed Vortex Induced Vibration (VIV), circa 1500 AD in the form of "Aeolian Tones," engineers have been trying to spoil vortex shedding and suppress VIV to prevent damage to equipment and structures. Furthermore, von Karman at California Institute of Technology proved that the Tacoma Narrows bridge collapse in 1940 was due to VIV. Here fluid-structure interaction phenomenon occurs due to the nonlinear resonance of cylinders or spheres through vortex shedding lock-in. VIV is also called synchronization between vortex shedding and cylinder or sphere oscillations. In this research, the terms VIV, synchronization, vortex shedding lock-in, and nonlinear resonance are used to refer to the same phenomenon.

In the condition of the constant Strouhal range, once the vortex shedding frequency for a stationary cylinder approaches the natural frequency of oscillation of the cylinder from below, the cylinder can begin periodical and vortex shedding can begin to correlate on the cylinder axis. This results in an oversized increase within the forces working on the cylinder. In this range, vortex shedding frequency and the oscillation frequency, collapse into the natural frequency of the system in flow. It is interesting to note here that sustained oscillations extend over a range of velocity values rather it can be talked about the range of Reynolds Number and the vortex shedding is controlled by the vibrating cylinder like types of research was carried out by (Bernitsas *et al.*, 2009; Raghavan *et al.*, 2009; Raghavan and Bernitsas, 2010; Chang, 2011). Today the scenario of the natural water channels in India is very critical since the water depths of such channels are decreasing day by day due to immense sediment loading due to the soil erosion at the upstream of the channels

Inspired from the earlier works, in this research a horizontally submerged cylinder has been considered against flat plate of 2 cm, 3 cm, 4 cm and 5 cm kept vertically at its downstream. The total flow phenomena have to be studied in order to bring out the

best possible combination for the hydrokinetic energy harvester to harness optimum amount of electricity.

1.3 Scope of this research

The prior work gives the hint of the way the present scope of work to be explored.

Main aspect of the dissertation lies under desired points:

- To understand and study about an electro-mechanical device where the flow field generated across a cylinder having two degrees of freedom in transverse direction of the flow of water in open channel due to Vortex Induced Vibration (VIV).
- To introduce obstruction like flat plate/s at downstream of the cylinder in order to increase the VIV.
- To analyze the flow mechanism where there is a combined effect of horseshoe vortex caused by the structures and vortex induced vibration on the cylinder and also to find out the location where the VIV would be maximum.
- If possible to generate a miniscule amount of electrical energy through the above noted device and to find out the ways to make the model feasible.

Chapter 2: Basic theories in relation to water kinematics, flow past a cylinder, vorticity and circulation, significance of various non-dimensional numbers in respect to the flow over the cylinder, various types of velocity measurement techniques and various types of electrical generators are been discussed in this chapter.

Chapter 3: Earlier in the literature it was depicted that if there is some modifications in the VIVACE plausible then the modified hydrokinetic energy harvester generate much more amount of electricity as it could think about. In this chapter feature of horseshoe vortex due to a flat vertical plate has been experimentally found out and have been analyzed.

Chapter 4: Aim of this chapter is to find out the flow fields between a vertical plate and a submerged horizontal cylinder. Numerous experiments had been carried out by altering the plate sizes to 2 cm, 3 cm, 4 cm and 5 cm at the downstream of the submerged cylinder. From the nature of the flow fields as generated from the experiments and analysis perfect combination of the plate and submerged moving cylinder could be found that would enhance effective power generations. Moreover the same characteristics of the vortices could be visualized at every instant of the depth of the water flow where the moving cylinder would traverse.

Chapter 5: Along-with the knowledge of flow fields it also becomes important to understand the electrical aspects of the hydrokinetic energy device that is to be developed. Taking the view of the results coming out from the above hydraulic aspects the electric aspects are to be developed. Then after developing the hydrokinetic generator the electrical parameters like voltage, current and power where recorded for various types of conditions like with or without modifications.

Chapter 6: This chapter comprises of the concluding remarks about the thesis and discussion about the future possibilities of similar works in this arena. Major areas that could have been developed in order to produce bulk amount of power in this research are also discussed here.

References

Bernitsas M.M. and Raghavan K. (2005). Fluid Motion Energy Converter. *USPTO*, 11/272,504.

Bernitsas M.M., Ben-Simon Y., Raghavan K. and Garcia E.M.H. (2009). The VIVACE Converter: Model tests at Reynolds numbers around 10^5. *Journal of Offshore Mechanics and Arctic Engineering*, 131(1), 1-13.

Billah K.Y. and Scanlan R.H. (1991). Resonance, Tacoma Narrows bridge failure, and undergraduate physics textbooks. *American Journal of Physics*, 59 (2), 118-124.

Carberry J. (2001). Wake States of a Submerged Oscillating Cylinder and of a Cylinder beneath a Free-Surface. *Ph.D. thesis, Monash University*.

Chang C.C., Kumar R.A. and Bernitsas M.M. (2011). VIV and Galloping of Single Circular Cylinder with Surface Roughness at $3.0\times10^4 \leq Re \leq 1.2\times10^5$. *Journal of Ocean Engineering*, 38, 1713-1732.

Gharib M.R. (1999). Vortex-Induced Vibration, Absence of Lock-in and Fluid Force Deduction. *Ph.D thesis, California Institute of Technology.*

Govardhan R. (2000). Vortex Induced Vibration of Two and Three Dimensional Bodies. *Ph.D thesis, Cornell University*, Ithaca.

Jia-kun L.I. (2012). Research on Prospect and Problem for Hydropower Development of China. *Procedia Engineering*, 28, 677-682.

Khalak A. and Williamson C.H.K. (1996). Dynamics of a Hydroelastic Cylinder with Very Low Mass and Damping. *Journal of Fluids and Structures*, 10(5), 455-472.

Klamo J.T. (2006). Effects of Damping and Reynolds Number on Vortex- Induced Vibrations. *Ph.D thesis, California Institute of Technology*.

Pontes M.T. and Falcao A. (2001). Ocean Energies: Resources and Utilization. *Proceedings of 18th WEC Congress*, Buenos Aires.

Raghavan K. (2007). Energy Extraction from a steady flow using Vortex Induced Vibration. *Ph.D thesis, California Institute of Technology, The University of Michigan*.

Raghavan K. and Bernitsas M.M. (2010). Experimental Investigation of Reynolds Number Effect on Vortex Induced Vibration of Rigid Cylinder on Elastic Supports. *Journal of Ocean Engineering*, 38(5-6), 719-731.

Raghavan K., Bernitsas M.M. and Maroulis D. (2009). Effect of Bottom Boundary on VIV for Energy Harnessing at $8\times10^3 < Re < 1.5\times10^5$. *Journal of Offshore Mechanics and Arctic Engineering*. 131(3), 031102-2-13.

Sumer B.M. and Fredsoe J. (1997). Hydrodynamics around Cylindrical Structures. *World Scientific Publication Company Limited.*

Technomare (1996). Wave Energy Project Results: The Exploitation of Tidal Marine Currents.

Triantafyllou M.S., Dahl J.M. and Hover F.S. (2006). Two-Degree-of-Freedom Vortex-Induced Vibrations Using a Force Assisted Apparatus. *Journal of Fluids and Structures,* 22(6-7), 807-18.

WaveNet (2003). Results from the Work of the European Thematic Network on Wave Energy, European Community.

Williamson C.H.K. and Govardhan R. (2004). Vortex-Induced Vibrations. *Annual review of fluid mechanics,* 36, 413-55.

Williamson C.H.K. and Jauvtis N. (2004). A High-Amplitude 2t Mode of Vortex Induced Vibration for a Light Body in Xy Motion. *European Journal of Mechanics,* 23, 107-114.

WMCE (2003). Ocean Energy Systems, Status and Research and Development Priorities.

Zhang Boting. (2010). Water conservancy and hydropower construction and a new round of western development. *Journal Grid and Clean energy*, 26 (10), 1-5.

2.1 Introduction to water kinematics

Kinematics is the branch of classical mechanics which describes the motion of points, bodies, and systems of bodies without consideration of the masses of neither the objects nor the forces that may have caused the motion. It treats variables such as displacement, velocity acceleration, deformation, and rotation of fluid elements without referring to the forces responsible for such motion. Kinematics as a field of study is often referred to as the "geometry of motion" and hence finds its application in fluid mechanics, describing the motion of water. Kinematics begins with a description of the geometry of the system and the initial conditions of known values of the position, velocity and or acceleration of various points that are a part of the system, then from geometrical arguments it can determine the position, the velocity and the acceleration of any part of the system. Fluids tend to flow easily, which causes a net motion of molecules from one point in space to another point as a function of time (Ojha *et al.*, 2010).

2.2 Flow past a cylinder

Many practical situations occur where it is found that the cylinders or any other shaped structure are mounted vertically or horizontally over the flow of the water. As a result, the flow separation occurs in both type practical scenarios. Due to its adverse geometry circular cylinders in a cross-flow have been a topic of research for over a hundred years, both for their practical and fundamental importance. Practically, circular cylinders exist in many engineering and industrial applications such as offshore raised platform, power lines, bridge supports, and heat exchangers. In the design of these structures, knowledge is needed in general of the forces, frequencies, heat transfer and flow behavior.

In a favorable streamwise pressure gradient, the flow is accelerated by the pressure force and thereby the boundary layer thickness keeps thin. In contrast, when the flow encounters an adverse streamwise pressure gradient along the solid boundary, the flow is decelerated by the pressure force, thereby causing the boundary layer to thicken. Then, the flow cannot advance too far in the region of adverse pressure gradient due to the insufficient kinetic energy that the fluid flow possesses. As a result, the boundary layer is deflected from the wall, known to be the separated boundary layer, which progresses into the main flow, as shown in Fig. 2.1. In general, the flow downstream the separation point (point S) experiences the adverse pressure gradient and turns to the reverse direction of the main flow that exists in the upper region of the separation line. As a result of the flow reversal, the boundary layer (δ) is thickened rapidly. The separation point is defined as the limit between the main and the reverse flow in the immediate vicinity of the wall. Further, in explaining the separation phenomenon by the potential flow theory, the streamlines within the boundary layer in the vicinity of the boundary layer separation are shown in Fig. 2.1. At the separation point, a streamline originates from the wall at a certain angle due to the merger of two limiting streamlines moving in the opposite direction. The separation point can be determined

by the condition that the velocity gradient normal to the wall becomes zero on the wall, that is $\left.\frac{\partial u}{\partial z}\right|_{z=0}^{s} = 0$.

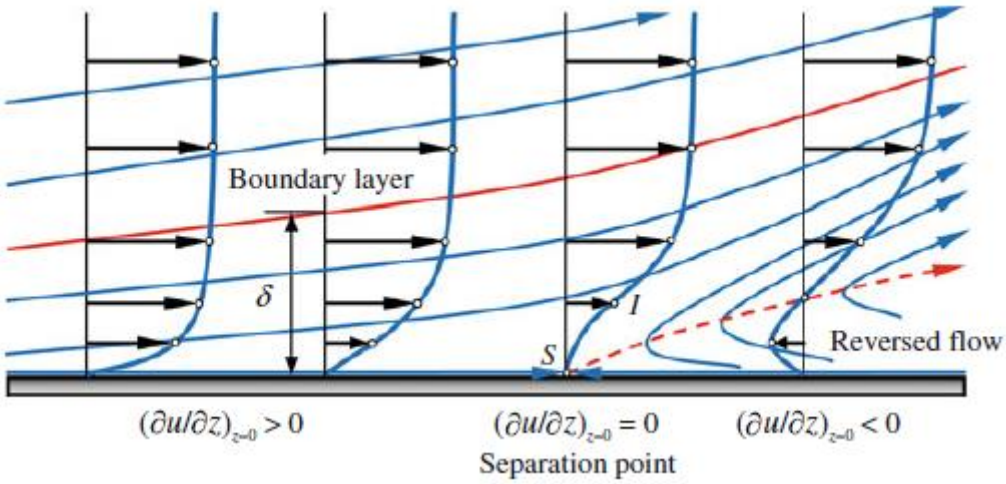

Fig 2.1 Concept of separation of boundary layer (Dey, 2014)

2.2.1 Vertically mounted cylinder

If a cylinder is vertically mounted in an open channel, the flow at the upstream will undergo a separation of the turbulent boundary layer and will roll up to form the well-known horseshoe-vortex system, which is swept around the cylinder. This type of flow occurs in a variety of situations, such as flow around bridge piers, around buildings and structures (stacks, cooling towers, gas tanks), and at different types of junctions.

Fig 2.2 Flow situations leading to scour around a vertically mounted cylinder

From Fig. 2.2 it is clear that in practical application when the cylinder is mounted vertical in sand bed a scouring phenomenon happens, which results in dunes and holes nearby the mounted cylinder. This type of study had been of interest of various researches in this field for decades.

2.2.2 Horizontally mounted cylinder

Scenarios are also there where we see underwater conveying elements like under water cables and pipelines. Due the occurrence of the flow separation here also the disturbance in the surrounding sand bed happens due to the adverse pressure gradient over the cylinder surface. Figure 2.3 shows the flow separation that occurs on the horizontally mounted cylinder. Here λ = wavelength of mushroom shaped vortices; a = amplitude of oscillatory flow and B is the axially periodic vortices when the flow past a cylinder.

Many of the previous studies examined two-dimensional flow around a circular cylinder that is free of end effects. In these situations, slender bodies exhibit alternating vortex shedding causing large fluctuating pressure forces that can lead to noise, vibration, or even structural failure when the vortex shedding frequency coincides with the bodies' own natural frequency. For example, vortex shedding was deemed partially responsible for the collapse of the Tacoma Narrows Bridge in Washington State in 1940.

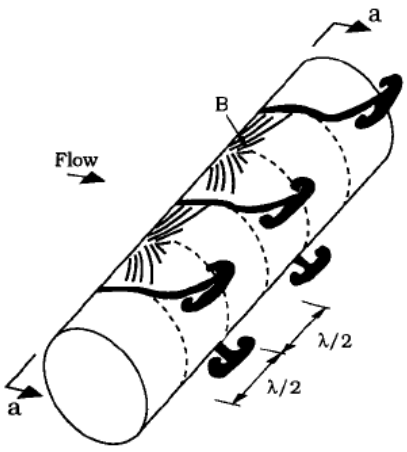

Fig. 2.3 Flow separation occurring around a horizontally placed cylinder

2.3 Vorticity

Vorticity is a vector field that gives a microscopic measure of the rotation at any point in the fluid. In its simple words, vorticity is the rotation of the fluid. It is the tendency for elements of the fluid to 'Spin'. The rate of rotation can be expressed various ways. Considering a bowl of water sitting on a table in a laboratory, the water may be spinning in the bowl. The two processes are separate, and two types of vorticity can be hence considered.

Vorticity is mathematically defined as the curl of the velocity field and is hence a measure of local rotation of the fluid. This definition makes it a vector quantity. Hence it is a vector field that gives a microscopic measure of the rotation at any point in the fluid.

More formally, vorticity can be related to the amount of "circulation" or "rotation" (or the local angular rate of rotation) in a fluid. The average vorticity (ζ) in a small region

of fluid flow is equal to the circulation (Γ) around the boundary of the small region, divided by the area (*A*) of the small region. Here *u* and *w* are the longitudinal and transverse velocity in *x* and *z* direction of a coordinate axis system.

$$\zeta = \frac{\partial u}{\partial z} - \frac{\partial w}{\partial x} = \frac{\Gamma}{A} \tag{2.1}$$

Notionally, the vorticity at a point in a fluid is the limit as the area of the small region of fluid approaches zero at the point:

$$\zeta = \frac{\Gamma}{A} \tag{2.2}$$

Mathematically, vorticity is a vector field and is defined as the curl of the velocity field:

$$\vec{\zeta} = \vec{\nabla} \times \vec{u} \tag{2.3}$$

An irrotational fluid has no vorticity. Somewhat counter-intuitively, an irrotational fluid can have a non-zero angular velocity (e.g. a fluid rotating around an axis with its tangential velocity inversely proportional to the distance to the axis has a zero vorticity).

2.4 Circulation

The circulation (Γ) is defined as the integral of the velocity vector around a closed path. i.e.

$$\Gamma = \oint \vec{v}.\vec{ds} = \iint_A \zeta \, dA \tag{2.4}$$

The existence of closed streamlines in a flow pattern implies that there are loops for which $\Gamma \neq 0$ and thus that the flow is not irrotational everywhere. The circulation Γ, of the vortex can be estimated at different azimuthal planes from the vorticity contours by using Stokes theorem, where $\vec{v}$ the velocity is vector; $\vec{ds}$ is the differential displacement vector over a closed curve and *A* is the area enclosed.

Using Stokes theorem, the line integral of the velocity field along the closed path, can be expressed as a surface integral of the curl of the velocity field normal to an arbitrary area bounded by the path. But, as already defined, that curl operation is called vorticity. Hence, circulation can be referred to as flux of vorticity. Conversely, it can also be said that that vorticity at a point is essentially circulation per unit area. The last two statements characterize the two quantities, vorticity and circulation, as microscopic and macroscopic respectively. Both these quantities are essentially a measure of the rotation of the fluid flow.

2.5 Vortex shedding

Vortex shedding is an oscillating flow that takes place when a fluid such as air or water flows past a bluff (as opposed to streamlined) body. In this study the bluff body is a cylinder that is placed horizontally, transverse to the direction of flow of water, at some distance away from the bed of the flume.

The vortex shedding phenomenon occurs for all flow regimes having Reynolds number (Re)>40. For these values of Re, the boundary layer over the cylinder surface separates due to the adverse pressure gradient imposed by the divergent geometry of the flow environment at the rear side of the cylinder, as a result of this a shear layer is formed. The boundary layer formed along the cylinder contains a significant amount of vorticity. Pipelines from offshore petroleum fields frequently pass over the areas with uneven seafloor. In such cases the pipeline may have free spans when crossing depressions. Hence, if dynamic loads can occur, the free span may oscillate and time varying stresses may give unacceptable fatigue damage. A major source for dynamic stresses in free span pipelines is vortex induced vibrations (VIV) caused by steady current. This effect is in fact dominating on deep water pipelines since wave induced velocities and accelerations will decay with increasing water depth. The challenge for the industry is then to verify that such spans can sustain the influence from the environment throughout the lifetime of the pipeline. The aim of the present project is to improve the understanding of vortex induced vibrations (VIV) of free span pipelines, and thereby improve methods, existing computer programs and guidelines needed for design verification. This will result in more cost effective and reliable offshore pipelines when laid on a very rugged seafloor. The VIV for multiple span pipelines were investigated and the dynamical interaction between adjacent spans has been shown. The interaction may lead to increase or decrease of response of each span depending on the current speed and the properties for the two spans. The extension of the contact zone between the spans and seafloor parameters will also be important for the interaction effect. The influence from temperature variation on vortex induced vibrations has been demonstrated. The response frequency is influenced through changes in pipe tension and sag. Both increased and decreased response of the frequency may be experienced. Moreover, it is shown that the influence from snaking of the pipe on the temperature effect is small, at least for large diameter pipes. A free span pipeline will necessarily oscillate close to the seabed. The presence of the seabed will therefore have some influences on the ambient flow profile and also on the flow pattern around the cylinder during oscillation. Hydrodynamic parameters may therefore vary when the pipe is close to the seabed. In the present work, the influence from spatial varying current profiles is investigated for both single and multiple span pipelines. It is shown that the difference between using uniform and spatial varying current profiles is significant for some current speeds. It is also shown that use of spatial varying current profiles can be even more important for multiple span pipelines. The comparison of vortex induced vibration analysis (VIVANA) results with Marine Technology (MARINTEK) test results has been given. It shows VIVANA predicts the cross-flow response generally much higher than the test measurements, especially for

the higher mode responses. To improve understanding of this phenomenon, the VIVANA model was tuned to the test model and results are compared in different cases. Attempts were made to obtain a better agreement by adjusting some of the input parameters to VIAVANA. The response frequencies are also tuned in order to have a better agreement on the results. It is been concluded that the method used here by VIVANA is not able to describe VIV for free spanning pipelines adequately. It is not possible to find a set of parameter in a rational way that will give reasonably correct results. The discrepancy between the analysis and test results are highlighted which confirms the interaction between the in-line and cross-flow vibrations. Discussions are given and addressed on different reasons which may cause this phenomenon. An improved strategy for non-linear analysis of free span pipeline is outlined. Time domain analysis for free span pipeline has been performed. The difference between time and frequency domain analysis has also been investigated by varying boundary conditions, pipe properties and axial tension. A significant difference is shown between results from time and frequency domain analysis at each end of the span where the pipe is started to interact with the seafloor. Due to high fatigue at this point, the importance of using non-linear time domain analysis is therefore obvious and highly recommended. This vorticity is fed into the shear layer formed downstream of the separation point and causes the shear layer to roll up into a vortex with a sign identical to that of the incoming vorticity (Vortex A). Likewise, a vortex, rotating in the opposite direction, is formed at the other side of the cylinder (Vortex B), (Sumer and Fredsoe, 2006). The pair formed by these two vortices is actually unstable when exposed to the small disturbances for Reynolds numbers Re> 40. Consequently, one vortex will grow larger than the other if Re > 40. Further development of the events leading to vortex shedding has been described by Sumer and Fredsoe, 2006 in the following way:

The larger vortex (Vortex A) presumably becomes strong enough to draw the opposing vortex (Vortex B) across the wake. As seen from Fig. 2.4a. The vorticity in Vortex A is in the clockwise direction, while that in Vortex B is in the anti-clockwise direction. The approach of vorticity of the opposite sign will then cut off further supply of vorticity to Vortex A from its boundary layer. This is the instant where Vortex A is shed. Being a free vortex, Vortex A is then conveyed downstream by the flow. Following the shedding of Vortex A, a new vortex will be formed at the same side of the cylinder, namely Vortex C as seen in Fig. 2.4(b). Vortex B will now play the same role as Vortex A, namely it will grow in size and strength so that it will draw Vortex C across the wake as depicted in Fig. 2.4(b). This will lead to the shedding of Vortex B. This process will continue each time a new vortex is shed at one side of the cylinder where the shedding will continue to occur in an alternate manner between the sides of the cylinder as shown in Fig. 2.5.

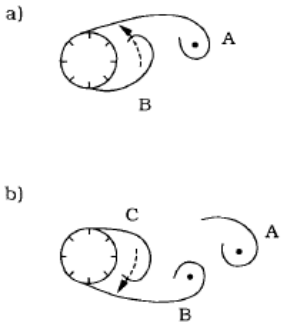

Fig 2.4 (a) Prior to shedding of Vortex A, Vortex B is being drawn across the wake; (b) Prior to shedding of Vortex B, Vortex C is being drawn across the wake.

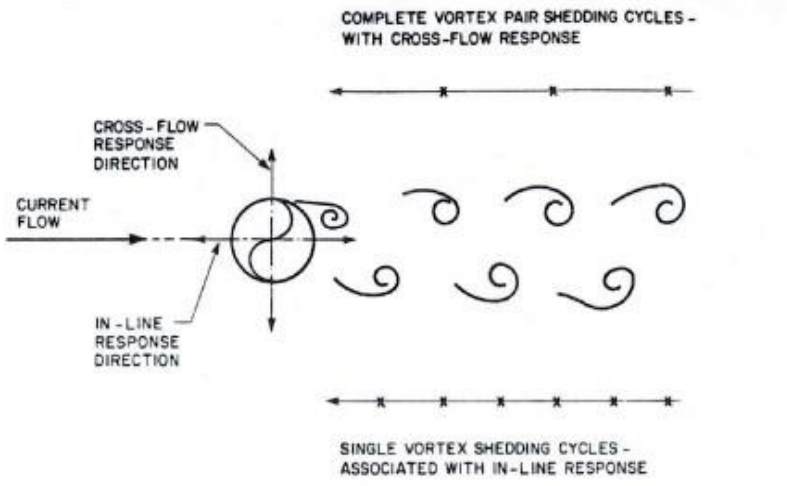

Fig.2.5 Staggered alternate vortex shedding - in-line and cross-flow response.

The tangential velocity (u_t) of particle on a stationary cylinder in uniform flow can be given by using potential theory, e.g. White (1998), as follow $u_t = -2U \sin\theta$ here U is the free stream velocity and θ is the angle on the cylinder. Therefore, the pressure distribution on the cylinder surface is given by

$$p = \frac{1}{2}\rho U^2 - 2\rho U^2 \sin 2\theta + p_0 \tag{2.5}$$

Using equation 2.5 shows the pressure distribution is symmetrical. Furthermore, the integrating of pressure around the cylinder surface will result to a net force equal to zero and confirm the so called D'Alembert's paradox which states that a body in an inviscid fluid i.e. $\nabla^2\varphi = 0$ has zero drag. Consideration of the flow as a potential flow or irrotational flow neglecting the viscous shear is not the actual situation that normally is found in reality. Flow retardation due to viscous action close to the surface of the cylinder leads to the development of a flow separation on it.

2.6 Flow around a submerged cylinder

Having already discussed the importance of study of flow around a cylinder, we shall discuss the different regimes of flow around a smooth, circular cylinder.

2.6.1 Lift forces on submerged cylinder

Knowledge of hydrodynamic forces on pipelines is of increasing importance in connection with the rapidly increasing number of off-shore pipelines. These pipelines are normally exposed to a complex wave-current climate. Furthermore, the seabed may be erodible so that scour takes place under the pipe. Thus the evaluation of forces on cylinders some distance away from the bottom becomes of interest.

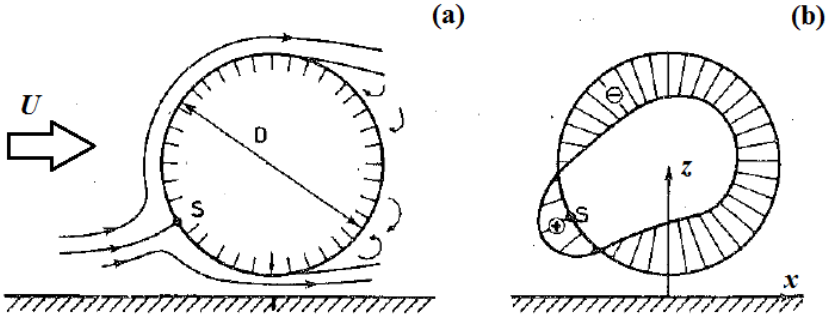

Fig. 2.6 (a) Flow around cylinder, (b) Pressure distribution around cylinder.

From the potential theory it is known that due to flow separation the stagnation point (*S*) which happens to be shifting as the gap between bed and submerged cylinder increase or decrease. Fig. 2.6 visualizes the phenomenon of the flow and pressure distribution around the submerged cylinder.

Pressure distribution on the surface of the circular cylinder

In order to understand the potential flow theory in more detail the pressure distribution over the cylinder surface as shown in Fig. 2.7 can be derived mathematically as:

$$v = u_\theta = -2U\sin\theta \tag{2.6}$$

Applying Bernoulli's principle,

$$\frac{p_\infty}{\rho g} + \frac{U^2}{2g} = \frac{p}{\rho g} + \frac{-2U\sin\theta^2}{2g} \tag{2.7}$$

$$C_p = \frac{p - p_\infty}{\frac{1}{2}\rho U^2} = (1 - 4\sin^2\theta) \tag{2.8}$$

Where, p_∞ is the pressure in a uniform flow, U is the velocity of a uniform flow, p is the pressure on the cylinder, θ is the polar coordinate and v is the velocity on the cylinder.

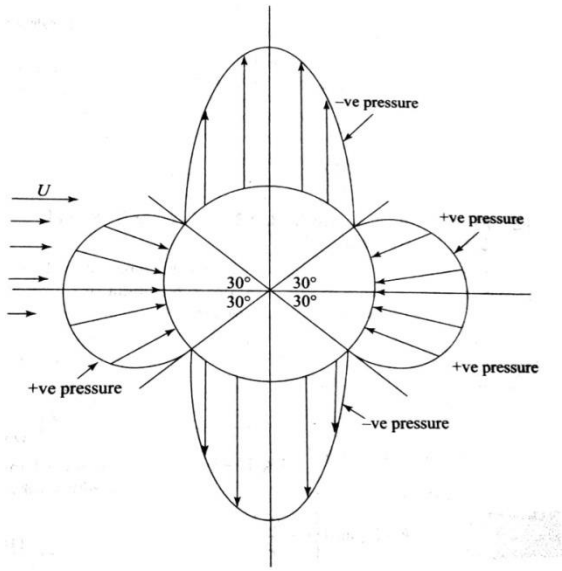

Fig. 2.7 The pressure distribution on the surface of the circular cylinder

The flow around the cylinder will exert a resultant force on the cylinder. There are two contributions to this force, one from the pressure and the other from the friction. The in-line component of the mean resultant force due to pressure (the in-line mean *pressure* force) per unit length of the cylinder is given by

$$\overline{F_p} = \int_0^{2\pi} \overline{p}\cos(\phi) r_0 d\Phi \tag{2.9}$$

$$\overline{F_f} = \int_0^{2\pi} \overline{\tau_0}\cos(\phi) r_0 d\Phi \tag{2.10}$$

$$\overline{F_D} = \overline{F_p} + \overline{F_f} \tag{2.11}$$

where, $\overline{F_p}$ is the form drag force, $\overline{F_f}$ is the friction drag force, $\overline{F_D}$ is the resultant drag force, $\overline{p}$ is the mean pressure, $\emptyset$ is phase difference between cylinder vibration and flow velocity and r_0 is the cylinder radius. The regime of flow around a circular cylinder varies as the Reynolds number is changed. Also, effects such as the surface roughness, the cross-sectional shape, the incoming turbulence, and the shear in the incoming flow influence the flow. However, except for very small Reynolds numbers (Re ~ 40) there is one feature of the flow which is common to all the flow regimes, namely the vortex shedding. As a consequence of the vortex-shedding phenomenon, the pressure distribution around the cylinder undergoes a periodic change as the shedding process progresses, resulting in a periodic variation in the force components on the cylinder. Fig. 2.8 shows a sequence of flow pictures of the wake together with the measured pressure distributions and the corresponding force components, which are calculated by integrating the pressure distributions over the cylinder surface (the time span covered in the figure is slightly larger than one period of vortex shedding). With *D*

= Diameter of the cylinder, Re = Reynolds number, U = Flow velocity and c_p = pressure coefficient the Fig. 2.8 can be elaborated as:

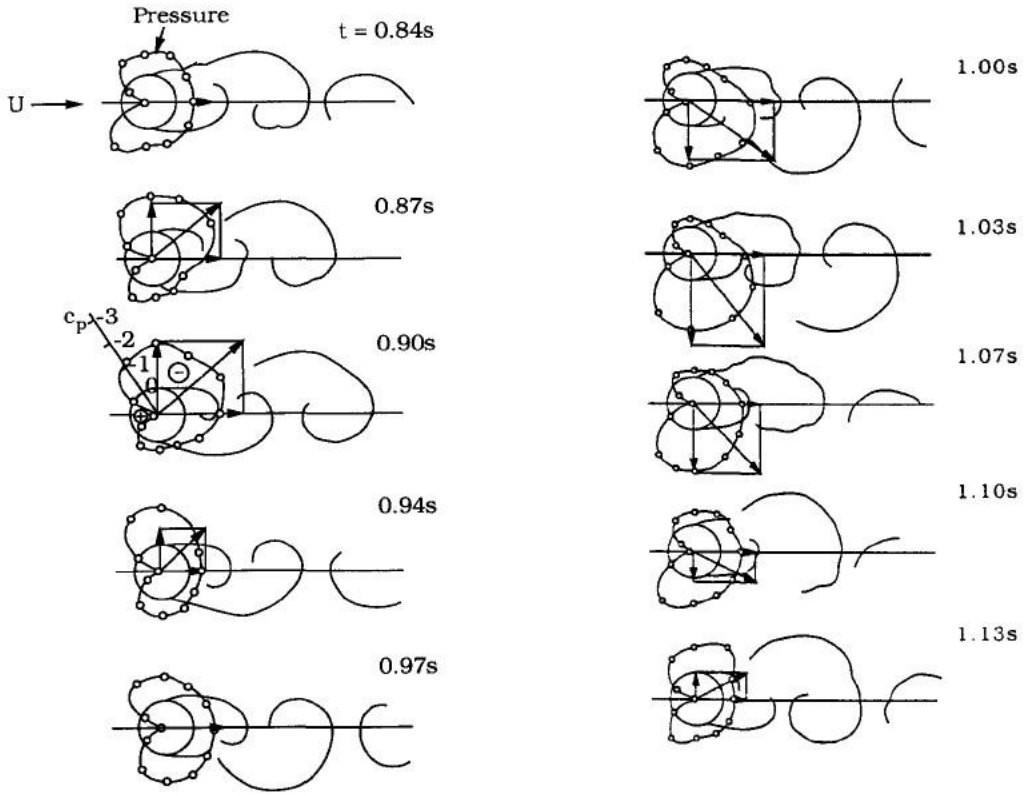

Fig. 2.8 Time development of pressure distribution and the force components, as the vortex shedding process Re = 1.1×10^5, D = 8 cm and U = 1.53 m/s. (Drescher, 1956)

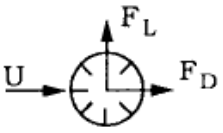

Fig. 2.9 Drag and lift forces occurring on horizontal placed cylinder.

In Fig. 2.9 the distribution of lift and drag forces are shown. Here U is the uniform velocity in the direction of flow, F_D is the drag force and F_L is lift force. It says that the lift force is always perpendicular to the water flow across the cylinder.

2.6.2 Significance of Reynolds number

The non-dimensional quantities describing the flow around a smooth circular cylinder depend on the cylinder Reynolds number (Re) with ν is the kinematic viscosity,

$$\mathrm{Re} = \frac{DU}{\nu} \tag{2.12}$$

From Fig. 2.10 shows a clear view of flow separation where flow after passing the cylinder wake region consisting of wake vortices are formed. While the wake extends over a distance which is comparable with *D*, the boundary layer extends over a very small thickness, which is normally small compared with *D*. The boundary layer thickness, in the case of laminar boundary layer, for example given by Schlichting (1979) is

$$\frac{\delta}{D} = O\left(\frac{1}{\sqrt{\mathrm{Re}}}\right) \tag{2.13}$$

And it is seen that $\frac{\delta}{D} << 1$ for Re larger than $O\left(100\right)$, say.

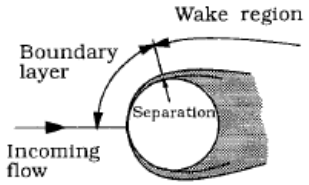

Fig 2.10 Definition sketch of boundary layer separation.

The flow regimes experienced with increasing Re, are summarized in Fig. 2.11. For very small values of Re no separation occurs. The separation first appears when Re becomes 5. For the range of the Reynolds number 5 < Re < 40, a fixed pair of vortices formed in the wake of the cylinder (Fig. 2.11 b). The length of this vortex formation increases with Re (Batchelor, 1967).

When the Reynolds number is further increased, the wake becomes unstable, which would eventually give birth to the phenomenon called vortex shedding in which vortices are shed alternately at either side of the cylinder at a certain frequency. Consequently, the wake has an appearance of a vortex street.

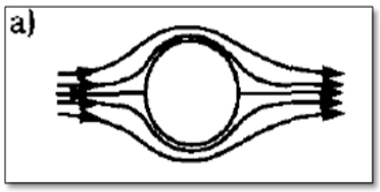

a) No separation. Creeping Flow
Re < 5

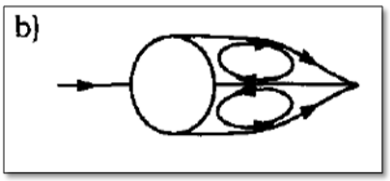

b) A fixed pair of symmetric vortices
5 < Re < 40

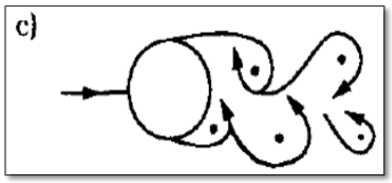

c) Laminar Vortex sheet
40 < Re <200

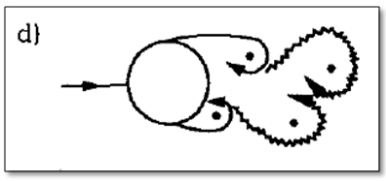

d) Transition To turbulence In the wake
200 < Re <300

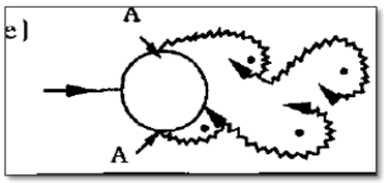

e) Wake completely turbulent.
A:Laminar Boundary layer separation
$300 < Re < 3.5 \times 10^5$
Subcritical

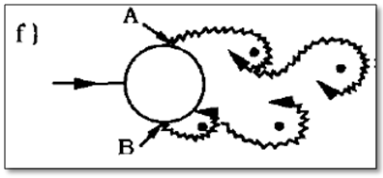

A:Laminar Boundary layer Separation
B: Turbulent Boundary layer Separation;
but boundary layer laminar
$3 \times 10^5 < Re < 3.5 \times 10^5$
Critical (Lower transition)

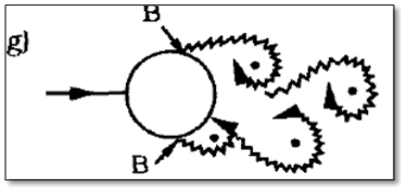

g) B: Turbulent boundary layer separation;
the boundary layer partly
laminar partly turbulent
$3.5 \times 10^5 < Re < 1.5 \times 10^5$

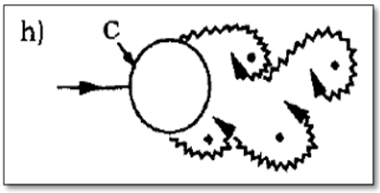

h) C: Boundary Layer completely
turbulent at one side
$1.5 \times 10^5 < Re < 4 \times 10^5$
Upper Transition

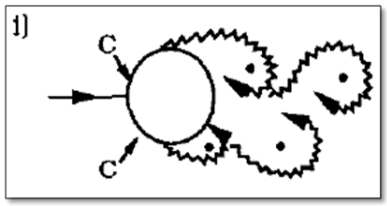

i) C: Boundary layer completely turbulent at two sides
$4 \times 10^6 < Re$
Transcritical

Fig 2.11 Regimes of flow around a smooth circular cylinder in steady current

For the range of the Reynolds number 40 < Re < 200 the vortex street is laminar (Fig. 2.11c). The shedding is essentially two-dimensional, i.e., it does not vary in the span-wise direction (Williamson, 1989).

With a further increase in Re, however, transition to turbulence occurs in the wake region (Fig. 2.11d). The region of transition to turbulence moves towards the cylinder,

as Re is increased in the range 200 < Re < 300 (Bloor, 1964). Bloor (1964) reports that at Re - 400, the vortices, once formed, are turbulent. Observations show that the two-dimensional feature of the vortex shedding observed in the range 40 < Re < 200 becomes distinctly three-dimensional in this range (Gerrard, 1978 and Williamson, 1988); the vortices are shed in cells in the span wise direction. (It may be noted that this feature of vortex shedding prevails for all the other Reynolds number regimes Re > 300.

For Re > 300, the wake is completely turbulent. The boundary layer over the cylinder surface remains laminar, however, for increasing Re over a very wide range of Re, namely 300 < Re < $3\times10^{5.}$ This regime is known as the subcritical flow regime (Fig. 2.11e).

With a further increase in Re, transition to turbulence occurs in the boundary layer itself. The transition first takes place at the point where the boundary layer separates, and then the region of transition to turbulence moves upstream over the cylinder surface towards the stagnation point as *Re* is increased.

In the narrow Re band 3×10^5< Re < 1.5×10^5 the boundary layer becomes turbulent at the separation point, but this occurs only at one side of the cylinder. The boundary layer in this region is partly laminar and turbulent. This flow regime is called the critical (or the lower transition) flow regime. The flow asymmetry causes a non-zero mean lift on the cylinder.

The side at which the separation is turbulent switches from one side to the other occasionally (Schewe, 1983). Therefore, the lift changes direction, as the one-sided transition to turbulence changes side, shifts from one side to the other (Schewe, 1983).

The next Reynolds number regime is the so-called supercritical flow regime where 3.5×10^5 < Re < 1.5×10^6 (Fig. 2.11g). In this regime, the boundary layer separation is turbulent on both sides of the cylinder. However, transition to turbulence in the boundary layer has not been completed yet; the region of transition to turbulence is located somewhere between the stagnation point and the separation point. The boundary layer on one side becomes fully turbulent when Re reaches the value of about 1.5×10^6. So, in this flow regime, the boundary layer is completely turbulent on one side of the cylinder and partly laminar and partly turbulent on the other side. This type of flow regime, called the upper-transition flow regime, prevails over the range of Re, 1.5×10^6 < Re < 4.5×10^6 (Fig. 2.11 h). Finally, when Re is increased i.e. Re> 4.5×10^6, the boundary layer over the cylinder surface is virtually turbulent everywhere. This flow regime is called the transcritical flow regime.

2.6.3 Significance of Keulegan Carpenter number

In fluid dynamics, the Keulegan Carpenter (*KC*) number also called the period number is a dimensionless quantity describing the relative importance of the drag forces over inertia force for bluff objects in an oscillatory fluid flow. Similarly, for objects that oscillate in a fluid at rest. For small KC number inertia dominates, while for large numbers the (turbulence) drag forces are important.

Keulegan-Carpenter number is given as:

$$KC = \frac{VT}{L} \tag{2.14}$$

Here, V = amplitude of the flow velocity oscillation

T = period of oscillation

L = characteristic length scale of the object, for instance diameter of a cylinder under wave loading.

When *KC* number is very small, separation behind the cylinder may not even occur. Large *KC* numbers on the other hand, mean that the water particles travel quite large distances relative to the total width of the cylinder, resulting in separation and probably vortex shedding. For very large *KC* numbers ($KC \to \infty$), one may expect that the flow for each half period of the motion resembles that experience in a steady current.

As described in the previous section hydrodynamic quantities describing the flow around a smooth, circular cylinder in steady currents depend on the Reynolds number. In the case where the cylinder is exposed to an oscillatory flow an additional parameter, the *KC* number appears.

Fig. 2.12 summarizes the changes that occur in the flow as the Keulegan-Carpenter number is increased from zero. The picture presented in the figure is for Re = 10^3. For very small values of *KC*, no separation occurs, as expected. The separation first appears when *KC* is increased to 1.1; this occurs in the form of the so-called **Honji instability**. The flow regime where separation takes place in the form of Honji instability occurs in a narrow *KC* interval, namely $1.1 < KC < 1.6$ (Fig. 2.12b).
With a further increase of *KC* number, however, separation begins to occur in the form of a pair of symmetric, ordinary, attached vortices as indicated in Fig. 2.12 c and d. This regime covers the *KC* number range $1.6 < KC < 4$ with the sub-range $2.1 < KC < 4$ where turbulence is observed over the cylinder as worked out by Sarpkaya (1986). It must be remembered that the limits for the indicated *KC* ranges in the figure are those for Re = 1000.

When *KC* is increased even further, the symmetry between the two attached vortices breaks down. (The vortices are still attached, and no shedding occurs, however). This regime prevails over the *KC* range $4 < KC < 7$ (Fig. 2.12e). The significance of this regime is that the lift force is no longer nil, and this is due to the asymmetry in the formation of the attached vortices. With a further increase of the Keulegan-Carpenter number, we come to the so-called **vortex-shedding regimes** *(KC* > 7).

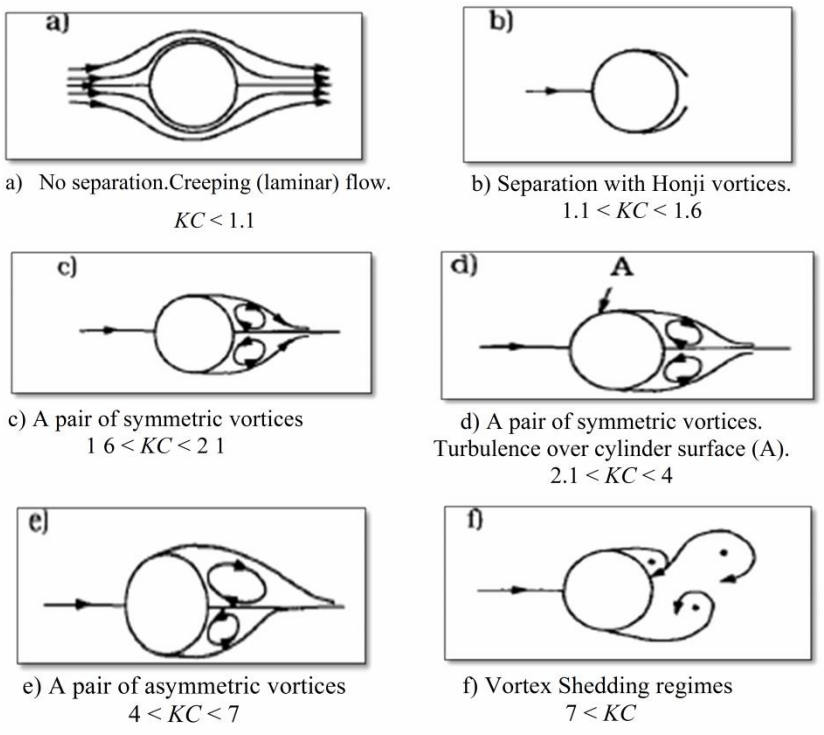

Fig. 2.12 Regimes of flow around a smooth, circular cylinder in oscillatory flow

2.6.4 Significance of Strouhal number

The vortex-shedding frequency, when normalized with the flow velocity U and the cylinder diameter D, can on dimensional grounds be seen to be a function of the Reynolds number;

$$St = St(\mathrm{Re}) \tag{2.15}$$

In which,

$$St = \frac{f_v D}{U} \tag{2.16}$$

And f_v is the vortex-shedding frequency, the normalized vortex-shedding frequency, named *St*, is called the Strouhal number. It is a non-dimensional parameter just like Reynolds Number. It is used in the momentum transfer in general, and in both von Karmann vortex streets and unsteady flow calculations in particular.

The Strouhal number represents a measure of the ratio of the *inertial forces* due to the *unsteadiness of the flow* or local acceleration to the inertial forces due to changes in velocity from one point to another in the flow field. The vortices observed behind gravel in a river, or measured behind the obstruction in a vortex flow meter, illustrate these principles.

2.7 Horseshoe vortex developed for a plate obstruction

The horseshoe vortex system emanating from the upstream of a vertical plate swirls while travelling in the main flow direction. Counter-clockwise rotating vortices take place downstream of the vertical plate submerged in the water channel. This horseshoe vortex system in real life many a times threatens the structures such as bridge piers which is places vertical to the flow directions due to occurrence of scour phenomena (Breusers *et al*., 1977; Dey *et al*., 1995 and Das *et al.,* 2013). The models of the scour phenomena occurring due to horseshoe vortex system were been vividly described in the researches of (Das and Mazumdar, 2015). Natural water channels containing erodible silts where there is high chance of scouring underneath such cylindrical structures due to the development of horseshoe vortex (Das *et al.,* 2014) along with transport of sediments due to equilibrium scour were depicted in the researches earlier (Das *et al.,* 2016).

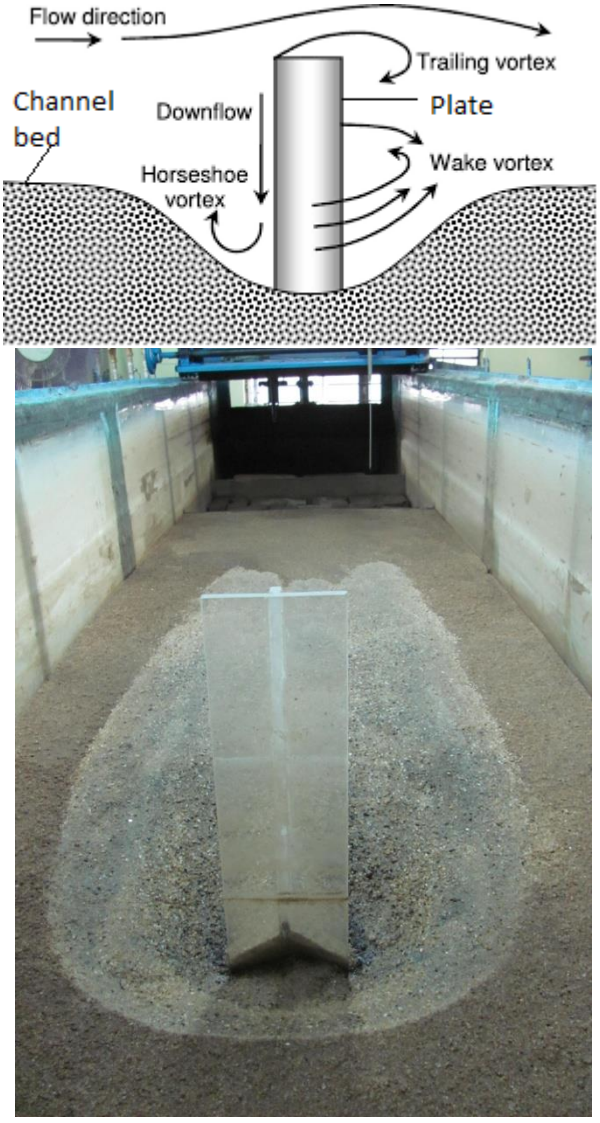

Fig. 2.13 Scour happening due to the effect of the horseshoe vortex generated from plate/pier

From Fig.2.13 the flow phenomenon happening due to the horseshoe vortex system is been represented. With reference to the above researches and Fig. 2.14 the system of horseshoe vortex can be understood as phenomena by which when the water flow hits any obstruction like a vertical plate as fixed perpendicular to the flow it goes vertically downwards and hits the water channel bed. Due to its circulatory motion the vortices try to split the sediment particles underneath the vertical plates and deposit them towards a position in downward direction of the plate due to the action of the wake vortex. At the same time this horseshoe vortex can aid to lift any device that works on the principle of vortex induced vibration as described in recent researches (Mukherjee *et al.,* 2016 a, b). Forthcoming detailed experimental discussion in this research about the effects of the horseshoe vortex developed for a flat plate obstruction may be clearer.

2.8 Velocity measurement

When coming to the discussions about the flow past a cylinder or plate, the measurement of the velocity becomes an important aspect. In previous researches earlier in 1990s before the wide introduction of the modern instruments the conventional direct methods of velocity measuring techniques like current meters were taken into considerations. After the development in electronic instrumentation a boom came into the velocity measuring techniques also by inventions of laser Doppler velocimetry, ultrasonic Doppler velocimetry and acoustic Doppler velocimetry were been utilized.

2.8.1. Introduction of various types of velocity measuring devices in open channel flow

As already discussed the measurement of velocity is an important aspect of many direct stream flow measurement techniques. A mechanical device called current meter; consisting essentially of a rotating element is probably the most commonly used instrument for accurate determination of the stream-velocity field.

Current Meters

The most commonly used instrument in hydrometry to measure the velocity at a point in the flow cross-section is the current meter. It consists essentially of a rotating element which operates due to the reaction of the stream current with an angular velocity proportional to the stream velocity. There are mainly two types of current meters:

1. Vertical-Axis Meters

These instruments consist of series of conical cups mounted around a vertical axis as shown in Fig. 2.14. The cups rotate in a horizontal plane and a cam attached to the vertical axial spindle records generated signals proportional to the revolutions of the cup assembly. The Price current meter and Gurley current meter are typical instruments

under this category. The normal range of velocities is from 0.15 to 4.0 m/s. The accuracy of these instruments is about 1.50% at the threshold value and improves to about 0.30% at speeds in excess of 1 m/s. Vertical-axis instruments have the disadvantage that they cannot be used in situations where there are appreciable vertical components of velocities. For example, the instrument shows a positive velocity when it is lifted vertically in still water.

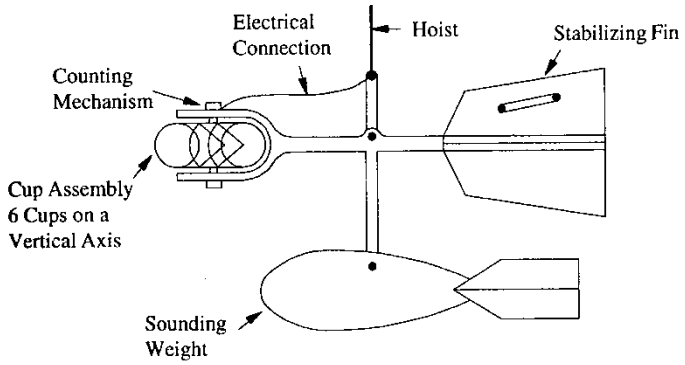

Fig. 2.14 Structure of vertical – axis current meter (Subramanya, 2008)

2. Horizontal-Axis Meters

These meters consist of a propeller mounted at the end of horizontal shaft as depicted in Fig. 2.15. These come in wide variety of size with propeller diameters in the range 6 to 12 cm, and can register velocities in the range of 0.15 to 4.0 m/s. Ott, Neyrtec and Watt-type meters are typical instruments under this kind. These meters are fairly rugged and are not affected by oblique flows of as much as 15˚. The accuracy of the instrument is about 1% at the threshold value and is about 0.25% at a velocity of 0.3 m/s and above.

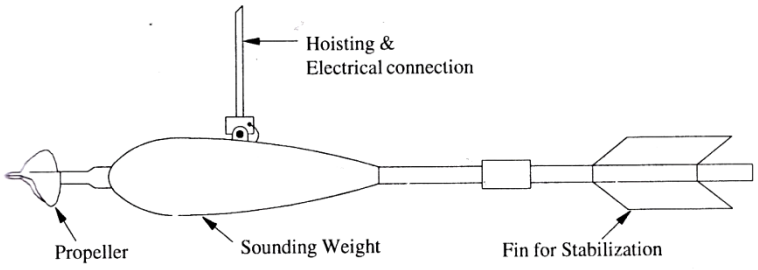

Fig. 2.15 Structure of horizontal – axis current meter (Subramanya, 2008)

When coming to the discussions about the modern velocity measuring technique i.e. detailed measuring the velocities across the grids so that the flow phenomena could be understood in more clear version three main instruments could be very useful but due to unavailability of the other two ADV is been used in this research purpose. Here are few descriptions about the three measuring instruments:

Laser Doppler velocimetry

Laser Doppler velocimetry (LDV) , also known as laser Doppler anemometry (LDA), is the technique of using the Doppler shift in a laser beam to measure the velocity in transparent or semi-transparent fluid flows, or the linear or vibratory motion of opaque, reflecting, surfaces. The measurement with LDA is absolute, linear with velocity and requires no pre-calibration. In its simplest and most presently used form, LDV crosses two beams of collimated, monochromatic, and coherent laser light in the flow of the fluid being measured as shown in Fig. 2.16. The two beams are usually obtained by splitting a single beam, thus ensuring coherence between the two. Lasers with wavelengths in the visible spectrum (390–750 nm) are commonly used; these are typically He-Ne, Argon ion, or laser diode, allowing the beam path to be observed. A transmitting optics focuses the beams to intersect at their waists (the focal point of a laser beam), where they interfere and generate a set of straight fringes. As particles (either naturally occurring or induced) entrained in the fluid pass through the fringes, they reflect light that is then collected by a receiving optics and focused on a photo detector (typically an avalanche photodiode).

The reflected light fluctuates in intensity, the frequency of which is equivalent to the Doppler shift between the incident and scattered light, and is thus proportional to the component of particle velocity which lies in the plane of two laser beams. If the sensor is aligned to the flow such that the fringes are perpendicular to the flow direction, the electrical signal from the photo-detector will then be proportional to the full particle velocity. By combining three devices (e.g.; He-Ne, Argon ion, and laser diode) with different wavelengths, all three flow velocity components can be simultaneously measured.

Another form of LDV, particularly used in early device developments, has a completely different approach akin to an interferometer. The sensor also splits the laser beam into two parts; one (the measurement beam) is focused into the flow and the second (the reference beam) passes outside the flow. A receiving optics provides a path that intersects the measurement beam, forming a small volume. Particles passing through this volume will scatter light from the measurement beam with a Doppler shift; a portion of this light is collected by the receiving optics and transferred to the photo-detector. The reference beam is also sent to the photo-detector where optical heterodyne detection produces an electrical signal proportional to the Doppler shift, by which the particle velocity component perpendicular to the plane of the beams can be determined.

Similar arrangements using optical heterodyning are also used in laser Doppler sensors for measuring the linear velocity of solids and for measuring vibrations of surfaces; the latter sensor is usually called a laser Doppler velocimeter, also abbreviated LDV.

Advantages of this instrument in this type of research:

1. Measurements could be done from outside the flume with greater accuracy.
2. Measurements could be done without hampering the flow field.

3. Very thin critical regions in the flow field could be measured.
4. All the output could be viewed in pictorial views at the same instant.

Disadvantages of this instrument in this type of research:

1. The price of the instrument is very high
2. The instrument must be handled with specific care as the laser rays coming out of the instrument is very dangerous to human skin and eye.

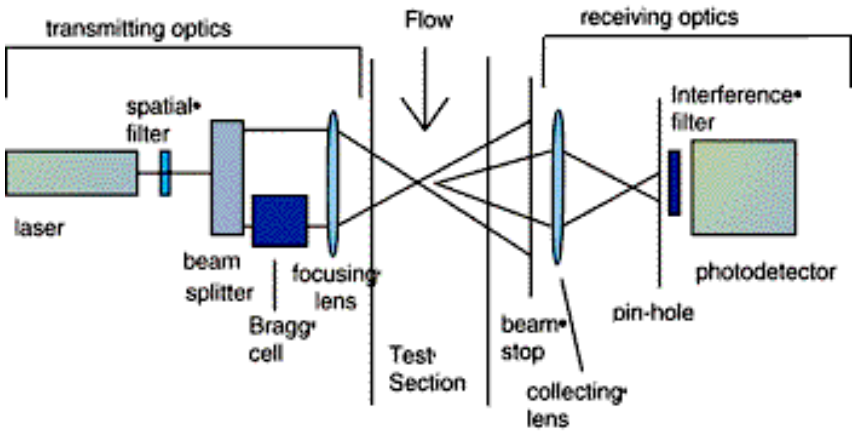

Fig. 2.16 Laser Doppler velocimeter arrangements (Azar, 1997)

Ultrasonic Doppler Velocimeter

Doppler ultrasound technique was originally applied in the medical field and dates back more than 30 years. The use of pulsed emissions has extended this technique to other fields and has open the way to new measuring techniques in fluid dynamics. The term "Doppler ultrasound velocimetry" implies that the velocity is measured by finding the Doppler frequency in the received signal, as it is the case in laser Doppler velocimetry. In fact, in ultrasonic pulsed Doppler velocimetry as shown in Fig 2.17, this is never the case. Velocities are derived from shifts in positions between pulses, and the Doppler effect plays a minor role. The velocities *u, v,* and *w* are the velocities found in respect to the coordinate axes of *x, y* and *z* respectively. The three dimensional velocities are received from three transmitters (Tr) as Tr1, 2 and 3 respectively which are emitted from Transmitter (Tre). Unfortunately, many publications, even recent ones, fail to make the distinction, resulting in erroneous system description and fallacious interpretation of the influence from various physical effects.

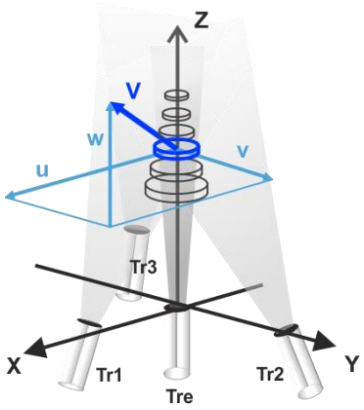

Fig. 2.17 Transmitters and Receivers of Ultrasonic Doppler Velocimeter

Advantages and limitations of UDV

The main advantage of pulsed Doppler ultrasound is its capability to offer spatial information associated to velocity values. Unfortunately, as the information is available only periodically, this technique suffers from the Nyquist theorem. This means that a maximum velocity ($v_{\max}$) exists for each pulse repetition frequency (*prf*), sound velocity (c) and probe frequency (f_e) as in equation 2.17:

$$v_{\max} = \frac{c}{4T_{prf} f_e \cos\theta} \tag{2.17}$$

Here θ is the angle between the velocity vectors *u*, *v* and *w* as given in Fig. 2.17 and shown at software interface of UDV in Fig. 2.18. In addition to the velocity limitation, there is a limitation in depth. The ultrasonic burst travels in the liquid at a velocity which depends on the physical properties of the liquid. The pulse repetition frequency gives the maximum time allowed to the burst to travel to the particle and back to the transducer. This gives a maximum depth ($P_{\max}$) of as given in equation 2.18:

$$P_{\max} = \frac{T_{prf}.c}{2} \tag{2.18}$$

From the above two equations, we can see that increasing the time between pulses (T_{prf}) will increase the maximum measurable depth, but will also reduce the maximum velocity which can be measured. The maximum velocity and maximum depth are thus related according to the following equation 2.19:

$$P_{\max} V_{\max} = \frac{c^2}{8 f_e \cos\theta} \tag{2.19}$$

More over the instrument cost is also very high.

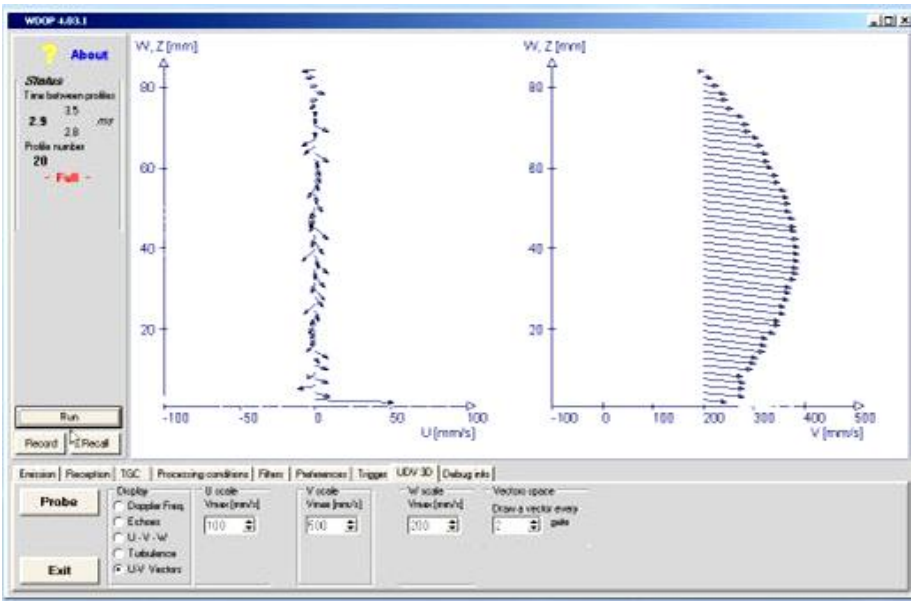

Fig.2.18 UDV software display window

Acoustic Doppler velocimeter

Acoustic Doppler velocimetry (ADV) is designed to record instantaneous velocity components at a single-point with a relatively high frequency. Measurements are performed by measuring the velocity of particles in a remote sampling volume based upon the Doppler shift effect as shown in Fig. 2.19. The probe head includes one transmitter and between two to four receivers. The remote sampling volume is located typically 5 or 10 cm from the tip of the transmitter, but some studies showed that the distance might change slightly. The sampling volume size is determined by the sampling conditions and manual setup. In a standard configuration, the sampling volume is about a cylinder of water with a diameter of 6 mm and a height of 9 mm, although newer laboratory ADVs may have smaller sampling volume (e.g. Sontek microADV, Nortek Vectrino plus). A typical ADV system equipped with N receiver's records simultaneously. N values with each sample. That is, for each receiver, a velocity component, signal strength value, a signal-to-noise (SNR) and a correlation value. The signal strength, SNR and correlation values are used primarily to determine the quality and accuracy of the velocity data, although the signal strength (acoustic backscatter intensity) may related to the instantaneous suspended sediment concentration with proper calibration. The velocity component is measured along the line connecting the sampling volume to the receiver. The velocity data must be transformed into a Cartesian system of coordinates and the trigonometric transformation may cause some velocity resolution errors. Although acoustic Doppler velocimetry (ADV) has become a popular technique in laboratory in field applications, several researchers pointed out accurately that the ADV signal outputs include the combined effects of turbulent velocity fluctuations, Doppler noise, signal aliasing, turbulent shear and other disturbances. Evidences included by high levels of noise and spikes in all velocity components. In turbulent flows, the ADV velocity outputs are a

combination of Doppler noise, signal aliasing, velocity fluctuations, installation vibrations and other disturbances.

Advantages:

1. It is very cheap instrument irrespective to above ones.
2. It can easily measure the velocity in 3-D without disturbing the flow field with high accuracy.

Disadvantages:

1. It has limitations in the measuring instances like every where measurement of the velocities points is not plausible as like in this research where the help of numerical modeling is also required.
2. In turbulence flow the measuring is not possible with accuracy.

Fig.2.19 Acoustic Doppler velocimeters

2.8.2 Measuring velocity with acoustic Doppler Velocimeter

An acoustic Doppler velocimeter (ADV) operates by the principle of Doppler shift. This concept is illustrated by a simple example: if you are standing at a railroad crossing and a train blows its horn as it passes by, you hear the horn at a higher pitch as the train approaches, and then a lower pitch as it leaves. As the train moves toward you, sound waves from the horn are compressed (meaning higher frequency) and you perceive the sound at a higher pitch. As the train leaves you, sound waves are no longer compressed and a lower-pitched, lower frequency noise is heard.

Vectrino Plus (make: Nortek, Norway)

The Vectrino (make: Nortek, Norway) is a high-resolution acoustic Doppler velocimeter used to measure turbulence and 3D water velocity in a wide variety of applications from the laboratory to the ocean. The basic measurement technology is

coherent Doppler processing, which is characterized by accurate data and no appreciable zero offset.

Technical Description

System Components

Probe: The probe is made of titanium and consists of four receiving transducers and a transmit transducer. It is mounted either on a fixed stem connected to the main housing through the probe end bell, or on a cable connected to the main housing through the same probe end bell.

Transducers: Each of the four receiving transducers is mounted inside a receiver arm. The transmit transducer is in the centre of the probe. The transducers are covered with hard epoxy.

Electronics Modules: The electronics module is located inside the pressure case and consists of a single board with the power transmitter, analog and digital signal processing, power conditioning, and interface circuits.

Temperature sensor: The temperature sensor (thermistor) is located inside the probe head.

Power and communication cable: The power and communication cable is connected to the end bell connector. The cable supplies external DC power (15–48 V) and provides a two-way serial communication with an external computer. It also provides four analog outputs (0-5 V DC) for input to an AD converter. The cable also provides synchronization options when the Vectrino is used as master or slave to synchronize measurements with other type of Vectrinos and/or other instruments.

Cable Wiring: The connector type is either a splash-proof connector or an MCBH-12-FS waterproof connector. The Vectrino power lines are diode protected, hence, about wiring the Vectrino power backwards is not the matter of problem.

Principle of Acoustic Doppler Velocimeter: Doppler Theory: The Vectrino uses the Doppler Effect to measure current velocity. The Doppler effect is the change in pitch that is heard when either the source of a sound or the listener is in motion. When a vehicle with a siren is heard, the pitch is higher when the vehicle is heading towards us, and lowers when it is going away. The change in pitch depicts how fast the vehicle is moving.

The Vectrino transmits short pairs of sound pulses, listens to their echoes, and, ultimately, measures the change in pitch or frequency of the returned sound.

Sound does not reflect from water, but from particles suspended in the water. These particles are typically suspended sediment or seeding particles, and move with the same average speed as the water. The velocity that is measured is consequently the velocity of the water.

The Vectrino velocimeter operating principle: A pulse is transmitted from the centre transducer, and the Doppler shift introduced by the reflections from particles suspended in the water, is picked up by the four receivers.

Mounting an ADV: Following guidelines need to be followed when mounting an ADV:

- It is to be assured that there are no obstructions between the sensor and the focal point (sampling volume) located about 5 cm from the transducers.
- The effect of large objects on the flow itself is to be considered. A rough rule of thumb is that objects disturb the flow as far as 10 diameters away from the object. Flow disturbance is greatest directly downstream in the wake behind the object.
- All acoustic transducers must be submerged during data collection. Operating your Vectrino when the transducers are out of water will not cause any damage, but your data will be meaningless. For side-looking probes, it is possible to collect 2D-data with only the lower receiver arms submerged.
- The best quality is achieved if the main flow direction is perpendicular to the transmit axis. Flow directly into the transmit axis should be avoided.
- Mounting structure has to be firmly fixed. Small vibrations in the mount can generate large accelerations in the data.

Signal to noise ratio (SNR): (Vectrino, 2004)

SNR is defined as follows:

$$SNR = 20\log_{10}\frac{Amplitude_{signal}}{Amplitude_{noise}} \tag{2.20}$$

While performing the experiments, some noise will always be present, so $Amplitude_{signal}$ should be read as $Amplitude_{signal+noise}$. However, for SNR values in the magnitude applicable to typical Vectrino situations, the difference is negligible.

Sampling rate: It sets the output rate for the velocity, amplitude, correlation and pressure data.

Sampling volume height: The height is user adjustable. Data accuracy increases if it is increased.

Transmit length: If it is increased then SNR ratio will be increased.

Salinity: Speed of sound depends upon salinity of water. The salinity is zero for fresh water and typically 35 ppt for the ocean.

Application of ADV in this research

This research aims towards determination of velocity profiles and the acoustic Doppler velocimeter (ADV) plays a major role in it. So, taking reference from the study of underwater pipeline as done by Dey and Singh (2008) here the cylinder would be kept

fixed at various depths of water and with help of acoustic Doppler velocimeter the trend and vortex strength immerging due to structures on the moving cylinder could be found out. Here tests will be done placing structures or fixed plates as shown in Fig. 2.20 of width 2 cm, 3 cm, 4 cm and 5 cm respectively in front of the cylinder. Moreover the experiments can also be done by moving the plates closer and away from the cylinder in the flow direction. After studying the above characteristics if possible the actual analysis of electrical power can be done by utilizing load cells or basic magnetic phenomenon. Getting the optimum calibrated device is finally the goal of the research work.

While the experiments are undergone with the help of ADV there is a high chance of missing few points, there the Finite difference schemes like forward, backward and central differences can be utilized. More over there are many grid points located in between the plate and cylinder where the readings cannot be taken there the above discussed methods of both implicit and explicit method could be useful provided the stability criteria to be fulfilled.

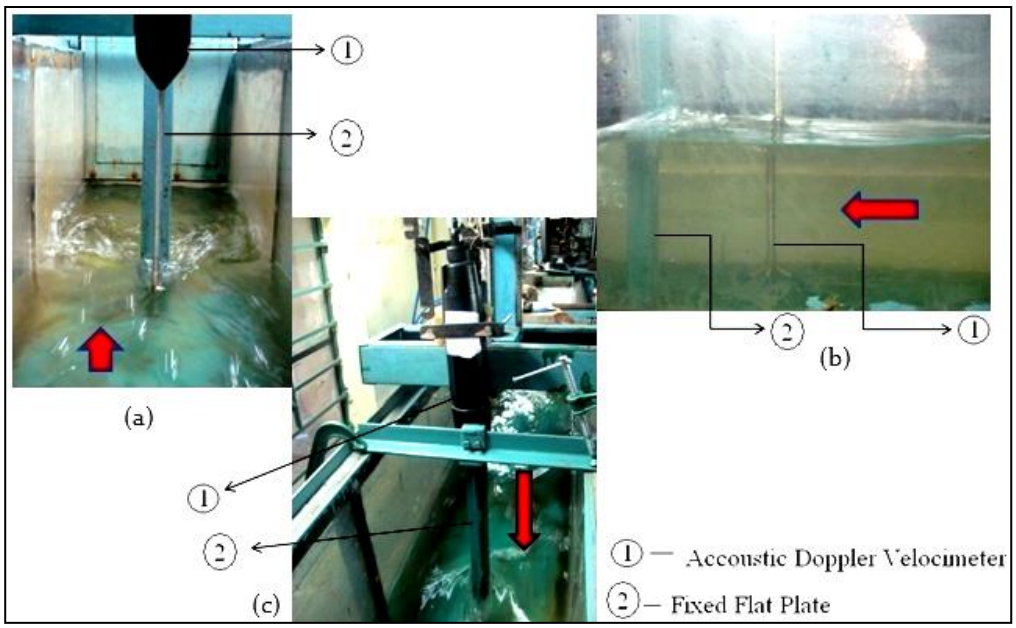

Fig. 2.20 Arrangements of Acoustic Doppler velocimeter in this research

2.9 Various types of electrical generator

Basically to harness power two principle types of generator are been employed which are rotating type and linear type respectively. There are also photovoltaic cells by which the solar energy can be converted into electrical energy. But when dealing with hydro energy basically rotating or linear type generators are been employed.

Rotating type generators

Generator is a machine that converts mechanical energy into electrical energy. It works based on principle of faraday law of electromagnetic induction. The Faraday's law

states that whenever a conductor is placed in a varying magnetic field, EMF is induced and this induced EMF is equal to the rate of change of flux linkages. This EMF can be generated when there is either relative space or relative time variation between the conductor and magnetic field. So the important elements of a generator are:

Generators are basically coils of electric conductors, normally copper wire, that are tightly wound onto a metal core and are mounted to turn around inside an exhibit of large magnets. An electric conductor moves through a magnetic field, the magnetism will interface with the electrons in the conductor to induce a flow of electrical current inside it. The conductor coil and its core are called the armature, connecting the armature to the shaft of a mechanical power source, for example an motor, the copper conductor can turn at exceptionally increased speed over the magnetic field. The point when the generator armature first starts to turn, then there is a weak magnetic field in the iron pole shoes. As the armature turns, it starts to raise voltage. Some of this voltage is making on the field windings through the generator regulator. This impressed voltage builds up stronger winding current, raises the strength of the magnetic field. The expanded field produces more voltage in the armature. This, in turn, make more current in the field windings, with a resultant higher armature voltage. At this time the signs of the shoes depended on the direction of flow of current in the field winding. The opposite signs will give current to flow in wrong direction.

Types of generators

The generators are classified into types.

- Alternating Current (AC) generators
- Direct Current (DC) generators

AC generators

These are also called as alternators. It is the most important means of producing electrical power in many of the places since now days all the consumers are using AC. It works based on principle of the electromagnetic induction as shown in Figs. 2.21-2.22. These are of two types one is induction generator and other one is synchronous generator. The induction generator requires no separate DC excitation, regulator controls, frequency control or governor. This concept takes place when conductor coils turn in a magnetic field actuating a current and a voltage. The generators should run at a consistent speed to convey a stable AC voltage, even no load is accessible.

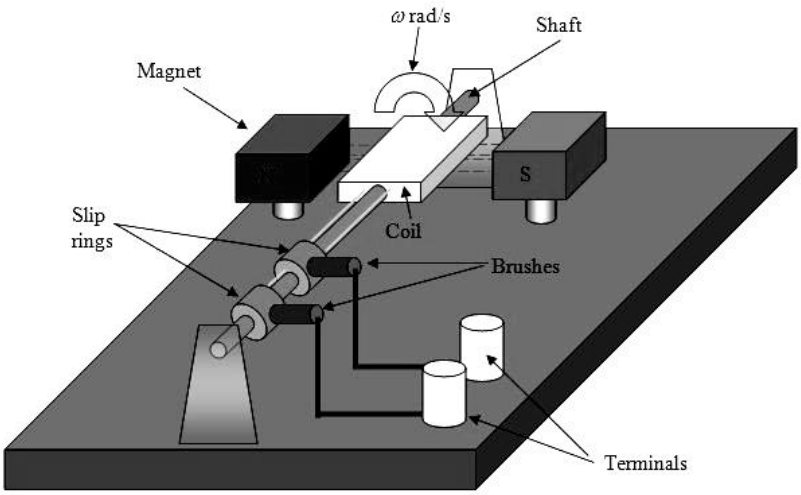

Fig. 2.21 Principle of A.C. Generator

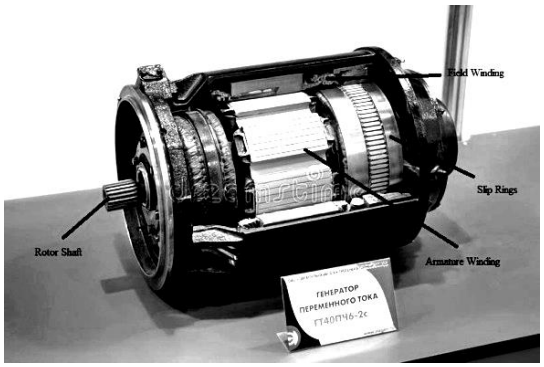

Fig. 2.22 Real view of a AC Generator (model breakdown) at the International Aviation and Space salon MAKS-2015

Synchronous generators are large size generators mainly used in power plants. These may be rotating field type or rotating armature type. In rotating armature type, armature is at rotor and field is at stator. Rotor armature current is taken through slip rings and brushes. These are limited due to high wind losses. These are used for low power output applications. Rotating field type of alternator is widely used because of high power generation capability and absence of slip rings and brushes.

It can be either three phase or two phase generators. A two-phase alternator produces two completely separate voltages. Each voltage may be considered as a single-phase voltage. Each is generated voltage completely independent of the other. The three-phase alternator has three single-phase windings spaced such that the voltage induced in any one phase is displaced by 120º from the other two. These can be connected either delta or wye connections. In delta connection each coil end is connected together to form a closed loop. A delta connection appears like the Greek letter delta (Δ). In wye connection one end of each coil connected together and the other end of each coil left open for external connections. A wye connection appears as the letter Y.

These generators are packaged with an engine or turbine to be used as a motor-generator set and used in applications like naval, oil and gas extraction, mining machinery, wind power plants etc.

Advantages of AC generators

- These generators are generally maintenance free, because of absence of brushes.
- Easily step up and step down through transformers.
- Transmission link size might be thinner because of step up feature
- Size of the generator relatively smaller than DC machine
- Losses are relatively less than DC machine
- These Generator breakers are relatively smaller than DC breakers

DC generators

DC generator is typically found in off-grid applications. These generators give a seamless power supply directly into electric storage devices and DC power grids without novel equipment. The stored power is carries to loads through dc-ac converters. The DC generators could be controlled back to an unmoving speed as batteries tend to be stimulating to recover considerably more fuel.

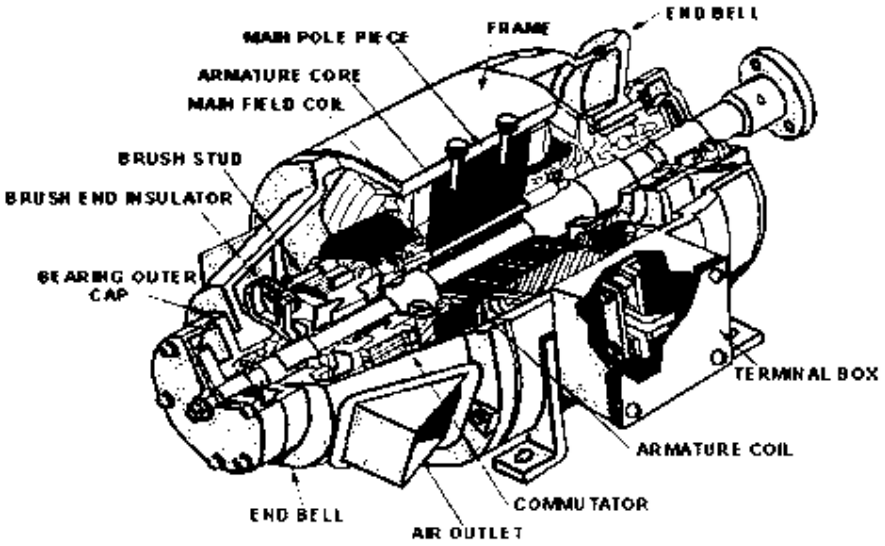

Fig. 2.23 Structural view of a D.C. Generator

Classification of DC generators

D.C Generators as shown in Fig. 2.23 are classified according to the way their magnetic field is developed in the stator of the machine.

- Permanent-magnet DC generators
- Separately-excite DC generators and
- Self-excited DC generators.

Permanent magnet DC generators do not require external field excitation because it has permanent magnets to produce the flux. These are used for low power applications like dynamos. Separately-excite DC generators requires external field excitation to produce the magnetic flux. We can also vary the excitation to get variable output power. These are used in electro plating and electro refining applications. Due to residual magnetism present in the poles of the stator self-excited DC generators can able to produce their own magnetic field ones it is started. These are simple in design and no need to have the external circuit to vary the field excitation. Again these self-excited DC generators are classified into shunt, series, and compound generators. These are used in applications like battery charging, welding, ordinary lightening applications etc.

Advantages of DC generators

- Mainly DC machines have the wide variety of operating characteristics which can be obtained by selection of the method of excitation of the field windings.
- The output voltage can be smoothed by regularly arranging the coils around the armature. This leads to fewer fluctuations which is desirable for some steady state applications.
- No shielding need for radiation so cable cost will be less as compared to AC.

The design process of a generator system aims at the specification of an optimal drive train configuration for the given application, which is a wave or water energy converter (WEC) in this case. As there are a lot of criteria which affect the choice of the system (e.g. technical feasibility, economics and complexity, among others), the result of the design process is likely to be a compromise between the different requirements on the generator system. In order to address the large number of different aspects which need to be taken into account, an approach with a systematic design process is recommended. In the following the different steps of the design process are described. The design process starts with investigating the requirements on the generator system, which depend on the characteristics of the WEC. From this investigation a list of criteria is compiled, which is used later to benchmark different systems. Based on these criteria, it can be investigated which components are generally available – e.g. components used in industrial applications or similar fields like wind energy conversion – and which components need to be developed for the application. The result is a list of candidate systems including the available generator systems, which generally meet the requirements of the application. The next step is a thorough benchmark of the candidate system according to the list of criteria referring to the generator system. Finally, as usually different systems show different characteristics in accordance to the criteria, the results of the benchmark have to be summarized and assessed to provide a final decision on the generator system. So a systematic approach of the design process could be split up into the following phases: Investigation on the requirements of the generator system depending on the application (function principle of the WEC, rated power, installation site, etc.); Compilation of a list of criteria on the generator system, - Choice of candidate system; Benchmarking of the candidate systems according to the list of criteria; Specification of the generator system. By

applying such a systematic approach, a high quality of the design process can be achieved. On the other hand, the quality depending highly on good knowledge and experience in the field of drive train systems. As such, knowledge and experience are crucial factors for identifying the requirements of the drive train, candidate systems, weak spots, etc. Two further aspects must be mentioned here which should not be underestimated: One is the interaction of the generator system with the rest of the PTO system and the overall WEC. The Power –Take-off (PTO) systems of the WECs considered in this study consist of several parts. Looking at an Oceanic Wave Current (OWC) WEC, the energy conversion chain consists of three steps: In the air chamber the wave energy is converted into a bidirectional airflow through a duct; By the air turbine the kinetic energy from the airflow is converted into rotational mechanical energy and The generator system converts the mechanical into electrical energy which is fed into the grid. According to the working principle of an overtopped WEC, the energy conversion chain consists of the following steps: By the ramp the energy stored in the incident wave front is converted into potential energy, A water turbine is applied to convert the potential to rotational mechanical energy, The generator system converts the rotating mechanical energy to electrical energy. In the design process of wave energy projects often the following approach is used: The first step is the design of the hull and the turbine. Then a suitable generator system is identified. When this design approach is followed, constraints of the generator system (such as minimum generator size for a given rated power) are not considered during the turbine and hull design. So it is very unlikely that the outcome will be an optimal system. Thus it is recommended to assess the impact of the generator system on the overall system throughout the whole design process. Besides considering characteristic data of the generator systems (masses, common speed ranges of generators, etc.), simulations of the interactions with the hull are recommended. Only by performing simulations which take into account factors like predominating sea states, behaviour of the prime mover and control, the crucial quantities like the rated/maximum generator speed and torque, the required overload capacity and thermal dimensioning of the generator system can be investigated and determined in detail. The second aspect is the evaluation of the final design of the generator system by conducting a hardware-in-the-loop (HIL) test. During the design process described above, the most promising design of the generator system is chosen. This is done based on the information of the different types of generators and the simulations of the overall system. Nonetheless there is still a significant risk of the system not performing as expected, which can happen due to wrong or missing information about the different parts of the system or shortcomings in the simulation. Therefore it is highly recommended to verify the results in a HIL-test. A typical configuration of a HIL test bench is depicted in Figure 2.24. The original generator system components are tested by using a test drive which simulates the air or water turbine respectively. In this configuration it’s also possible to test the original control unit which will be applied on the WEC. With this procedure, the behaviour of the generator system and the interaction with the control unit can be tested and verified under realistic conditions. This way the risk of the system not performing as expected

can be reduced to a reasonable limit and additionally the commissioning time can be reduced (Bard and Kracht, 2012).

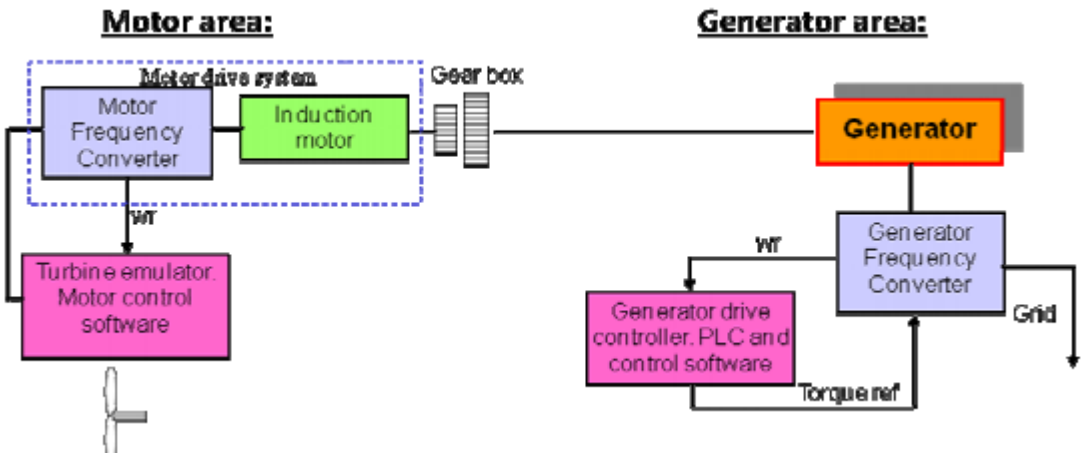

Fig. 2.24 Hardware-in-the-loop test bed configuration (Bard and Kracht, 2012)

Linear type generators

Since the 1970s various different designs and working principles for wave energy converters have been proposed, out of which a few were actually build, deployed and sometimes successfully tested. Nonetheless wave energy conversion is still an immature technology. In order to develop it further towards commercialization mainly two aspects need to be addressed. Firstly survivability in the extreme environment must be achieved at reasonable costs and secondly the overall efficiency of the devices needs to be increased. Accordingly research addresses fields like the structural design of the converters, the working principle, moorings etc. Also the generator system of the converters is a topic of on-going research. Some wave energy converters, e.g. oscillating water column or overtopping WECs, use rotating prime movers, allowing the application of rotating electrical machines for conversion from mechanical to electrical energy. Rotating electrical generators are widely used in conventional energy production and also in renewable energy systems like wind energy converters. A different situation is found, if one looks at generator systems for a WEC following for instance the working principle of a point absorber, converting the incident wave force into a translational movement of body. In this case some kind of linear actor is required for the next conversion step. Currently mainly hydraulics and electrical linear generators are discussed as candidate system for the application in this type of wave energy converters. But also alternative technologies like artificial muscles and mechanical conversion systems are proposed. Some of these technologies are used in various other fields, but only limited knowledge and experience on the application in WEC exists. Currently it's still unsure, which of the various generator technologies will finally make the race. Therefore it was found necessary to compare as many different options as possible in order to give device developers an overview of the options and a chance of a basic comparison of the different technologies.

Linear electrical machines are used as an alternative drive system in transportation and conveyor systems, where they replace pneumatic/hydraulic systems or rotating electric machines driving a spindle. Generally speaking linear machines are unwound rotating machines, either asynchronous or synchronous machines. In Figure 2.25 the principle layout of a permanent magnet synchronous linear generator is depicted. In the example the coils are placed on the stator and the magnets on the translator, mounting vice versa is also possible.

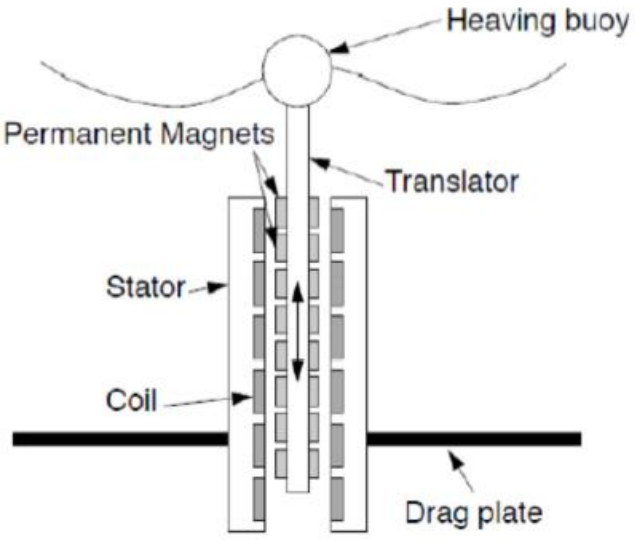

Fig. 2.25 A schematic of a linear electrical generator based on a permanent magnet generator (Drew *et al.*, 2009).

By mounting the coils on the stator no flexible connection to the coils is required and the number of magnets is reduced. If the stator is significantly longer than the translator the stator can be split up in several parts. This would allow switching of the generator parts, which are not active at a given time. This would result in a reduction of the losses in the generator as shown by Mueller *et al.* (2005). Almost all linear electrical machines are connected to the grid by means of a frequency converter (FC). In this configuration the behaviour is pretty similar to a rotating electrical machine grid connected by an FC.

A Power Take off (PTO) system comprising a linear electrical machine and an FC benefits from some clearly positive characteristics. Firstly the system shows excellent control behaviour and extremely short response times in the range of some milliseconds. The overall efficiency of the system – electrical machine and FC is comparably high. At full-load efficiencies well above 80% up to 95% can be expected. Also at part-load especially the permanent magnet synchronous machine shows a high efficiency. A further positive aspect is the overload capacity. Electrical machines typically have an overload capacity in the range of 700% and the thermal time constant is in the range of 10 minutes; is definitely sufficient for the short power peaks of a WEC. Looking at the FC reduced overload capacities (up to 200%) and thermal time constants (in the range of some seconds – some minutes) will be found.

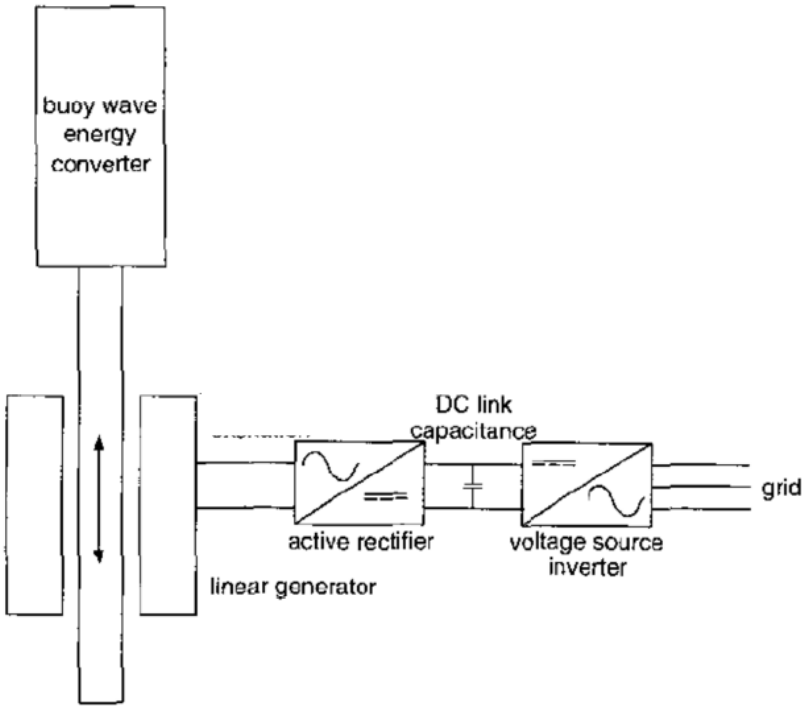

Fig. 2.26 Basic configuration of grid connection (Mueller *et al.,* 2002)

Also in terms of grid connection an electrical linear generator has own major drawback. The overall system normally comprises the generator itself and an FC for grid connection. The DC link capacitance in this configuration is too small to give any relevant means of power smoothing. Thus the overall system does not comprise any inherent power storage device. So the fluctuating power viewing from Figs. 2.26-2.27 is directly transferred to the grid. A good candidate system for power smoothing, which can relatively easy be integrated in this system, could for instance be a so-called super capacitor (O'Sullivan *et al.,* 2011). Despite the various drawbacks electrical linear generator are assumed to be a reasonable candidate system for the application in WEC. This is due to some benefits of the technology. Firstly the overall efficiency is comparably high due to the fact, that only two power steps are required to convert the power from the prime mover to useful power delivered to the grid. Secondly also the reliability is assumed to be high compared to other systems due to the low number of system components. Also in terms of maintenance the electrical linear generator shows some benefits, if at all only the bearings need maintenance, on a regular basis. In terms of risks to the environment it is advantageous, that only the bearings might contain oil for lubrication, which could pollute the environment in case of leakage. A further advantage is the controllability, allowing realizing control schemes as described above. And the high overload capacity allows to rate the generator significantly below the peak power of the device.

References

Azar K. (1997). Thermal measurements in Electronics Cooling, CRC Press, 4(1), 1-42.

Bard J. and Kracht P. (2012). Report on Rotating Generators. *Fraunhofer, IWES, Alborg Universtiy*, 1-34.

Batchelor G.K. (1967). An Introduction to Fluid Dynamics. *Cambridge University Press.*

Bloor M.S. (1964). The transition to turbulence in the wake of a circular cylinder. *Journal of Fluid Mechanics, Cambridge University Press*, 19, 290-304.

Breusers H.N.C., Nicollet G. and Shen H.W. (1977). Local scour around cylindrical piers. *Journal of Hydraulic Research*, 15(3), 211-252.

Das S. and Mazumdar A. (2015). Comparison of Field of Horseshoe Vortex at a Flat Plate and Different Shaped Piers. *International Journal of Fluid Mechanics Research*, 42(5), 418-448.

Das S., Das R. and Mazumdar A. (2012). Vortex flow field past a cylinder under clear water scour regime. *International Conference on Applications of Fluid Engineering, CAFÉ*, Greater Noida, India.

Das S., Das R. and Mazumdar A. (2014). Vorticity and Circulation of Horseshoe Vortex in Equilibrium Scour Holes at Different Piers. *Journal of The Institution of Engineers (India): Series A*, 95(2), 109-115.

Das S., Das R. and Mazumdar A. (2016). Comparison of Local Scour Characteristics around Two Eccentric Piers of Different Shapes. *Arabian Journal for Science and Engineering*, 41(4), 1199-1213.

Das S., Midya R., Das R. and Mazumdar A. (2013). A Study of Wake Vortex in the Scour Region around a Circular Pier. *International Journal of Fluid Mechanics Research*, 40(1), 42-59.

Dey S., Bose S.K. and Sastry G.L.N. (1995). Clear Water Scour at Circular Cylinders, *Journal of Hydraulic Engineering,* 121(12), 869-876.

Dey S. and Singh N.P. (2008). Clear-water scour below underwater pipelines under steady flow. *Journal of Hydraulic Engineering,* 134, 588-600.

Dey S. (2014). Fluvial Hydrodynamics. *GeoPlanet: Earth and Planetary sciences, Springer*, 592-594.

Drescher H. (1956). Messung der auf querangestromte Zylinder ausgeiibten zeitlich veranderten Drucke. *Z. f. Flugwiss,* 4(112), 17-21.

Drew B., Plummer A. and Sahinkaya A.N. (2009). A review of wave energy converter technology. *Proceedings of the Institution of Mechanical Engineers, Part A: Journal of Power and Energy*, 223 (8), 887-902.

Gerrard J.H. (1978). The wakes of cylindrical bluff bodies at low Reynolds number. *Philosophical Transactions of the Royal Society London, Series A*, 288(A1354), 351-382.

Mueller G. and Ponick B. (2005). Grundlagen elektrischer Maschinen. *WILEY-VCH – Verlag, 9th edition.*

Mueller M.A. (2002). Electrical generators for direct drive wave energy converters. *IEE Proceedings of Generations, Transmission, Distributions*, 149(4), 446-456.

Mukherjee B., Das S. and Mazumdar A. (2016a). Electrical Energy Generation by Enhancing Flow Induced Vibration. *2nd International Conference on Control, Instrumentation, Energy & Communication, CIEC*, Calcutta, India, 368-371.

Mukherjee B., Das S. and Mazumdar A. (2016b). Sustainable Electrical Energy Generation Technique in Shallow Water Channels. *IEEE Students' Technology Symposium*, Kharagpur, India, 147-151.

O'Sullivan D., Murray D., Hayes J., Egan M.G. and Lewis A.W. (2011). The Benefits of Device Level Short Term Energy Storage in Ocean Wave Energy Converters. *Energy Storage in the Emerging Era of Smart Grids, Prof. Rosario Carbone (Ed.).*

Ojha C., Berndtsson R. and Chandramoulli P. (2010). Fluid Mechanics and Machinery. *Oxford University Press, First Edition*, 172-173.

Sarpkaya T. (1986). Force on a circular cylinder in viscous oscillatory flow at low Keulegan-Carpenter numbers. *Journal of Fluid Mechanics*, 165, 61-71.

Schewe G. (1983). On the force fluctuations acting on a circular cylinder in crossflow from subcritical up to transcritical Reynolds numbers. *Journal of Fluid Mechanics*, 133, 265-285.

Schlichting G. (1979). Boundary Layer Theory. *McGraw-Hill Book Company, seventh edition.*

Subramanya K. (2008). Engineering Hydrology. *Tata McGraw Hill Book Company, third edition*, 101-131.

Sumer M. and Fredsoe J. (2006). Hydrodynamics around cylindrical structures. *Advanced Series on Ocean Engineering. World Scientific*, 26, 36-75.

Vectrino velocimeter user guide. (2004). *Nortek AS*, 27.

White F. (1998). Fluid Mechanics. *WCB McGraw Hill Publication. Fourth edition*, 215-260.

Williamson C.H.K. (1988). The existence of two stages in the transition to three dimensionality of a cylinder wake. *Physics of Fluids*, 31(11), 3165-3168.

Williamson C.H.K. (1989). Oblique and parallel modes of vortex shedding in the wake of a circular cylinder at low Reynolds number. *Journal of Fluid Mechanics*, 206, 579-627.

3.1 Introduction

Analysis of the flow phenomenon associated with a vertical plate kept in perpendicular to the flow in a water channel has been discussed in this chapter. Since in this thesis main focus lies on the modification of the electrical energy harnessing device that mainly runs on the principle of vortex induced vibration. Here the vertical flat plates are used as an obstruction to the water flow at the downstream of the horizontally laid cylinder. In this regard four types of vertical plates were considered whose profile plots of velocity vectors, velocity contours, turbulence intensities, turbulent shear stresses, turbulent kinetic energy and vorticity were calculated and generated. By analyzing the results from each of the obstruction, the flow phenomena generating from each of plates and its probable effect basically the horseshoe vortex on the horizontally fixed cylinder have been accessed. In the later part of thesis the complex phenomena has also been seen and analyzed. As a result, while designing the whole hydrokinetic energy converter the role of the vertical plates and the horizontal cylinder is most important. Hence analyzing the flow phenomena of the vertical plates will aid to the proper design of the electrical energy generator. Strict maintenance of 52 lps water flow and 20 cm flow depth for water recirculation in flume were followed. In such water flow, turbulence condition is obvious and the vortex formation is also in expectation as depicted in earlier researches. Acoustic Doppler Velocimeter (ADV) helped to determine the velocity and its direction while vortices were being created at the upstream of the vertical plate. The circulation of the horseshoe vortex as created by the plate is determined by using Stokes theorem and backward difference technique.

Keywords: *flow fields; horseshoe vortex; hydrokinetic energy generator; hydrodynamic structure.*

3.2 Earlier works on this research

In fluid mechanics, vorticity or circulation per unit area is the tendency for elements of the fluid to spin. It becomes important to be acquainted with the magnitude of circulation as it implies the strength of the vortex. Hence it can be said that the circulation or vortex strength (Γ) will increase if the Reynolds number increases and also if the viscous effect is negligible. When discussing about the vertical plates the earlier researches mostly of the horseshoe vortex leading to the scour phenomena comes into play. Earlier researches of Melville and Coleman (2000) stated that the strength of the horseshoe vortex depends on pier or plate Reynolds number and relative inflow depth. The horseshoe vortex systems underneath the cylindrical structures were explained in the works of Baker (1979); Dey and Raikar (2007, 2008). Further on if a cylinder was vertically set in an open channel; the upstream flow will undergo a separation of the turbulent boundary layer and rolls up to form the well-known horseshoe-vortex system also visualized by Das *et al.* (2013, 2014) is swept around the cylinder. The calculations for the turbulence kinetic energy and other related parameters were shown by Dey (2014). From the work of Das and Mazumdar (2015) experimental investigation on the kinematics of horseshoe vortex around a flat plate

was reflected. In order to have a comparative study, the velocity measurements within clear water equilibrium scour hole at circular, square, and equilateral triangular piers of sides equaling the width of the flat plate has been taken by an acoustic Doppler velocimeter. The contours and spatial distributions of the time-averaged (mean) velocities, turbulence intensities and turbulent kinetic energy at different azimuthal planes were deduced. Velocity vector plots of the flow fields at azimuthal planes were used to show further flow features. The horseshoe vortex flow and turbulence characteristics were discussed from the standpoint of similarity with velocity and turbulence intensity characteristics scales. The measuring technique of high-image density particle image velocimetry (PIV) has been employed in order to obtain instantaneous representations of the unsteady flow for a specified flow field. The time history of velocity and time-averaging of PIV data, particularly near the juncture, reveal valuable information about the behaviour of the horseshoe vortex system as suggested in the work of Sahin *et al.* (2007). Sahin *et al.* (2010) has also investigated horseshoe vortex formation around a vertical flat plate mounted in the water channel experimentally. In order to demonstrate the development of the horseshoe vortex system in the junction of the horizontal and vertical plates a Particle Image Velocimetry (PIV) and dye visualization techniques were used. Instantaneous and time-averaged velocity vector fields, corresponding streamline topology, vorticity values were analyzed. Boundary layer separation, developing vortices, secondary or counter-rotating vortices, merging of developing and counter-rotating vortices which results in a primary horseshoe vortex system and corner vortex have been demonstrated qualitatively and quantitatively in that research. In-depth study of horseshoe vortex flows, near the juncture of a vertical plate and a base plate, is performed using flow visualization technique, fiber laser Doppler velocimetry and particle image velocimetry systems in the study of Lin *et al.* (2002). In that study the flow patterns were classified into four major categories while the Reynolds number based on the free stream velocity and the width of vertical plate, varies with a range of 400-11000, and the height-to-width ratio changes from 0.5 to 4.0. Four major categories were defined as (1) steady vortex system, (2) periodic oscillation vortex system with small displacement, (3) periodic breakaway vortex system, and (4) turbulent-like vortex system. Zhihua *et al.* (2011, 2014) adapted the vortex control baffle for the horseshoe vortex generated at the stern foil–body junction. Results from the numerical simulation of the flow around the fully appended submarine model indicated that the effect of the vortex control baffle plate greatly improved the performance of the submarine wake. Muzzammil and Gangadhariah (2003) experimentally observed that the primary horseshoe vortex, formed in front of a circular pier, is the prime cause responsible for scour during the entire process of scouring. Simple and effective method to obtain the time-averaged characteristics of the vortex in terms of parameters relating variables of the flow, pier, and channel bed was employed.

Turbulent vertical structures under broken solitary waves using three-dimensional smoothed particle hydrodynamics (SPH) method were studied by Farhani *et al.* (2014). The numerical model predicted that water surface evolution and horizontal velocity very well in comparison with the experimental results. The numerical results detect

organized coherent structures characterized as reversed horseshoe (hairpin) vortices being generated at the back of the broken spilling wave and traveling downward. The counter rotating legs of the reversed horseshoe structures appear to be a continuous form of the previously found obliquely descending eddies. The reversed horseshoe structures are associated with the turbulence motion of sweep events (down welling motion) and transport momentum and turbulent kinetic energy downward into the water column. Vortex-roll-up turning plays an important role on the generation and evolution of three dimensional reversed horseshoe structures from the span-wise breaking wave rollers.

3.3 Present need of analysis of horseshoe vortex due to a flat plate

The work undertaken here is based on the modification of the electrical energy generator that basically runs on the principle of vortex induced vibration. A vertical plate placed at the downstream of a horizontal cylinder in a water channel has been considered as the modification. The horseshoe vortex generated at the upstream of the vertical plate aids to the lift of the freely moving horizontal cylinder in the transverse direction to the flow of water. Hence a separate analysis of the flow phenomena related to the vertical plate becomes necessary. From the vortex strength or circulation finally obtained, the design of plates could be accessed i.e. what should be the optimum width of the vertical plate that should be placed as an obstruction for the hydrokinetic energy converter. For purpose of comparative study the plates of width 2 cm, 3 cm, 4 cm and 5 cm were taken into consideration.

3.4 Experimental setup and method

The experimental arrangement, data acquisition system and variables measured in the model study are been described in this research. Typical investigation of flow fields for a hydrodynamic structure which consists of a vertical plate (in z axis) perpendicular to flow of water which is in x axis alongwith velocity measurement by ADV at the upstream of the plate has been carried out through various experiments. All the experiments were conducted in the Fluvial Hydraulics Laboratory of the School Water Resources Engineering in Jadavpur University, Kolkata. The experiments were carried out in a re-circulating flume 3.96 m long, 0.355 m wide, and 0.45 m deep including free board. The water depth of 20 cm was achieved in maximum to maintain the depth average velocity of 72.5 cm/s. The working section of the flume is made up of cast iron bed and Plexiglas side walls along two sides for most of its length to facilitate visual observations as seen from Figs. 3.1-3.2. The axis representation in Fig 3.1 depicts as x axis which is in line to the flow direction, y which is transverse to the flow direction and z axis which is vertical to the flow direction. The re-circulating flow system was served by two centrifugal pumps located at the upstream end of the flume whose technical details are: power capacity of the motors were 10 and 7.5 hp respectively having variable speed, here the water flows through two sets of 20 cm diameter pipe line which runs directly into the flume. The rotational speed of each of

the pump is 1430 rpm with a maximum discharge of 26 lps each, so that a total flow of 52 lps was achievable.

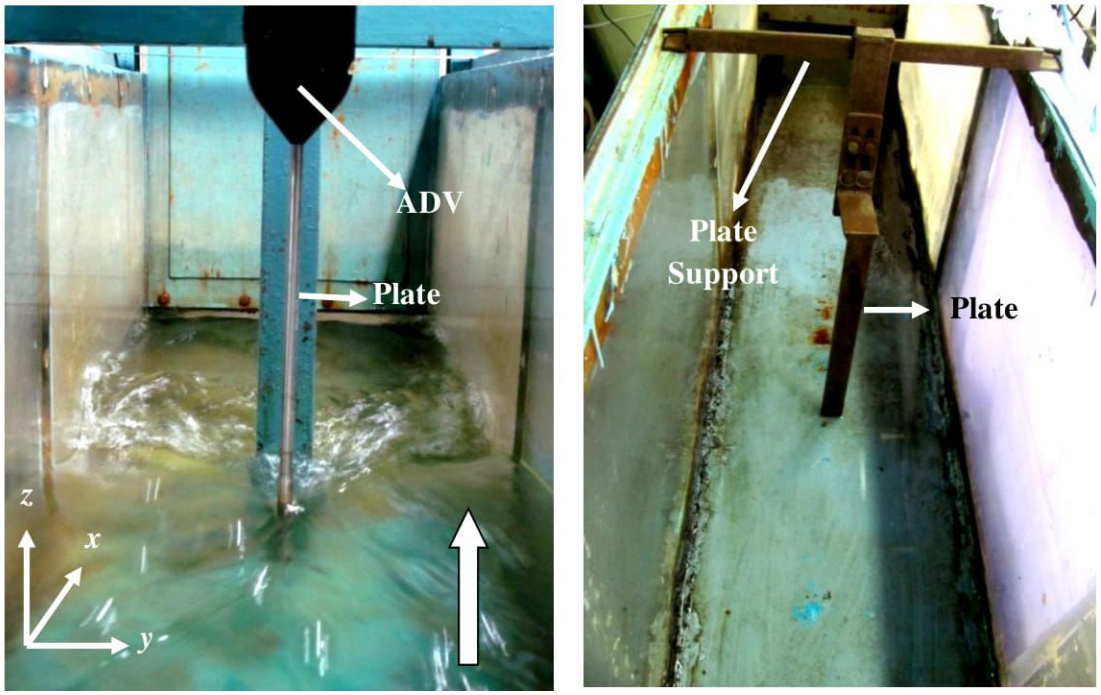

Fig. 3.1 Experimental arrangement and measuring instrument

Hence for the reigning setup of the flume the attainable depth average velocity is 72.5 cm/s. To measure the discharge, water flows through both magnetic and analog type flow meters.

Flat plates of widths 2, 3, 4 and 5 cm were used for the purpose of experiment. For each plate different set of ADV measurements were taken. The plates were hung from top to the bed of the flume with the help of special metallic supports in order to get it fixed in vertical position. The selection of the maximum width of 5 cm is based on the studies by **Kozakiewicz *et al.* (1992)** where for a gap (flume wall and vertical plate) to plate or pier width ratio upto 3 the proximity of the wall effect can be neglected.

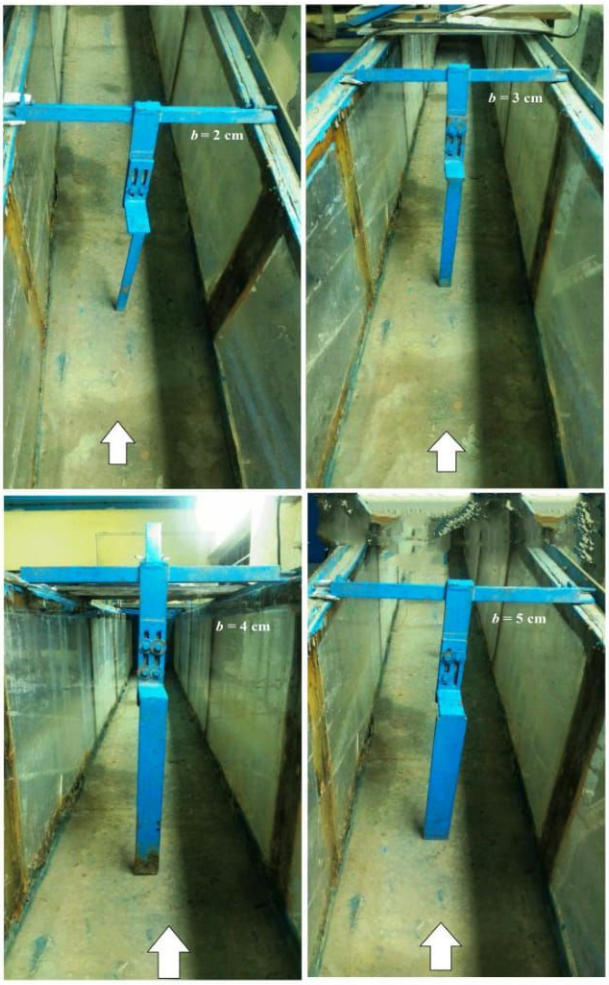

Fig. 3.2 Experimental arrangements of plates b = *2* cm, 3 cm, 4 cm and 5 cm

The instantaneous 3D velocity data were captured by a 5-cm four-receiver Nortek-make down looking probe Vectrino Plus. It follows acoustic Doppler principle. The Vectrino functions on Doppler effect for providing instant 3D velocity readings at 100 Hz sampling rate. An adjustable sampling volume of 0.6 cm diameter having 0.2–0.5 cm sampling height was set to measure velocities. Horizontally, the minimum resolution during the Vectrino measurement was 1 cm. The measurement by the ADV probe was not possible in the zone 4.5 mm above the bed surface, because the ADV requires a measuring volume of 0.09 cm^3 as depicted by Dey and Raikar (2007). The measurement by Vectrino probe was not possible below in the section 0.45 cm above flume bed. Output readings from Vectrino were converted software Vectrino+ version 1.18. During the Vectrino data filtering, the minimum SNR (signal-to-noise ratio) and minimum correlation limit were maintained at 16 or above and 70%, respectively. A sampling duration of one minute was considered ensuring a statistically time-independent averaged velocity. Near the range of the plate and flume bed, relatively long sampling durations (3 minutes) were taken since it was found that in that region correlation value was very low.

From Fig. 3.3 arrangement of the vertical plate and the points where the velocity is to be measured is detailed keeping h as the water depth. For the detailed measurement with the help of ADV, a grid system was prepared. Since in this experiment the main focus is on the horseshoe vortex phenomena so the main axis of consideration is x and z axis. The analysis of the measurements as taken by ADV has been shown in details in the result and discussions part of this chapter.

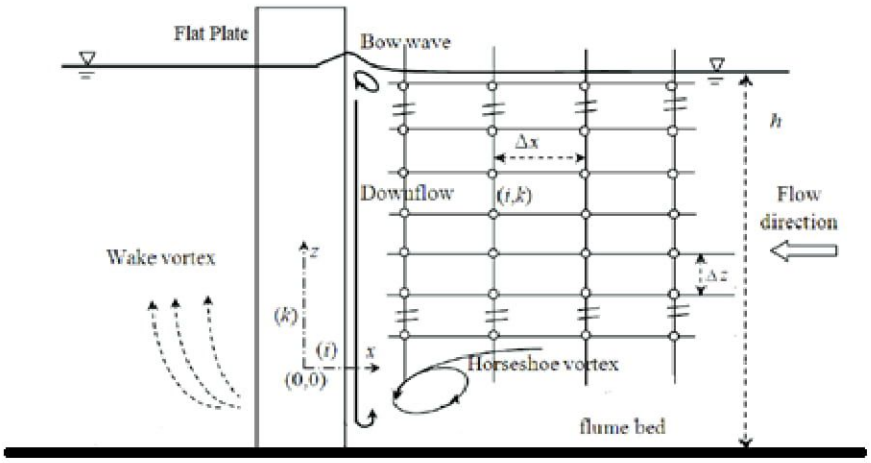

Fig. 3.3 Grid points formation for measuring the velocity to analyze the horseshoe vortex

3.5 Result and discussion

The experiment was separately carried out using four plates of width 2, 3, 4 and 5 cm respectively denoted by notation b. Notably for each experiment one plate was placed at 3.55 m away from the intake side of the flume in order to receive water at its end in addition to the baffle plates at the intake point. The depth average flow velocity was maintained as 72.5 cm/s To measure and plot contours for time-averaged flow velocity vectors, time-averaged longitudinal flow velocity (u), time-averaged flow transverse velocity (v), time-averaged flow vertical velocity (w) the instrument ADV and Origin Lab Software had been used. Here the axis considered as the vertical plate is supposed to be fixed at the origin and in respect to the plate, any coordinate in the upstream is considered negative and the downstream considered as positive accordingly. Each and every aspect of the flow velocities u, v and w are viewed from the x-z plane. Moreover concentration of the study mainly lies near the region of the boundary layer of the vertical plate. Since beyond this region the effect of the horseshoe vortex is supposed to be diminished. For justification the measurements at the upstream beyond the region of concentration is also taken. Same velocity profile was observed at the region at upstream beyond 12.5 cm for measurements taken with or without the plates. Due to the limitations of ADV, the measurements could not be taken less than 2.5 cm away upstream from the vertical plate.

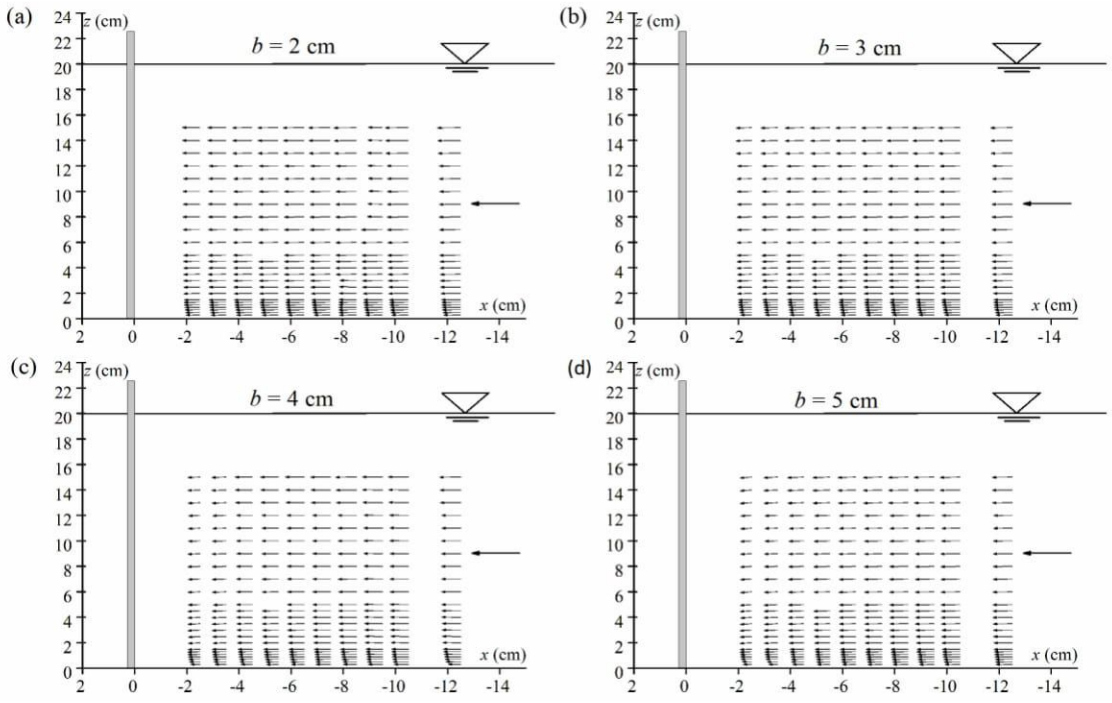

Fig. 3.4 Time averaged velocity vectors at the upstream of plates of different width

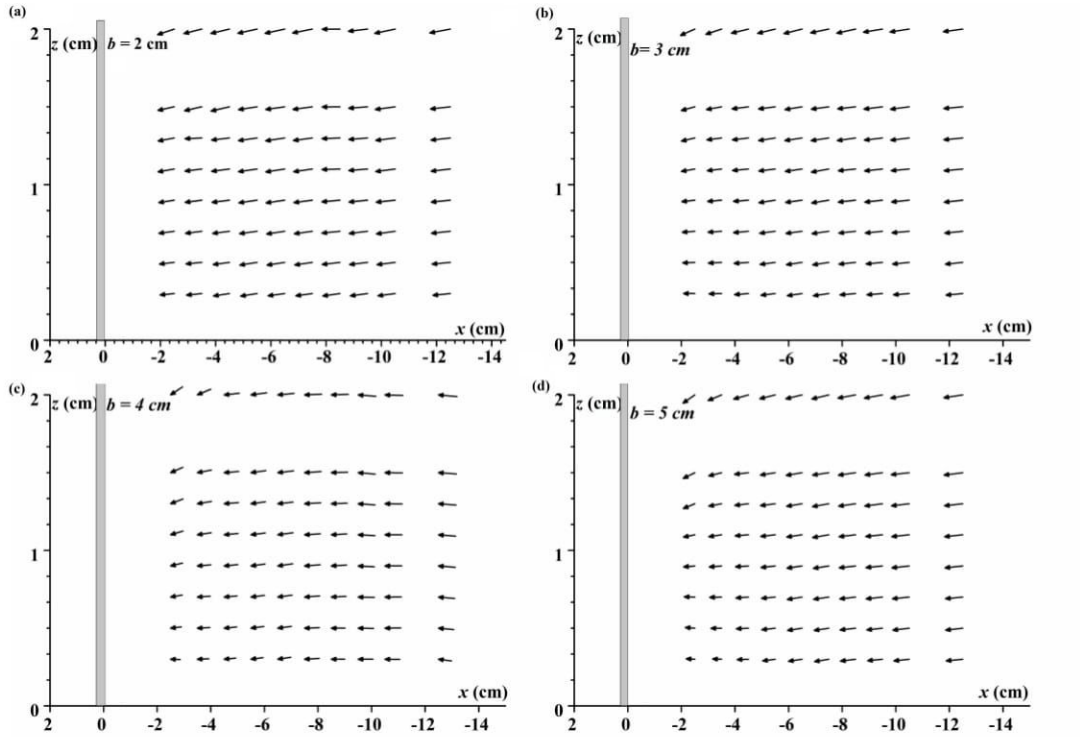

Fig. 3.5 Time averaged velocity vectors (near bed) at the upstream of plates of different width

Time averaged velocity vectors

The time-averaged velocity vectors (V), whose magnitude and direction are $\sqrt{u^2+w^2}$ and *arctan (w/u)* as visualized in Fig. 3.5, depicts that the flow directions are tends to move downward as it approaches towards the plate. The phenomenon of the water flow striking the obstructions and moving vertically downward towards the flume bed happens for each considered plates. Since the depth average velocity is very high of 72.5 cm/s as considered for the experiments. Hence forth a least effect of the horseshoe vortex can be visualized for all the considered plates. Since the approaching u will force the water that is flowing in reverse direction due to the horseshoe vortex from the plates laterally in the resultant direction of x and y. There is reduction of magnitude of the velocity vectors found near plate. The reason for justification the point is the effect of horseshoe vortex generated by the plates. The phenomenon is found upto water depth of 2 cm. Above 2 cm towards the upstream water level the changes in magnitude are very less this happens because the effect of horseshoe vortex is diminished in that region. The magnitude found in Fig. 3.4-3.5(a-d) depicts that with the increase of plate widths considered the magnitude of the velocity vectors decreases. Overall a trend of downflow of water been observed in the Figs. 3.4-3.5(a-d).

Velocity Contours

Three dimensional flow velocities were measured with the help of ADV. From Fig. 3.6 the contours of velocities u, v and w were found out. From Fig. 3.6(a) while viewing the contours of time-averaged longitudinal flow velocity (u), it can be said that how the change in the magnitude of width of the plate changes the magnitude of the u velocity. Fig. 3.6(a) depicts that longitudinal velocity near the plates increases with the decrease of plate width. The profile shows that the magnitude of maximum longitudinal velocities found near the plates are 63 and 58 cm/s for plate widths b = 2 cm and 3 cm respectively. Longitudinal velocity of magnitude 53 and 43 cm/s was observed for the plate widths b = 4 and 5 cm. The results clearly say that where the area of contact with the water flow is more there the longitudinal flow velocities are mostly affected. This happens since the flow approaches towards the stagnation point where the velocity is zero. When the width of the plate is more than other widths considered, maximum amount of the longitudinal flow strikes the surface of the plate and the flow tends to move downward. Hence as a result, much of the energy of the longitudinal flow is exhausted and the approaching flow velocities are reduced. Though the measurements are taken in flat bed flume where there is no sand or silt particles as flume bed but still the phenomenon of losing the energy due to varied width are visible. Only difference between the flume with sand bed and without sand bed is the magnitude of the approaching velocity which is obviously higher in the case of bed without sand. The longitudinal velocity is found mostly affected from Fig. 3.6(a) near the boundary layer region of the flume bed and the vertical plate. The velocities farther from the boundary layer of the flume bed and the plate also may be called as turbulent outer layer are

found less affected since the velocities found to be nearer to the depth average velocity i.e. 72.5 cm/s. of large eddies. This happens because the effect of horseshoe vortex generated due to the plate are been broken up by the approaching flow of the flume which produce strong mixing of flow. This layer possesses approximately 80 to 90 % of the flow region. Interesting thing to note is also that maximum longitudinal velocity was found to be 88, 81, 78 and 75 cm/s respectively for the plate widths 2, 3, 4 and 5 cm respectively at a distance 12.5 cm away from the plate in the upstream at the turbulent outer layer. This also suggests that the stretch of effect of the horseshoe vortex generated due to the plates also depends on the width of the hydrodynamic structures. More the width considered further shall be the extent of the horseshoe vortex. Both transversal and vertical velocities found to be much less in compared to the longitudinal velocities since the concentration lies in the horseshoe vortex of the vertical plate. Still due to the horseshoe vortex there is some movement found in the streamlines in y and z directions and are justified with the magnitude of transverse and vertical flow velocities i.e. v and w velocities. The positive magnitudes of velocities from Fig 3.6(b-c) for all the plate widths are viewed near the flume bed and turbulent inner layer and the negative values are found in the turbulent outer layer. The lateral movement as seen from Fig. 3.6(b) is almost same for each of the plates considered due to the fact that lateral movement in the high turbulent flow is always depending upon its longitudinal flow velocity. This distinction happens since the horseshoe vortex which is elliptical in shape diverts the longitudinal flow to transverse or vertical flow so in turbulent layer where the horseshoe vortex is dominant there the transverse or vertical flow velocities also exists.

At the turbulent outer layer where the horseshoe vortex is very low there the longitudinal velocities are predominant and whatever the magnitude of the transverse and vertical velocity exists there is due to the flow diversion due to the vertical plate obstruction and the downflow of water due to the vertical plate respectively. The positive value of w depicts that the water is directed upward and it is seen upto water depth of 2 cm near the plate and flume bed as seen from Fig. 3.6(c). Positive w = 0.5, 1 and 1.1 cm/s were found for b = 3, 4 and 5 cm respectively. Positive w as seen for plate width b = 2 cm was very close to zero. The results depicts again that the prevalence of the longitudinal flow velocity is very much dependent on the plate width b. Rest of the region which is also termed as turbulent outer layer there w is found to be negative that depicts a trend of downflow of water due to the vertical plate. Negative w as seen from Fig. 3.6(c) were found maximum as -3, - 3.5, -5 and -5.6 cm/s for b = 2, 3, 4 and 5 cm respectively. The velocity of downflow of water also depends upon the contact area of the obstruction. Hence the negative w is increased with the increase of the considered plate widths.

Finally it can be said that when the longitudinal flow approaches the plate and a stagnation pressure decreasing with water depth establishes itself. It produces a (weak) pressure gradient along the front of the plates and induces a downward flow from high to low velocities. Since there is also a (strong) pressure gradient around the plate, the downstream flow will be laterally diverted.

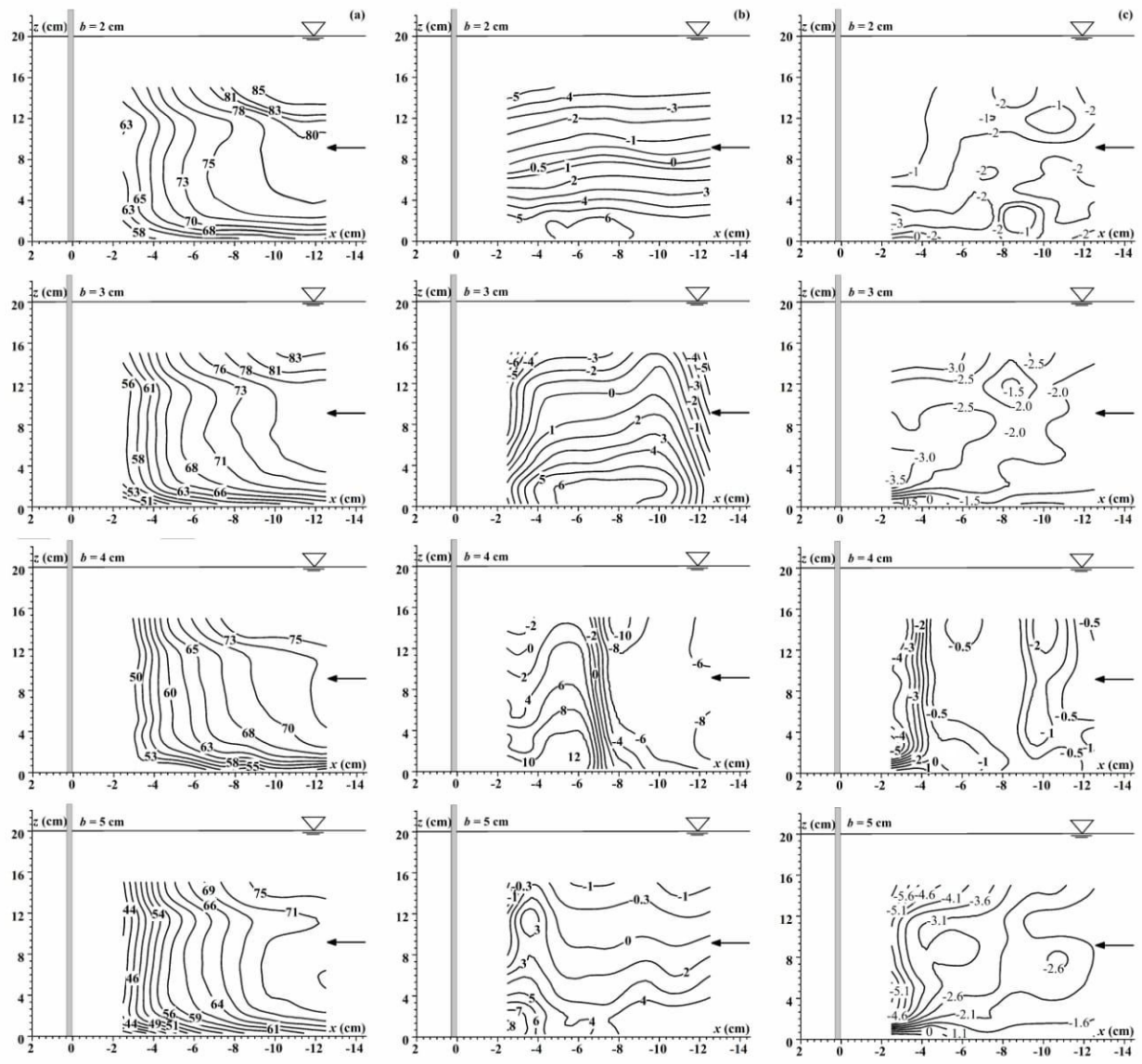

Fig: 3.6 Velocity contours (in cm/s) at the upstream of the plate: (a) longitudinal; (b) transversal and (c) vertical flow velocity

Turbulence Intensities

From Fig. 3.7 the contours of turbulence intensities at the upstream of the plates are represented. The turbulence intensities for longitudinal, transversal and vertical flow velocities are formulated respectively as: $u^+ = \sqrt{\overline{u'u'}}$, $v^+ = \sqrt{\overline{v'v'}}$ and $w^+ = \sqrt{\overline{w'w'}}$, respectively where u' , v' and w' are the fluctuations of u, v and w, respectively. Fig 3.7(a-c) reveals that the distribution the turbulence intensities u^+, v^+ and w^+ are almost similar except some deviation is seen for turbulence intensities for longitudinal flow and vertical flow velocity for the experiments carried out for the plate width of 2 cm.

Since for the plate width of 2 cm, the area exposed to the longitudinal flow is very low in respect to the other plate widths considered. There the fluctuations are found for the longitudinal velocities since the turbulence due to the approaching longitudinal

velocity becomes dominant in respect to the horseshoe vortex generated from the plate of width 2 cm at a distance of 10.5 to 12.5 cm upstream of the plate. At any particular coordinate, the magnitudes of the turbulence intensities of longitudinal velocity are less for the widths 3, 4 and 5 cm is less in compared to the width of 2 cm is only due to the prevalence of the horseshoe vortex as shown in Fig. 3.7(a). The u^+ was found maximum in the range of 3 to 8 cm at the upstream of the plate for plate widths b = 3, 4 and 5 cm respectively. From Fig. 3.7(a-c) the turbulence intensities of three types of flow velocities are more at the turbulent inner layer i.e. near the plate and the flume bed in respect to the turbulent outer layer due to prevalence of the horseshoe vortex for all the widths considered.

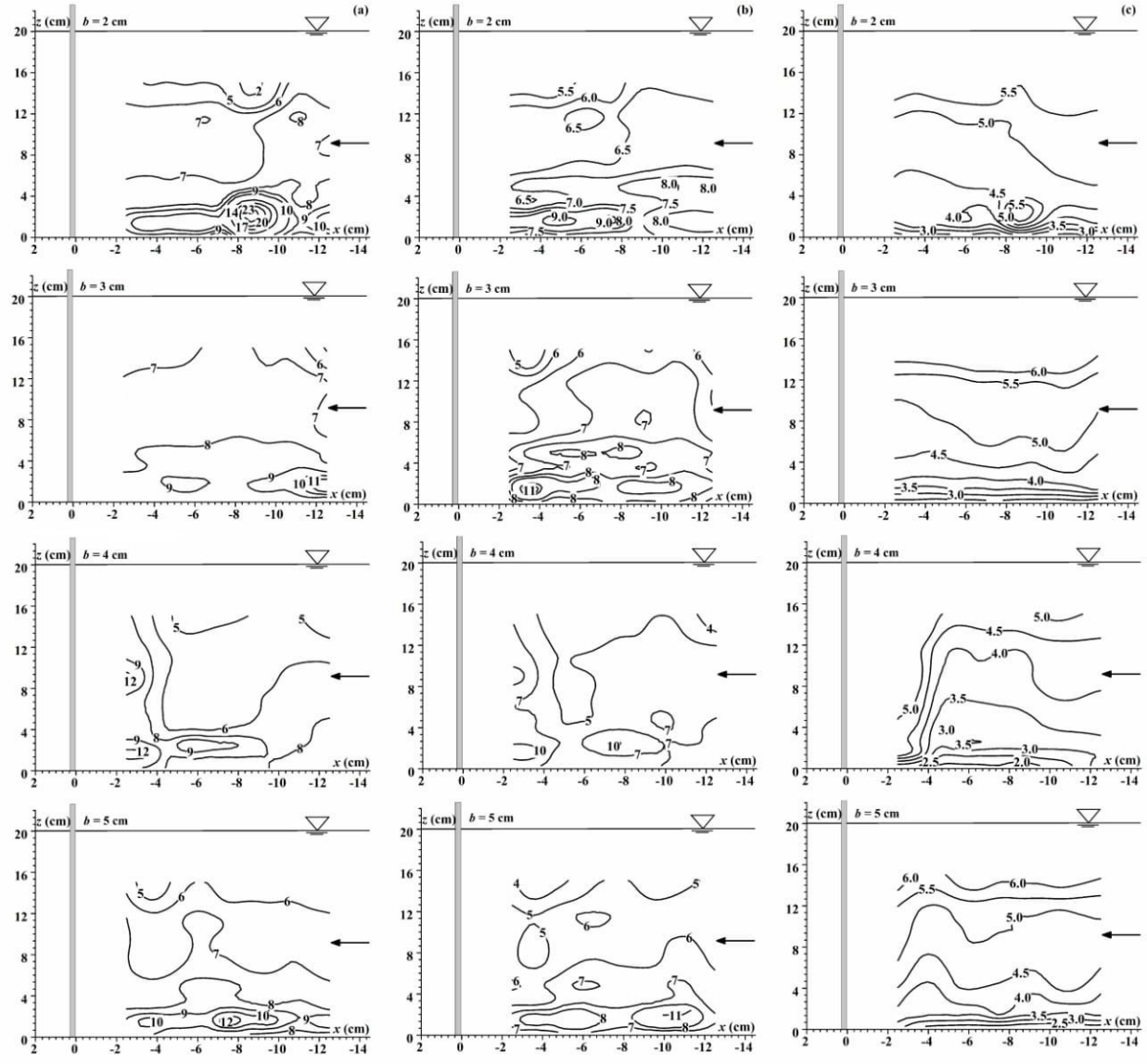

Fig. 3.7 Contours for turbulence intensities (in cm/s) at the upstream of the vertical plate for: (a) longitudinal (u^+); (b) transversal (v^+) and (c) vertical flow velocity (w^+)

Higher core of turbulent intensity for transverse velocity is found basically at the upstream of the vertical plate where the water heading towards the plate is forced to diverge where the water tries to move towards the wall of the flume after hitting the obstruction. The higher core of turbulence intensity of the vertical flow velocity is supposed to be near the stagnation point at the upstream surface of the vertical plate where the water tends move downward after colliding with the obstruction and the same water will flow in the longitudinal direction. The core of w^+ is also supposed to be higher near the surface of the vertical plate where the water after striking the vertical plate moves downward.

Turbulent shear stresses

Fig. 3.8 depicts know how about the turbulent shear stresses as $\tau_{vu} = -\rho\overline{v'u'}$, $\tau_{vw} = -\rho\overline{v'w'}$ and $\tau_{wu} = -\rho\overline{w'u'}$ where ρ = density of water in any plane. Notably the experimental setup is mainly visualized from the negative sign indicates that since the stresses act opposite to the flow velocities among *u, v* and *w* when the particular stresses are been considered. The concentrations while discussing the turbulent shear stress just lays in the region the boundary layer of the flume bed and the vertical plate. Visuals from Fig. 3.8(a) derive the activities of the water flow in *x-y* plane where it is observed that turbulent shear stress τ_{vu} is having magnitudes negative values for all the considered plates. The values of the turbulent shear stress in *x-y* plane are nearly same for the plates considered. Negative values suggest the dominance of approaching *u* and are seen just at the upstream of the plate where the flow starts to divert due to the obstruction. But since the approaching longitudinal velocity is very high so it overcomes the stresses offered by the plate. Notably the negative value tends to positive value that is the flow resistance offered by the plates is seen in increasing order with the increase of the plate width.

From Fig. 3.8(b) turbulent shear stress τ_{vw} are observed having both positive and negative values in respect to *y-z* plane. The negative values of τ_{vw} are seen all over the region above 2 cm water depth. This justifies the following concept that the water after striking the obstruction just moves downward and here in two instances the water is striking the obstruction. According to the width of the plate the magnitude of positive values of τ_{vw} depends. The positive magnitude suggests the water flow in the upward direction due to the existence of the horseshoe vortex. It is seen that near flume bed and the upstream of vertical plate except for b = 2 cm rest of the plates are having very low positive magnitude. For plate b = 2 cm the magnitude just able to achieve the zero line while approaching towards the positive value. Hence visuals from *y-z* plane shows that vey less effect of obstruction is given the plate b = 2 cm in respect to the other considered plates. Fig. 3.8(c) describes about the turbulent shear stress τ_{wu} in the *x-z* plane. Here since the measuring was mainly done by traversing the ADV in *x-z* plane hence the picture of the horseshoe vortex might be clearer. Where negative value of τ_{vw} suggests the dominance of the approaching longitudinal velocity (*u*) and positive value predicts the dominance of the horseshoe vortex and shown that the reverse flow of water after striking the plate. The results from Fig. 3.8(c) also say that more the area of contact to the flow of

water more is the turbulent shear stress in the opposite direction to the approaching flow. For plate width b = 5 cm the shear stress in x-z plane is 1.52, 2.36, 4.33 times greater than the plate widths b = 4, 3 and 2 cm respectively. In support to the explanation and observation, as the plate widths are increased the positive values of stresses in the x-z plane are also increased. In the other hand at the turbulent outer region the negative values decreases with the increase of the plate widths. This says that with the increase in area of the contact to the water the downflow of the water also increases.

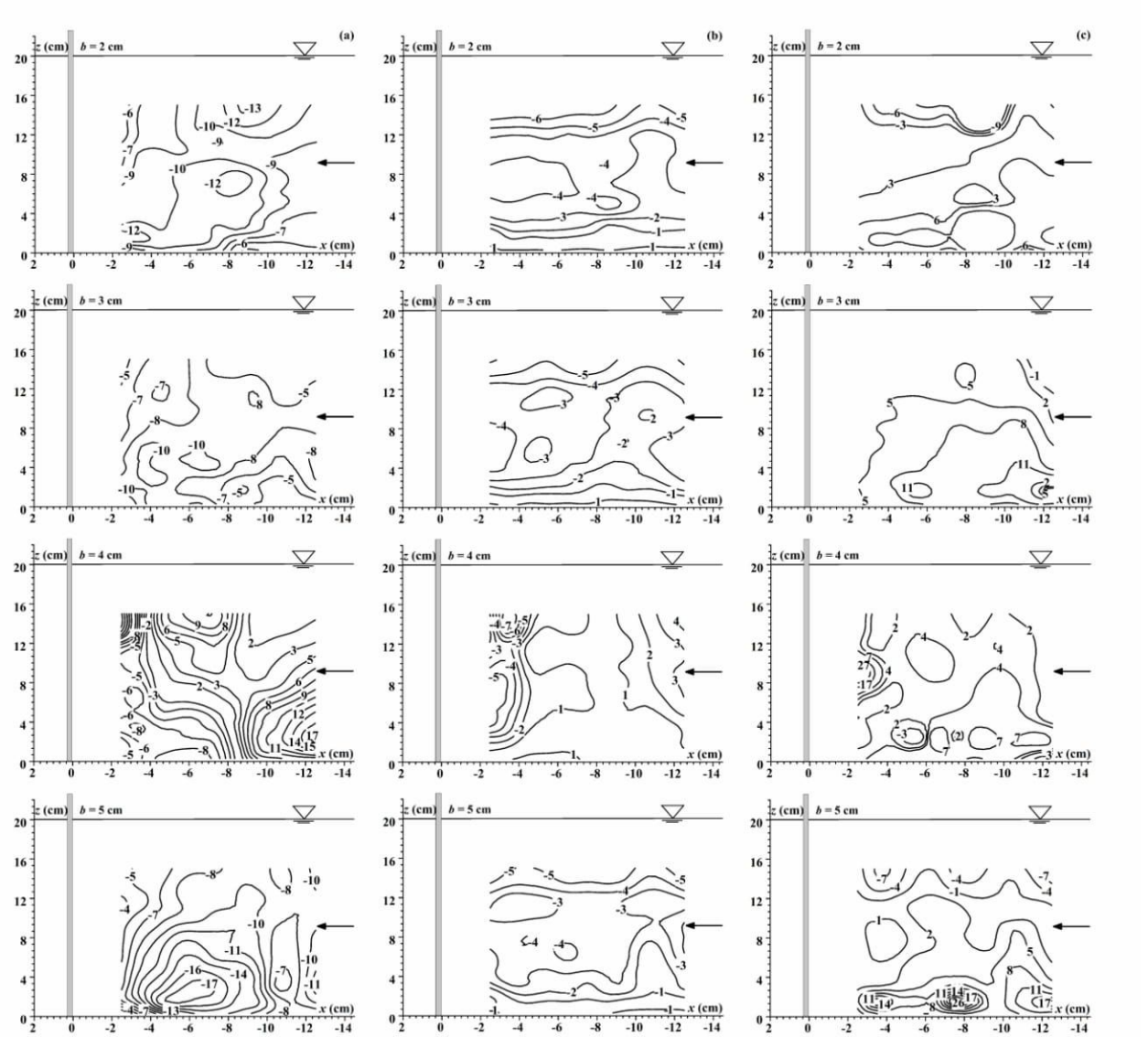

Fig. 3.8 Contours for turbulent shear stresses (in cm^2/s^2) at the upstream of the vertical plate for: (a) $-\overline{v'u'} = \tau_{vu}/\rho$; (b) $-\overline{v'w'} = \tau_{vw}/\rho$ and (c) $-\overline{w'u'} = \tau_{wu}/\rho$

Vorticity and Circulation

Fig. 3.9(a-d) shows the vorticity, more formally, that can be related to the amount of "circulation" or "rotation" (or the local angular rate of rotation) in water. The average vorticity (ζ) in a small region of fluid flow is equal to the circulation (Γ) around the boundary of the small region, divided by the area (A) of the small region as shown in equation (3.1) as :

$$\zeta = \frac{\partial u}{\partial z} - \frac{\partial w}{\partial x} = \frac{\Gamma}{A} \tag{3.1}$$

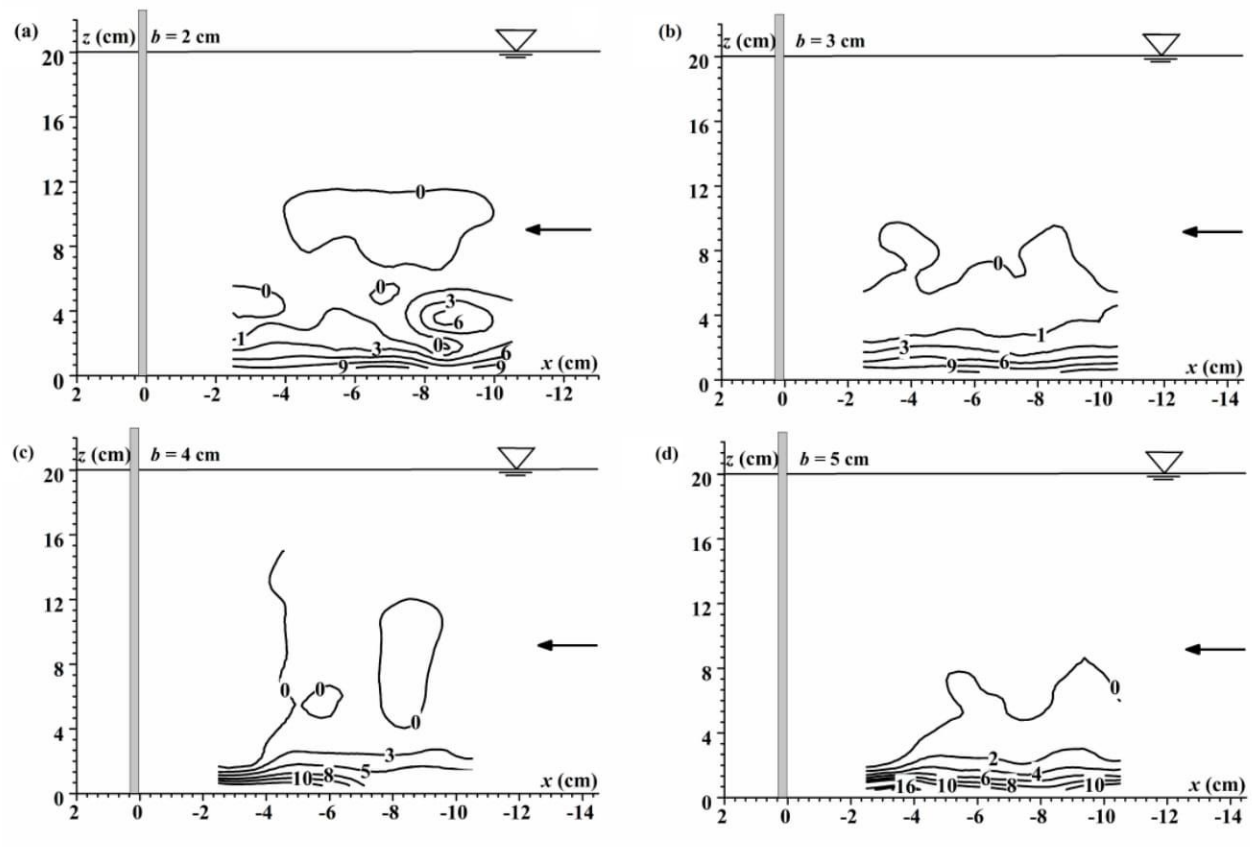

Fig: 3.9 Contours of vorticity (in s^{-1}) for the plate width b equal to (a) 2 cm, (b) 3 cm, (c) 4 cm, (d) 5cm.

Notionally, the vorticity at a point in a fluid is the limit as the area of the small region of fluid approaches zero at the point referring the equation (3.2):

$$\zeta = \frac{\Gamma}{A} \tag{3.2}$$

The left hand convention that is positive in anticlockwise direction is adopted to define the vorticity. As per the data observed the partial difference equation (PDE) $\left(\frac{\partial u}{\partial z} - \frac{\partial w}{\partial x}\right)$

is been converted to Finite difference equation (FDE) by the help of first order backward difference technique in the form:

$$\zeta = \frac{u_{i,k} - u_{i,k-1}}{\Delta z} - \frac{w_{i,k} - w_{i-1,k}}{\Delta x} + O(\Delta z, \Delta x) \tag{3.3}$$

In equation (3.3) the index i runs in x direction and index k runs in z direction. The limiting behaviour of the truncation error (T.E.) is characterized by using the order of (O) notation. $O(\Delta z, \Delta x)$ has a precise mathematical meaning and it is called "terms of order Δz and Δx". The T.E. part was neglected during the calculation. From Fig. 3.9(a-d) the concentration of the vortex cores for all the plate widths considered lie near the plates and the flume bed termed as the turbulent inner layer. The magnitude of vorticity also reveals that with the increase of the plate width from 2 to 5 cm the core of vorticity near the plate and flume bed is also concentrated. The higher magnitude of the vorticity also signifies the vortex core. The reason behind it is again the prevalence of the boundary layer due the surfaces of flume bed and the vertical alongwith the horseshoe vortex generated from the vertical plate. The circulation of the horseshoe vortex from the vorticity contours as seen from Fig. 3.9(a-d) are derived by using Stokes theorem as:

$\Gamma = \oint \vec{V} \vec{ds} = \iint_A \zeta \, dA$ where, $\vec{V}$ is the velocity vector, $\vec{ds}$ is the differential displacement vector over a closed curve, A is the area enclosed by successive vorticity contours. The total circulation or the vortex strength at the upstream of the different plates of width b is reflected in Table 3.1.

Table 3.1 Circulations for different plate width (b)

Circulation (m^2/s)			
***b* = 2 cm**	***b* = 3 cm**	***b* = 4 cm**	***b* = 5 cm**
1.19×10^{-2}	1.55×10^{-2}	1.94×10^{-2}	2.05×10^{-2}

The circulations were estimated for different plates near the boundary layer of the plate and flume bed. The magnitude of circulation was estimated to be highest for plate width b = 5 cm. This depicts the prevalence of the horseshoe vortex. The reason is justified from the earlier discussions that more the area of contact to the water flow more will the prevalence of the horseshoe vortex generated. The vortex strength is found to be increased with the increase in the width of the vertical plate.

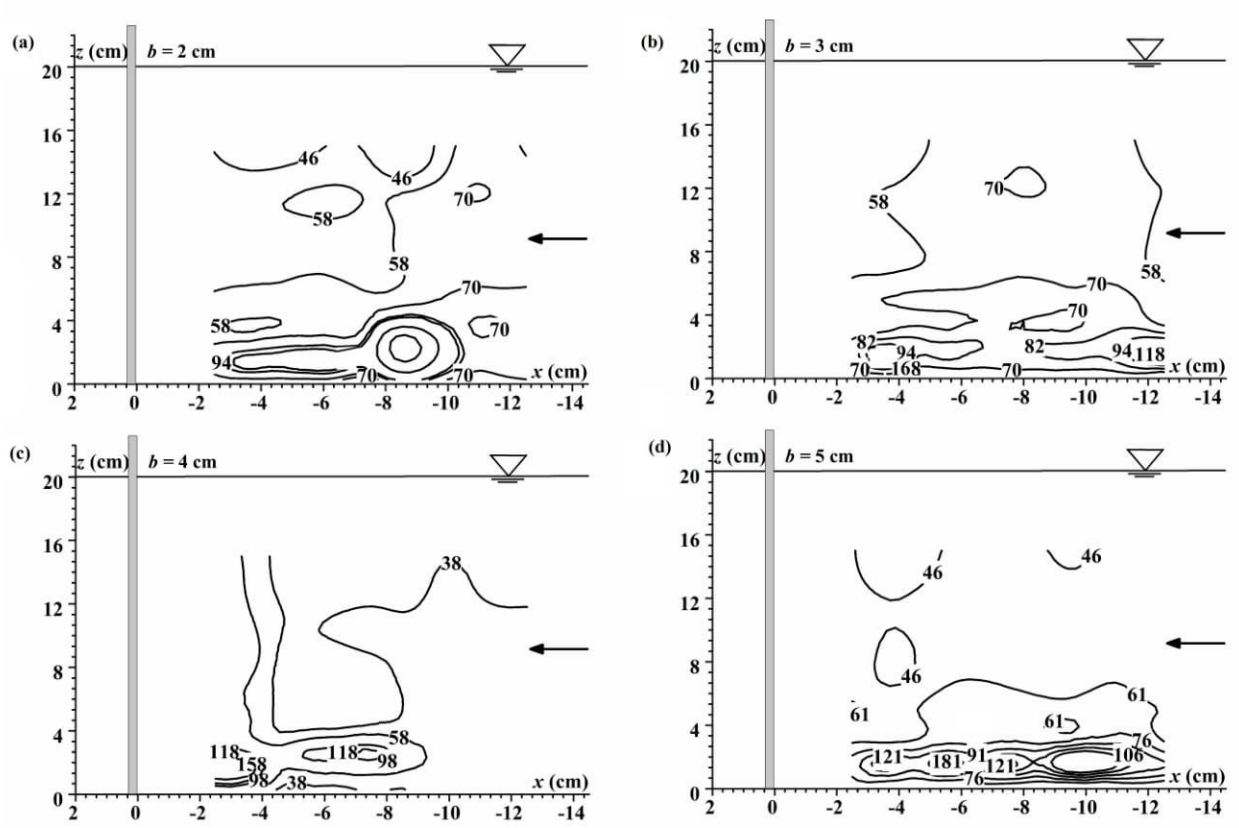

Fig: 3.10 Contours of turbulent kinetic energy (in cm/s) for flow fields arousing from the plate width *b*: (a) 2 cm, (b) 3 cm, (c) 4 cm, (d) 5cm.

Turbulence Fields

The turbulence intensities are the root-mean-square (RMS) values of the velocity fluctuations. The contours of the turbulent kinetic energy $\left[k = 0.5\left(u^{+2} + v^{+2} + w^{+2}\right)\right]$ as shown in Fig. 3.10 to illustrate the distributions of k for the turbulence intensities of longitudinal, transverse and vertical velocities for all sizes of the plate width considered. For plate width b = 2 cm, a core of higher turbulent kinetic energy is found in the region of turbulent outer layer beyond the distance of 8.5 cm upstream of the plate. Interestingly the magnitude of the turbulent kinetic energy is much higher than the other bigger sized plates, this says that due to small area of contact to the water flow the prevalence of the horseshoe vortex is not happened. The turbulence occurring from the source point is the main reason of the increase of core of higher turbulent energy. But for the other sized plates a core of higher turbulent kinetic energy is seen at the upstream of the vertical plate depicts dominance of the horseshoe vortex. As the width is changed from 3 to 5 cm the kinetic energy is also observed to be increased. The highest core of kinetic energy as generated by the horseshoe vortex from the plates starts from the distance of 3, 4, 5 and 5.5 cm upstream of the vertical plate width b = 2, 3, 4 and 5 cm respectively, as shown in Fig. 3.10(b-d). It is also observed that maximum values of kinetic energy for all the considered plates extend upto atleast 5.5 cm.

3.6 Conclusions

The main aspect to get from this chapter is to know the flow phenomena at the upstream of different types of plate widths 2, 3, 4 and 5 cm as considered here. Since the work undertaken here is based on the modification of the electrical energy generator that basically runs on the principle of vortex induced vibration. A vertical plate placed at the downstream of a horizontal cylinder in a water channel has been considered as the modification. Hence the selection of the vertical plate in the process of the modification becomes an important factor. From this chapter flow phenomena for different plates from various views of time averaged velocity vectors, velocity contours, turbulence intensities, turbulent shear stresses, vorticity and turbulent kinetic energy are found out. Major concern for this work also lies with the turbulence coming from the source point to maintain a velocity of 72.5 cm/s in the flume. Hence for plate width b = 2 cm, the horseshoe vortex strength is very less in compared to the turbulence at the source point. The horseshoe vortex phenomena basically come into existence from plate width of 3, 4 and 5 cm. The major outcomes from this chapter can be summarized as:

1. From the contours of velocity vectors for different plate widths there is downflow of water been observed near to the plates which can be said as starting of the horseshoe vortex.
2. Longitudinal flow velocity as it approaches towards the plate decreases with the increase in the plate widths. This happens due to the flow approaching towards the stagnation point at the obstruction plate. The magnitudes of the transverse and vertical flow velocity increases for each plate due to the effect of the horseshoe vortex and the flow striking obstruction plate.
3. Viewing the results from the contours of the turbulent intensities and shear stress it is clear except the plate width b = 2 cm, the effect horseshoe vortex generated from the plates are dominant.
4. The results of vorticity and turbulent kinetic energy depict that the core of the concentration of vorticity or turbulent kinetic energy mainly lies near the plate and the flume bed. The results of the vorticity and circulation say that horseshoe is generated from each of the plates. But the difference lies in the strength. The magnitude for both the aspects **are highest for plate width b = 5 cm.**

From the summary of the points coming out of the study depicts that plate width b = 2 cm or less value in this type of flow condition may not have much vortex strength to lift the cylinder. So for selection of plates for the modification of the hydrokinetic energy generator which works on the principle of vortex induced vibration the outcomes of this chapter will be very useful.

Nomenclatures

b	=	Plate width [L];
h	=	Water depth [L]
u	=	Longitudinal flow velocity [LT^{-1}];
v	=	Transverse flow velocity [LT^{-1}];
w	=	Vertical flow velocity [LT^{-1}];
x, y, z	=	Coordinate axes [L];
i, j, k	=	Direction indices along x, y and z directions, respectively [—];
V	=	Time averaged velocity vectors [LT^{-1}];
ζ	=	Vorticity [T^{-1}];
$\vec{V}$	=	Velocity vector [LT^{-1}];
A	=	Area enclosed by successive vorticity contours [L^2];
$\overrightarrow{ds}$	=	Differential displacement vector over a closed curve [L];
Γ	=	Circulation [L^2T^{-1}];
$\Delta x, \Delta y, \Delta z$	=	Spacing of grid points in x, y and z directions, respectively [L];
$\tau_{uv}, \tau_{vw}, \tau_{wu}$	=	Turbulent shear stresses [$ML^{-1}T^{-2}$]

References

Baker G.R. (1979). The "cloud in cell" technique applied to the roll up of vortex sheets. *Journal of Computational Physics*, 31, 76-95.

Das S. and Mazumdar A. (2015). Comparison of Field of Horseshoe Vortex at a Flat Plate and Different Shaped Piers. *International Journal of Fluid Mechanics Research*, 42(5), 418-448.

Das S., Das R. and Mazumdar A. (2013). Circulation Characteristics of Horseshoe Vortex in Scour Region around Circular Piers. *Water Science and Engineering*, 6(1), 59–77.

Das S., Ghosh S. and Mazumdar A. (2014). Field of Horseshoe Vortex in a Scour Hole around Two Eccentric Triangular Piers. *International Journal of Fluid Mechanics Research*, 41(4), 296-317.

Dey S. (2014). Fluvial Hydrodynamics. *GeoPlanet: Earth and Planetary sciences, Springer*, 592-594.

Dey S. and Raikar R.V. (2007). Characteristics of Horseshoe Vortex in Developing Scour Holes at Piers. *Journal of Hydraulic Engineering*, 133(4), 399-413.

Farahani R.J. and Dalrymple R.A. (2014). Three-dimensional reversed horseshoe vortex structures under broken solitary waves. *Coastal Engineering*, 91, 261–279.

Kozakiewicz A., Sumer B.M. and Fredsoe J. (1992). Spanwise correlation on a vibrating cylinder near a wall in oscillatory flows. *Journal of Fluids and Structures,* 6, 371-392.

Lin C., Chiu P. and Shieh S. (2002). Characteristics of horseshoe vortex system near a vertical plate–base plate juncture. *Experimental Thermal and Fluid Science*, 27, 25-46.

Melville B.W. and Coleman S.E. (2000). *Bridge Scour*. Colorado, USA: Water Resources Publications, LLC.

Muzzammil M. and Gangadhariah T. (2003). The mean characteristics of horseshoe vortex at a cylindrical pier. *Journal of Hydraulic Research*, 41(3), 285-297.

Raikar R.V. and Dey S. (2008). Kinematics of Horseshoe Vortex Development in an Evolving Scour Hole at a Square Cylinder. *Journal of Hydraulic Research*, 46(2), 247-264.

Sahin B., Akilli H., Karakus C., Akar M.A. and Ozkul E. (2010). Qualitative and quantitative measurements of horseshoe vortex formation in the junction of horizontal and vertical plates. *Measurement*, 43, 245-254.

Sahin B., Ozturk N.A. and Akilli H. (2007). Horseshoe vortex system in the vicinity of the vertical cylinder mounted on a flat plate. *Flow Measurement and Instrumentation*, 18, 57-68.

Zhihua L., Ying X. and Chengxu T. (2011). Numerical simulation and control of horseshoe vortex around an appendage–body junction. *Journal of Fluids and Structures*. 27, 23–42.

Zhi-hua L. and Ying X. (2014). The method to control the submarine horseshoe vortex by breaking the vortex core. *Journal of Hydrodynamics*, 26(4), 637-645.

4.1 Introduction

This chapter is a presentation of complex flow phenomena in between the flow past a horizontally placed cylinder and a vertical plate placed at its downstream. Curiosity in research for the investigation of flow fields around the underwater laid cylinders has enhanced due to the rapid increase in submerged pipes or cables. Since in natural water channels containing erodible silts, there is high chance of scouring underneath such cylindrical structures due to the development of horseshoe vortex along with transport of sediments. Moreover in this thesis major emphasis had been given to a new type of power generation technique utilizing vortex induced vibration. In previous chapter several experimental investigations were done in order to understand the flow phenomena at the upstream of a vertically mounted plate. Interestingly it was found that the horseshoe vortex that is aroused from the vertically mounted plates aids to lift a freely moving horizontally laid cylinder of a hydrokinetic energy generator that works on the principle of vortex induced vibration. To understand the effect of the horseshoe vortex the experiments were carried out taking into consideration about the complex flow that had occurred in between the horizontally placed cylinder fixed at different water depth with varied width of vertically mounted plates. Experimental setup that had been established in the work at varied instances consists of a cylinder of 5 cm diameter which is placed 5.5 cm horizontally away from the vertical plates having 2, 3, 4 and 5 cm width. In such water flow, turbulence condition is obvious and the vortex formation is also in expectation as depicted in earlier researches. Acoustic Doppler Velocimeter (ADV) had been used to determine the velocity and its direction while vortices were being created around the cylinder and in its wake, and also to record the velocity and observe its characteristics in the boundary layer. With the determination of flow fields of the underwater composite hydrodynamic structures various other environmental issues come into play. These types of under-laying structures not only helps in dispersion of sediment decomposition in the river bed but also in this juncture help to get a free passage and movement area for aquatic fauna for a shallow type of water channel. Seeing so many advantages of this type of study could really boost to maintain aquatic ecological balance in addition to the territorial environment and socio-economic development.

Key words: *flow fields; hydrokinetic energy generator; vortex induced vibration; submerged cylinder.*

4.2 Review of earlier works

Investigation of flow fields around the underwater laid pipes are attaining curiosity in juncture to rapid increase in submerged pipes or cables. Such cylindrical cross-sectional structures faces wave-current climate of complex nature. The flow fields occurring due to the development of turbulence has been studied in the thesis of Lin (1944). Natural water channels containing erodible silts where there is high chance of scouring underneath such cylindrical structures due to the development of horseshoe vortex as discussed by Dey and Raikar (2007) along with transport of sediments due to

equilibrium scour were depicted in the researches earlier by Das *et al.* (2014, 2016). The phenomena of scour had proved to leave a cylindrical structure uncorroborated over a substantial distance resulting in fatigue failure due to flow-induced oscillation by wake-vortex shedding such types of works had been proven numerically by Eldho and Young (2001) and Roulund *et al.* (2005) and experimentally by Das and Mazumdar (2017); Jaman *et al.* (2017) and Das *et al.* (2017) occurring at the base of the vertically mounted piers that are also related with the movements of sediments of the river beds from one locations to other locations in the exposure of the works of Ettema *et al.* (2006) and Das *et al.* (2014, 2015).

Additionally problem of vortex-induced vibration of structures is important in various fields of engineering, as it is also a cause for concern in the dynamics of riser tubes bringing oil from the seabed to the surface, in flow around heat exchanger tubes, in the dynamics of civil engineering structures such as bridges and chimneys, and also in many other situations of practical importance. Graf and Istiarto (2002) experimentally investigated the three-dimensional flow field in an established (equilibrium) scour hole. An acoustic-Doppler velocity profiler (ADVP) was used to measure instantaneously the three components of the velocities in the vertical symmetry (stagnation) plane of the flow before and after the cylinder. The velocities, turbulence intensities, Reynolds stresses, bed-shear stresses and vorticity of the flow field was calculated in different azimuthal planes within the equilibrium scour hole at a circular pier. Results of the study showed that a vortex-system was established in the front and a trailing wake-vortex system of strong turbulence was formed in the rear of the cylinder.

Therefore, one of the imperative aspects of pipeline design is the prediction of the extent of scour below pipelines. Thus the evaluation of forces on cylinders some distance away from the bottom becomes of interest. Last 15 years, acoustic Doppler velocimeters (ADV) have become popular in the field of fluid dynamics. They are applied to study the three-dimensional flow field and turbulence in laboratory applications, as well as in rivers, lakes and the ocean. ADVs typically consist of one emitter surrounded by a number of receivers, each of them measuring one projection of the velocity vector. The reduction of noise of ADV in turbulence measurements in order to get accurate results was explained in the works of Blanckaert and Lemmin (2010).

In this research stresses were given upon the features of ADV as measurement process that are beneficially applicable for the study of flow fields and also determining and discussing velocity profiles occurring due to flow around a horizontally placed submerged cylinder, that is placed before another obstruction, i.e. a vertical plate. The references of the analysis of the shear flow is been understood from the observation of Dey *et al.* (2011). If a cylinder is set in an open channel, the flow upstream will undergo a separation of the turbulent boundary layer and rolls up to form the well-known horseshoe-vortex system is swept around the cylinder. This type of flow occurs in a variety of situations, such as flow around bridge piers, around buildings and structures (stacks, cooling towers, gas tanks), and at different types of junctions.

In the condition of the constant Strouhal number, when the vortex shedding frequency for a stationary cylinder approaches the natural frequency of oscillation of the cylinder from below, the cylinder will start oscillating and vortex shedding will start to correlate along the cylinder axis (Raghavan and Bernitsas, 2009; Chang *et al.* 2010). This leads to a large increase in the lift forces acting on the cylinder. By increasing the flow velocity further, the vortex shedding frequency will finally jump back to the linear curve defined by the Strouhal number. The changes taking place in the vortex shedding frequency in the synchronization ranges. In this range, vortex shedding frequency and the oscillation frequency, collapse into the natural frequency of the system in flow. It is interesting to note here that sustained oscillations extend over a range of velocity values rather it can be talked about the range of Reynolds Number and the vortex shedding is controlled by the vibrating cylinder like types of research carried out by Bernitsas *et al.* (2009) and Raghavan *et al.* (2009). Today the scenario of the natural channels in the world especially in India is very critical since the water depths of such channels are decreasing day by day due to immense sediment loading. Utilizing these types of devices shows that the discharges natural streams and channels have decreased with the water depth. So, the assessment of sediment loading becomes much important while viewing the environmental aspects in the natural water channels.

Inspired from the earlier works, in this research a horizontally submerged cylinder had been considered against four types of flat plates whose widths are 2 cm, 3 cm, 4 cm and 5 cm kept vertically at its downstream. The flow fields arousing from these structures were represented in the form of velocity and turbulence profiles. These profiles will show how the horseshoe vortex appearing at the upstream of the vertical plate affect the horizontally laid cylinder kept at various water depth.

4.3 Need for the analysis of complex flow

Main motive of the work has been to modify the electrical energy generator that works on the principle of vortex induced vibration. Since from the earlier it was known that on the utilization of vertical plate at the downstream of horizontally laid cylinder, the lift force acting on the cylinder is enhanced. The horseshoe vortex as generated from the vertical plates aids to the lift force on the cylinder and as a result the cylinder could easily move upwards. Previous chapter dealt with the separate analysis of the flow phenomena of the vertical plate. In this chapter combined flow phenomena arousing due to the horizontally laid cylinder and the vertical plate has been discussed. The experiments were carried out by fixing the cylinder at varied water depths. For each positions of the cylinder the analysis was carried out for different widths of plates as considered in this research. From the vortex strength and circulation finally obtained, gives a view about the confirmation of the design of plates and cylinder. From the analysis it can be accessed about the flow phenomena at every instance, when the cylinder is moving in transverse direction to the approaching flow direction of the flume.

4.4 Experimental setup and method

The experimental arrangement, data acquisition system and variables measured in the model study are described in this research. Typical investigation of flow fields for a composite hydrodynamic structure which consists of a submerged cylinder placed transverse to the flow of water and a vertical plate in line to flow of water alongwith velocity measurement by ADV around the cylinder has been carried out through various experiments. All the experiments were conducted in the Fluvial Hydraulics Laboratory of the School Water Resources Engineering in Jadavpur University, Kolkata. The experiments were carried out in a re-circulating flume 3.96 m long, 0.355 m wide, and 0.45 m deep including free board. Water flows in flume with a depth of 20 cm, and the water depth has been observed dropping to 17 cm after flowing past both the structures. The water depth of 20 cm was achieved in maximum to maintain the depth average velocity of 72.5 cm/s. The working section of the flume is made up of a cast iron bed and Plexiglas side walls along two sides for most of its length to facilitate visual observations as seen from Fig. 4.1. The axis representation in Fig. 4.1 depicts as *x* axis is in line to the flow direction, *y* axis is transverse to the flow direction and *z* axis is vertical to the flow direction. The re-circulating flow system was served by two centrifugal pumps located at the upstream end of the flume whose technical details are: power capacity of the motors were 10 and 7.5 hp respectively having variable speed, here the water flows through two sets of 20 cm diameter pipe line which runs directly into the flume. The rotational speed of each of the pump is 1430 rpm with a maximum discharge of 26 lps each, so that a total flow of 52 lps was achievable.

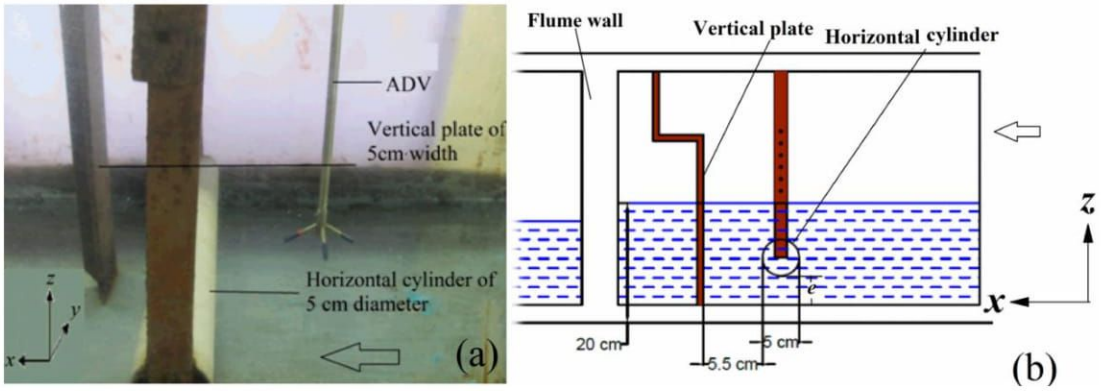

Fig. 4.1 Arrangement of hydrodynamic structures in water channel (a) Laboratory setup view; (b) Schematic elevation view

A cylinder of 5 cm diameter was used for the purpose of experiment. This cylinder was hung from top to the bed of the flume with the help of special metallic supports in order to get it in horizontal submerged position. Experiments were carried on by placing the coating iron plate vertically at the downstream of the cylinder, at a distance of **5.5 cm**. Notably the gap between the cylinder and the vertical plate was considered on the basis of highest amplitude as observed in the **model of modified VIVACE**. Figure 4.2 depicts about the optimization of longitudinal distance between the vertical plate and

the horizontally laid cylinder. It was seen that at a longitudinal distance ($L^* = X/D$) is $1.1D$ at the downstream of the cylinder, if a vertical plate is kept then a maximum amplitude of $A^* = 2$, where $A^* = a/D$ (a = amplitude of the cylinder movement in transverse direction). A gradual decrease in the amplitude has been observed when the longitudinal gap between the vertical plate and the cylinder is below $1.1D$. The justification for the reason of gradual decrease is because the horseshoe vortex created at the upstream of the plate requires a longitudinal gap to gain its full strength. Hence when the spaces between the vertical plate and the cylinder is decreased the external lift force as from the vertical plate is reduced since full development of the horseshoe vortex was not there. The shape of the horseshoe vortex is elliptical in cross section with its major axis approximately bisecting the horizontal cylinder 5.5 cm away from it. Moreover the dominance of the wake vortex generating by the cylinder is also another reason since the wake vortex generated from the upper side of the cylinder where the flow tends to move downwards, tries to break the effect of the horseshoe vortex whose purpose is to provide the water to flow in the upward direction. Steep decrease of the amplitude was seen when the plate is shifted beyond $1.1D$ at the downstream of the cylinder which depicts that the effect of the horseshoe vortex generated from the plates had diminished. Width of the vertical plates as considered are b = 2, 3, 4 and 5 cm, respectively.

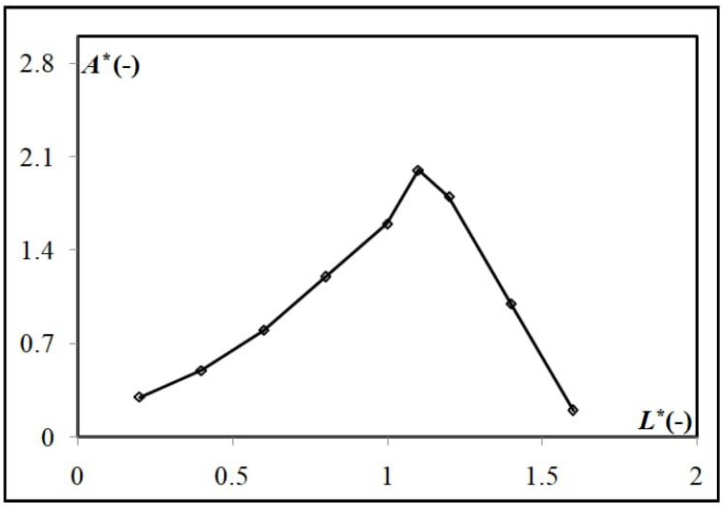

Fig. 4.2 Optimization of longitudinal gap between vertical plate and horizontally laid cylinder

Separate experiments were carried out by considering a vertical plate and the cylinder positions at e = 1, 2, 4, 6 and 8 cm respectively, as shown in Fig. 4.3, where e is the gap between cylinder and flume bed. The instantaneous three dimensional velocity data were captured by a 5-cm four-receiver Nortek-make down looking probe Vectrino Plus. It follows acoustic Doppler principle.

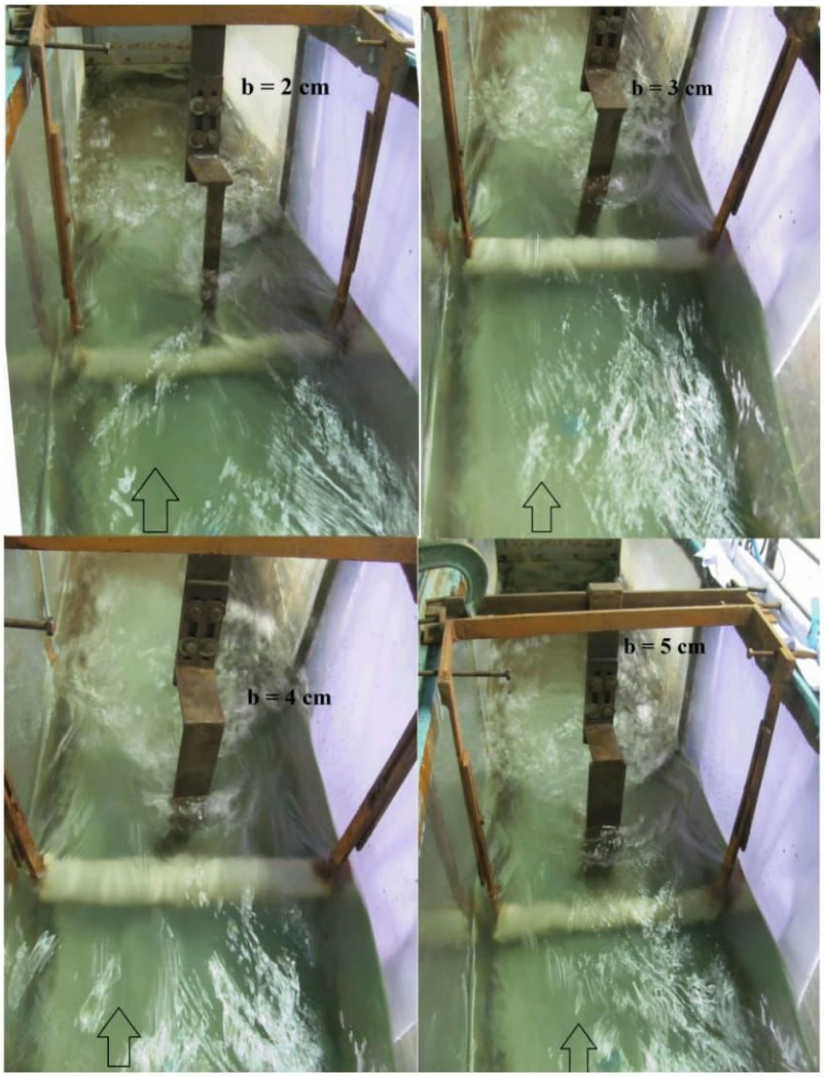

Fig. 4.3 Arrangement of plates having different vertical plate widths at the downstream of the horizontal cylinder in laboratory

The Vectrino functions on Doppler effect for providing instant 3D velocity readings at 100 Hz sampling rate. An adjustable sampling volume of 0.6 cm diameter having 0.2–0.5 cm sampling height was set to measure velocities. Horizontally, the minimum resolution during the Vectrino measurement was 1 cm. The measurement by the ADV probe was not possible in the zone 4.5 mm above the bed surface, because the ADV requires a measuring volume of 0.09 cm^3 as depicted in Dey and Raikar (2007). Output readings from Vectrino were converted by the software Vectrino+ version 1.18. During the Vectrino data filtering, the minimum SNR (signal-to-noise ratio) and minimum correlation limit were maintained at 16 and 70%, respectively. A sampling duration of one minute was considered ensuring a statistically time-independent averaged velocity. The space between the cylinder and plate, basically the boundary layer region, relatively long sampling durations (3 minutes) were taken since it was found that in that region correlation value was very low.

4.5 Result and discussion

The experiment was separately carried out using four plates of width 2, 3, 4 and 5 cm, respectively denoted by notation *b*. Notably for each experiment one plate was placed at 3.55 m away from the intake side of the flume in order to receive water at its end in addition to the baffle plates at the intake point. For each experiment, the horizontal cylinder was fixed at a distance of 5.5 cm upstream from the vertical plate. To understand the complex flow phenomenon throughout the water depth, for each experiment the cylinder has been fixed at various water depth. The gap (*e*) of the cylinder maintained with the flume bed is 1, 2, 4, 6 and 8 cm, respectively. The depth averaged flow velocity was maintained as 72.5 cm/s. To measure and plot contours for time-averaged flow velocity vectors, time-averaged longitudinal flow velocity (*u*), time-averaged transverse flow velocity (*v*), time-averaged vertical flow velocity (*w*) the instrument ADV and Origin Lab Software had been used. Here the axis considered as the vertical plate is supposed to be fixed at the origin and in respect to the plate; any coordinate at the upstream is considered negative and at the downstream is considered as positive, accordingly. Each and every aspect of the flow velocities *u*, *v* and *w* are viewed at the *x*-*z* plane. Moreover concentration of the study mainly lies near the region of the boundary layer of the cylinder and the gap between the cylinder and the vertical plate. For the purpose of parity and distinction of the values, the measurements at the upstream beyond the region of concentration was also taken. Due to the limitations of ADV, the measurements could not be taken less than 2.5 cm away upstream from the vertical plate. Also no measurements could be taken underneath the cylinder surface.

Time averaged velocity vectors

The time-averaged velocity vectors (*V*), whose magnitude and direction are $\sqrt{u^2+w^2}$ and $\arctan(w/u)$ as visualized in Figs. 4.4 - 4.5, depict that there is a flow separation seen just at the upstream of the cylinder. Flow separation is caused by the reduction of velocity in the boundary layer, combined with a positive pressure gradient basically known as adverse pressure gradient since it opposes the flow. Separation can therefore occur only when an adverse pressure gradient exists. Flow over a flat plate with zero or negative pressure gradient will never be separate before reaching the end of the cylinder no matter how big the cylinder is. The line of zero velocity dividing the forward and reverse flow leaves the surface at the separation point, and is known as the separation streamline. As a result of the reverse flow, large irregular eddies are formed in which much energy is dissipated as heat. The separated boundary layer tends to curl up in the reversed flow, and the region of disturbed fluid usually extends for some distance downstream. Since the energy of eddies are dissipated as heat, the pressure downstream remains approximately the same as at the separation point. Separation occurs with both laminar and turbulent boundary layers, and for the same reasons, but laminar layers are much more prone to separation than turbulent ones. This is because

in a laminar layer the increase of velocity with distance from the surface is less rapid and the adverse pressure gradient can more readily halt the slow-moving fluid close to the surface. A turbulent layer can survive an adverse pressure gradient for some distance before separating. For any boundary layer, however, the greater the adverse pressure gradient, the sooner the separation occurs. Separation of the boundary layer greatly affects the flow as a whole. In particular formation of a wake of disturbed fluid downstream, in which the pressure is approximately constant, radically alters the pattern of flow. The pressure is approximately constant, radically alters the pattern of flow. The effective boundary of the flow is then, not the solid surface but an unknown shape which includes the zone of separation. Because of the change in pattern of flow, the position of minimum pressure may be altered and the separation point may move towards the upstream where the pressure was originally low. Once a laminar layer has separated from the boundary it may become turbulent. The mixing of fluid particles which then occurs may, in some circumstances, cause the layer to re-attach itself to the solid boundary so that the separation zone is an isolated bubble on the surface. Although not a common occurrence this does sometimes happen at the leading edge of a surface where excessive roughness causes separation of the laminar layer, which followed by a turbulent layer downstream. After the flow separation had occurred past the horizontal cylinder then again there is a downward fall in the flow in front of the plate due to horseshoe vortex created by the plate. The horseshoe vortex is basically a forced vortex type of flow, because the whirl velocity increases in the outward direction from the vortex centre. Notably the shape of the vortex is elliptical in cross section with its major axis approximately bisecting the horizontal cylinder 5.5 cm away from it. This horseshoe vortex in-turn supposed to hit the bottom surface of the cylinder. The velocity vectors are not visible at the bottom side of the cylinder since it was beyond the scope of the ADV to measure in that region. From Figs. 4.4 - 4.5 the flow phenomena cylinder placed at varied gaps from the flume bed are visualized for the plate widths 2, 3, 4 and 5 cm respectively. The vector plot for each experiment shows the flow separation just at the upstream. As the plate width is increased, the magnitude in the horizontal distance upto 15.5 cm upstream of the vertical plate is decreased. This feature is observed upto the water depth of 6 cm above the flume bed. Same trend of changes in the magnitude has been observed in previous chapter. Interestingly due to the cylinder, the magnitude near the stagnation point of the cylinder has also decreased further. Due to the presence of the cylinder the downward movement of the flow of water is not observed near the surface of plate and the flume bed. The wake vortex generated from the horizontal cylinder becomes dominant upto the gap of 6 cm between flume bed and cylinder. When e = 8 cm a down flow of the water been observed near the plate and flume bed. The result suggests that beyond e = 6 cm both flow separation from the cylinder and the downward movement of the flow due to vertical plates are prominent. Moreover the flow separation underneath the cylinder is also not visualized clearly for e = 1 cm since the cylinder is very close to the flume bed, e is comparatively very less in respect to development of the flow separation. In the arranged discussion later on may give few hint about affects that the horseshoe vortex from the vertical plate on the cylinder.

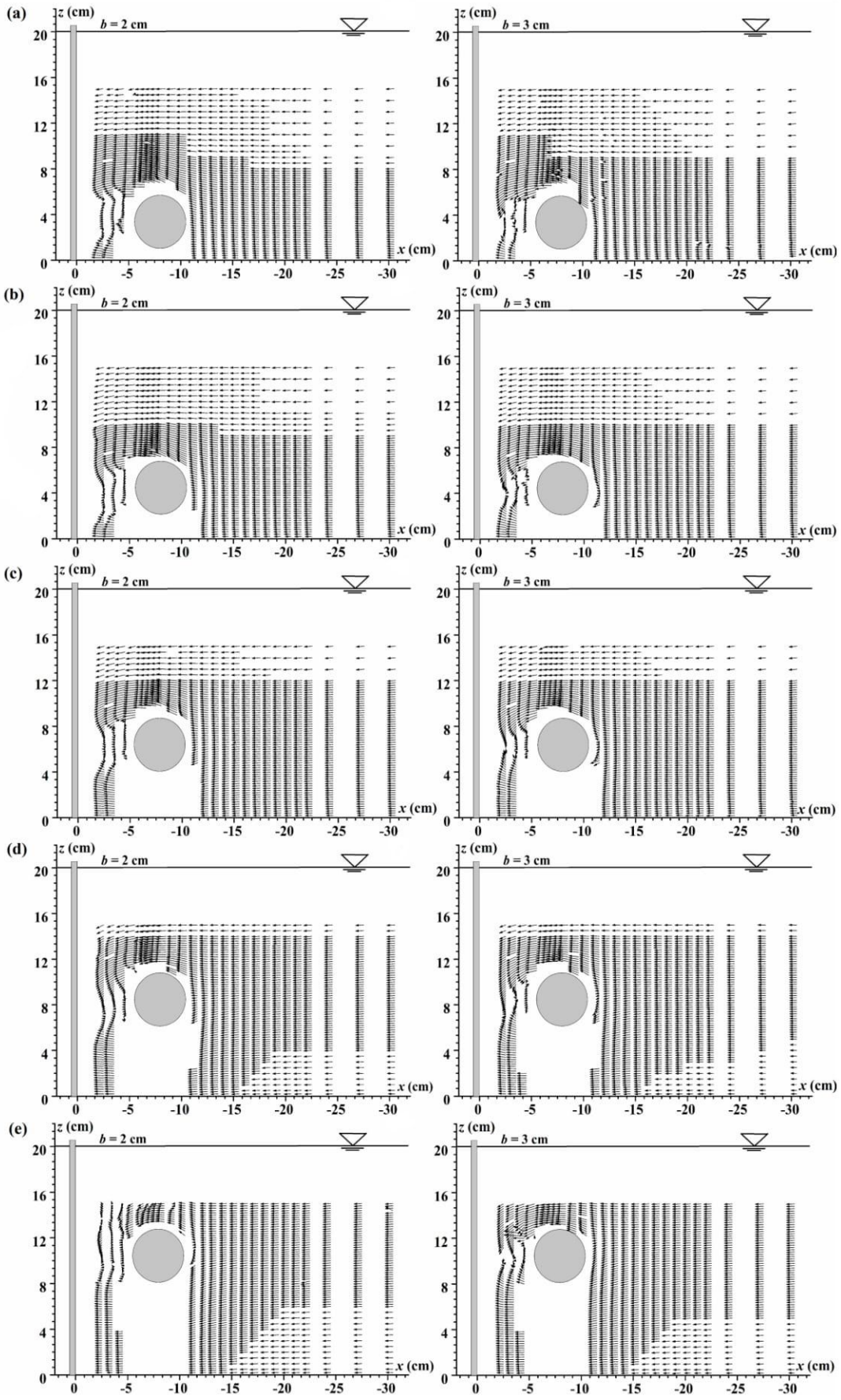

Fig. 4.4 Time averaged velocity vectors in and around the plate and cylinder for the vertical plate width 2 cm and 3 cm for cylinder and flume bed gap: (a) 1 cm; (b) 2 cm; (c) 4 cm; (d) 6 cm and (e) 8 cm

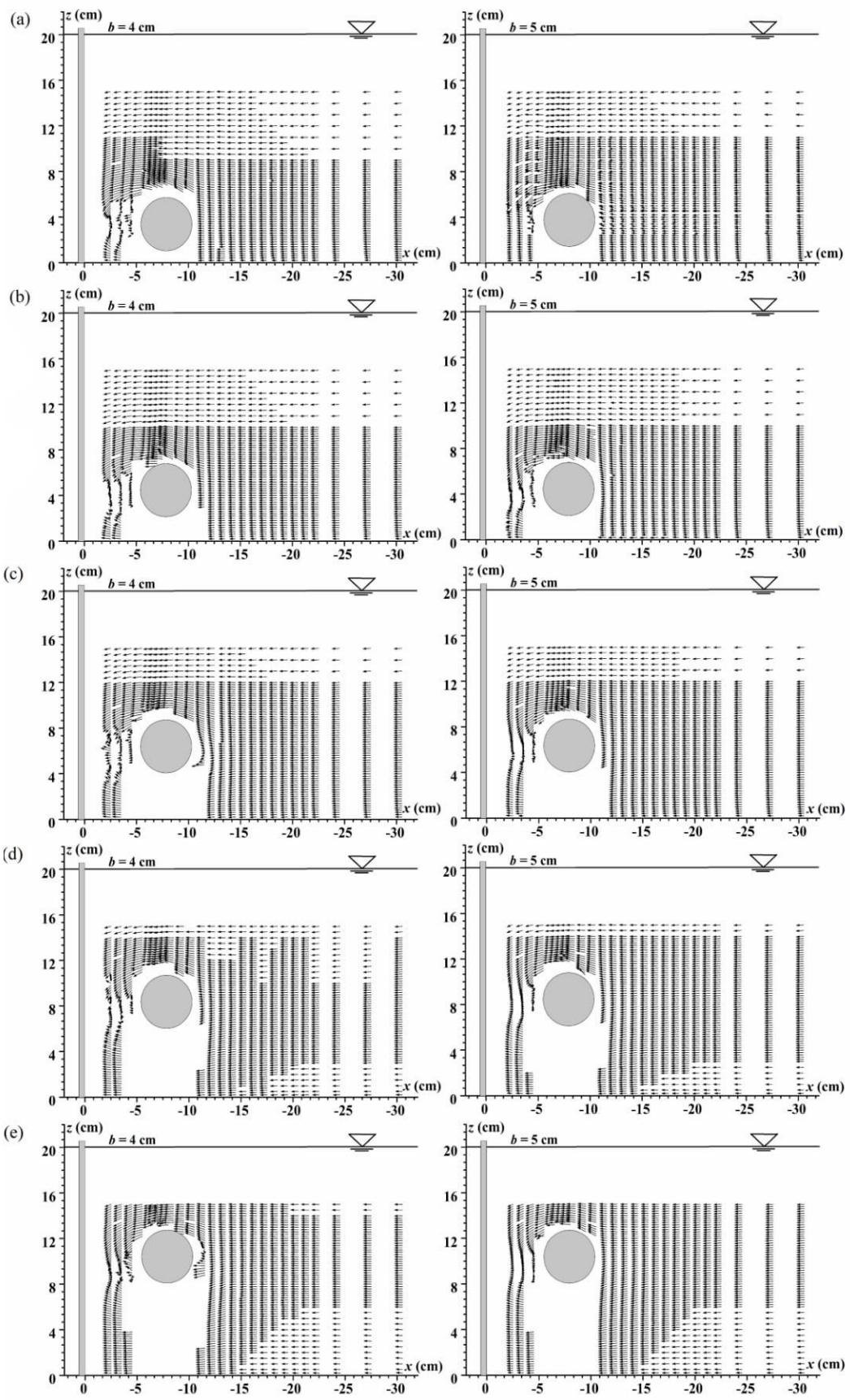

Fig. 4.5 Time averaged velocity vectors in and around the plate and cylinder for the vertical plate width 4 cm and 5 cm for cylinder and flume bed gap: (a) 1 cm; (b) 2 cm; (c) 4 cm; (d) 6 cm and (e) 8 cm

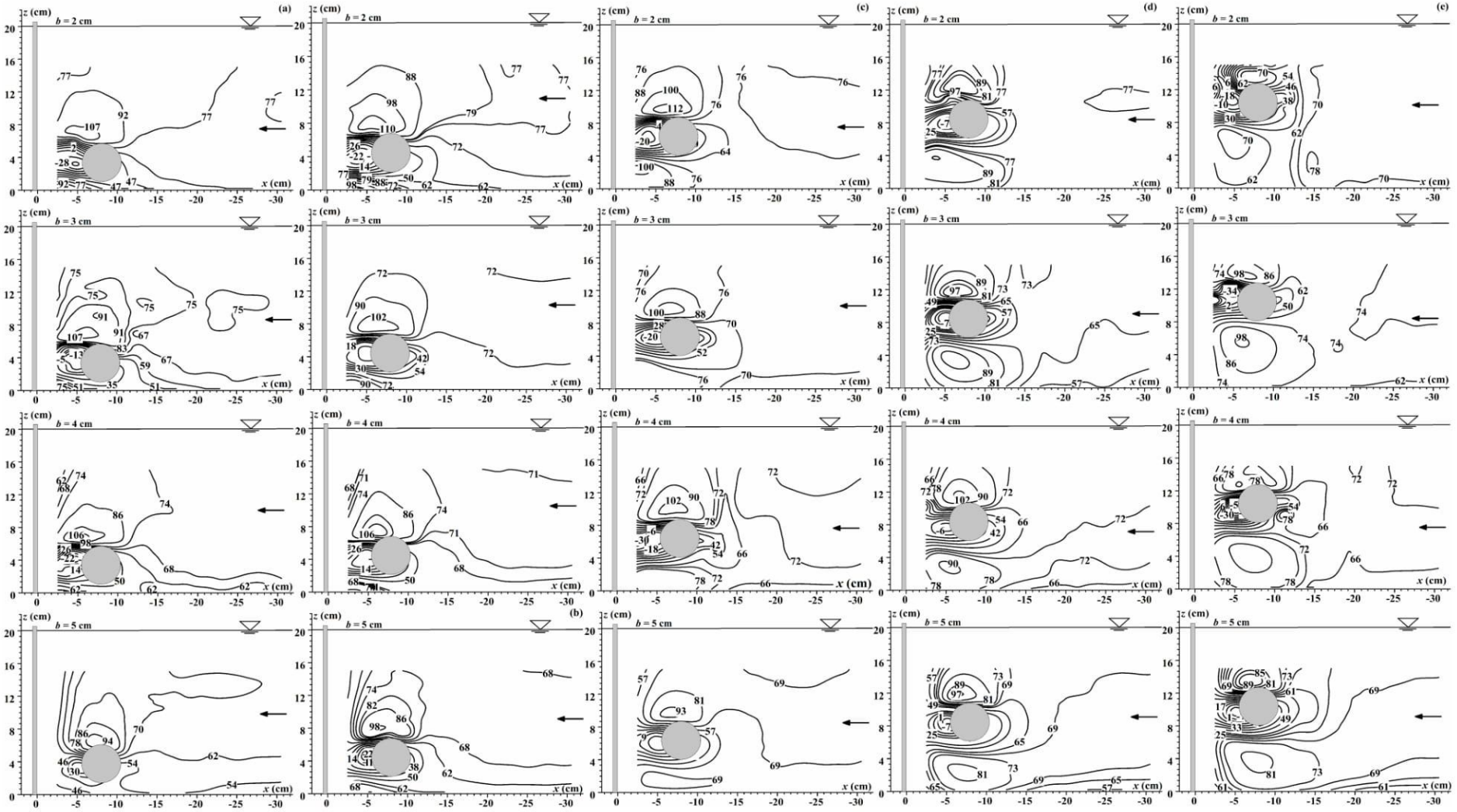

Fig. 4.6 Contours for longitudinal flow velocity u (in cm/s) in and around the plate and cylinder, for cylinder and flume bed gap: (a) 1 cm; (b) 2 cm; (c) 4 cm; (d) 6 cm and (e) 8 cm

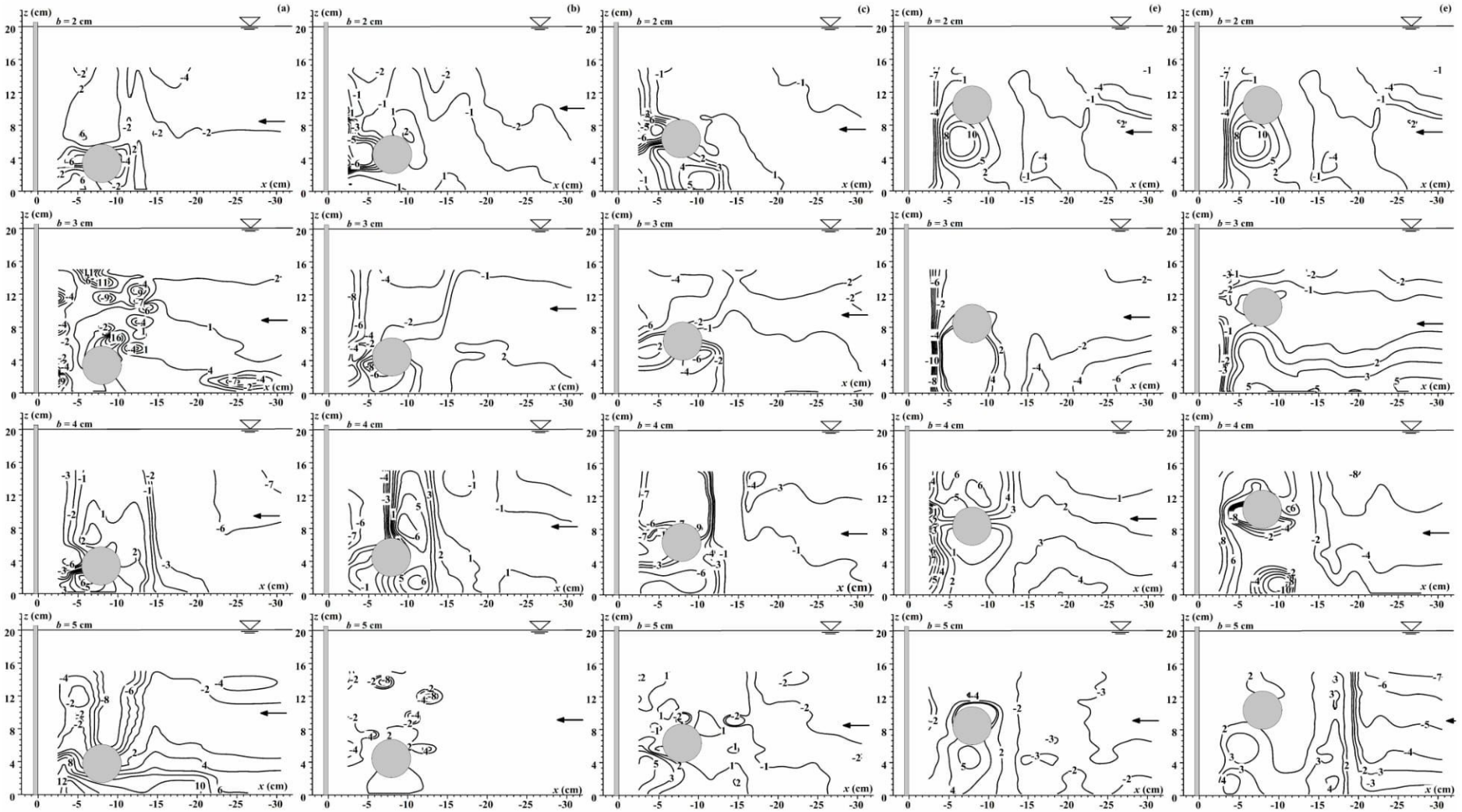

Fig. 4.7 Contours for transversal flow velocity *v* (in cm/s) in and around the plate and cylinder, for cylinder and flume bed gap: (a) 1 cm; (b) 2 cm; (c) 4 cm; (d) 6 cm and (e) 8 cm

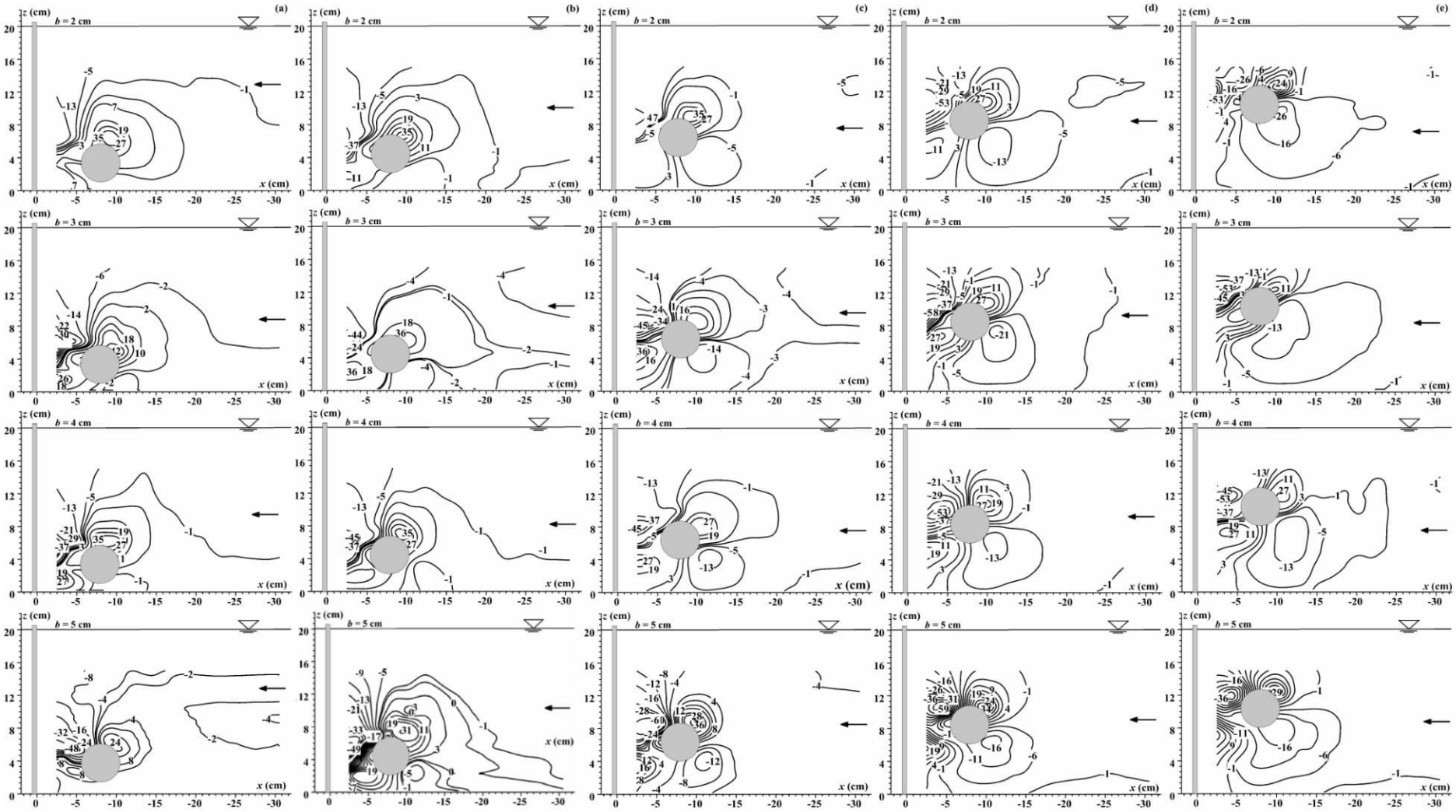

Fig. 4.8 Contours for vertical flow velocity *w* (in cm/s) in and around the plate and cylinder, for cylinder and flume bed gap: (a) 1 cm; (b) 2 cm; (c) 4 cm; (d) 6 cm and (e) 8 cm

Velocity Contours

Three dimensional flow velocities were measured with the help of ADV. From Figs. 4.6 - 4.8 the contours of velocities *u, v* and *w* were found out. The fluid in the boundary layer moves at a lower velocity than the fluid in the free stream. A point is reached at which negative velocities arise at the inner part of the boundary layer. The development of the negative velocity zone further implies that the pressures within the zone are low compared to those in the free stream. Fluid from further outward in the boundary layer is therefore drawn inwards to the low-pressure zone (Kirkil and Constantinescu, 2010). For each case in Fig. 4.6(a) the maximum *u* is found at the upper surface of the cylinder. The reason behind it is the instantaneous approaching longitudinal flow velocity *u* is supplemented with the mushroom shaped vortices that occurs due to a flow past over the horizontal cylinder (as shown in Fig. 4.9) in the *x* - direction. The magnitude of *u* at the upper surface of the cylinder again depends on the vertical plate kept at the downstream of the cylinder. Two main things are supposed to happen due to the plates. Firstly the horseshoe vortex would be generated a secondly when the flow strikes the plate then the flow is separated into three directions resulting in backflow in *x* direction, lateral flow in *y* direction and downflow in *z* direction. Now from earlier researches the *x* axis component of the horseshoe vortex would lead to the increase of the approaching longitudinal velocity but at the same the backflow arousing from the vertical plate in *x* direction reduces the *u* velocity. This opposition of the flow is more when the area of exposed to the flow is more. Hence the maximum *u* velocity observed at the upper surface of the cylinder for different plates considered are been justified. It is also found that the longitudinal flow velocities near the flume bed and the vertical plates considered at e = 1 cm were found to 92, 75, 62 and 46 cm/s respectively for the plate widths b = 2, 3, 4 and 5 cm respectively. The reason is justified by the fact that resistance offered to the longitudinal velocity increases with the area of solid surface contact with the water. Hence a decreasing trend of the longitudinal velocity is found for the increase in the plate widths as considered. The longitudinal velocity in that region also supplemented by the mushroom shaped vortices created underneath the cylinder (as shown in Fig. 4.9). The longitudinal velocities farther from the boundary layer of the flume bed and the plate also may be called as turbulent outer layer are found less affected since the velocities found to be nearer to the depth averaged velocity i.e. 72.5 cm/s.

When e = 2 cm as shown in Fig. 4.5(b) the longitudinal velocities for different widths as considered revealed to 1.02, 1.25, 1.45 and 1.57 times of the velocities as observed from Fig. 4.6(a). The reason is justified by the fact that the e = 2 cm had provided a sufficient gap for the development of the horseshoe from the plates and the mushroom shaped vortices at the downstream of the cylinder near the flume bed. From Fig. 4.6(c) at e = 4 cm the longitudinal velocities have started to reduce for the considered plate width at the upper side of the cylinder. The reason is justified by the fact; the supplementary effect of the horseshoe vortex developed by the plate reduces as the cylinder moves up. The longitudinal velocities in the lower part of the cylinder increases due to the fact the approaching flow gets more opening underneath the

cylinder. From Fig. 4.7(d) the visualization of the longitudinal velocity at the upper surface decreases further due to the reduction of the horseshoe vortex. The longitudinal flow underneath the cylinder tries to achieve the depth averaged flow velocities. It was found that at the upper surface the longitudinal flow velocity was found to be 0.906, 0.906, 0.958 and 0.969 times as the longitudinal flow velocities observed in Fig. 4.6(a) for b = 2, 3, 4 and 5 cm respectively. The longitudinal velocities found underneath the cylinder were found to be 88, 76, 72 and 69 cm/s for b = 2, 3, 4 and 5 cm respectively. Finally from Fig. 4.6(e) at e = 8 cm the longitudinal flow velocities were found to be near the depth averaged velocity at the upper surface of the cylinder which suggest that the effect of the horseshoe vortex had totally been diminished in that region. The same range of longitudinal velocities as found in the upper surface of the cylinder was observed underneath the cylinder for all the plate widths considered. The results clearly say that, where the area of contact with the water flow is more there the longitudinal flow velocities are mostly affected. This happens because the flow approaches towards the stagnation point where the velocity is zero. The separation point is defined as the limit between the main and the reverse flow in the immediate vicinity of the wall. When the width of the plate is more than other widths considered, maximum amount of the longitudinal flow strikes the surface of the plate and the flow is exhausted and the approaching flow velocities are reduced.

The horseshoe vortex developed from the plates also aids to the longitudinal flow velocity. So from Figs. 4.6(a-e) as the e is increased and at e = 8 cm, the longitudinal flow velocity over the cylinder is reduced to the upstream velocity. Whereas when e = 1-6 cm as considered the longitudinal velocity is much higher than the upstream velocity. The longitudinal velocities are mostly affected near solid walls i.e. flume bed, cylinder surface and the vertical plate. The velocities farther from the boundary layer of the flume bed and the plate also may be called as turbulent outer layer are found less affected since the velocities found to be nearer to the depth velocity i.e. 72.5 cm/s.

Viewing Figs. 4.7(a-e) both negative and positive values of transverse flow velocities are found at the range of water depth in relation to cylinder position. Magnitude of transverse velocities at the rear portion of the cylinder near the vertical plate is found to be -10 to 12 cm/s. The reason is justified by the fact; the separation first appears when Keulegan Carpenter number (KC) is increased to 1.1; this occurs in the form of the so-called Honji instability (Fig. 4.9). When this KC number is reached, the purely two-dimensional flow over the cylinder surface breaks into a three-dimensional flow pattern where equally-spaced, regular streaks are formed over the cylinder surface, as sketched in Fig. 4.9. Here λ = wavelength of mushroom shaped vortices; a is the amplitude of oscillatory flow and B is the axially periodic vortices when the water flow past a cylinder. These streaks can be made visible by flow visualization techniques. Observations show that the marked fluid particles, which were originally on the surface of the cylinder, would always end up in these narrow, streaky flow zones.

The observations also show that these streaks eventually are subject to separation in every half period prior to the flow reversal, each separated streak being in the form of a mushroom-shape vortex (Honji, 1981). Hence the mushroom shaped vortices

contribute to the transverse flow velocity. As the gap between the cylinder and the flume bed is increased the trends of the mushroom shaped vortices are more prominent near the bottom portion of the cylinder closed to the vertical plate, and vice versa. The magnitude and direction of the transverse flow velocity also depends upon the width of the plates, the contours from Figs. 4.7(a-e) suggests that as the width of the plates are increased the horseshoe vortex generated from the plates plays an important role to direct the Honji streaks developed due to the cylinder. More powerful the horseshoe vortex the more chances of the breaking up of the mushroom shaped vortices and change in direction. From previous chapter it is known that the horseshoe vortex strength is very high for width 5 cm in compared to lowest width of 2 cm as considered.

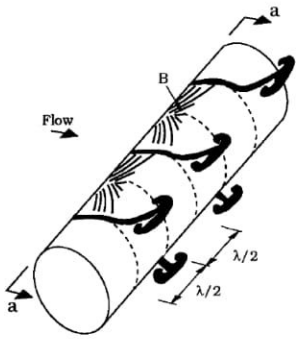

Fig. 4.9 Honji streaks, which are subject to separation in the form of mushroom-shaped vortices (Honji, 1981)

Depending upon the width of the plate, the magnitudes and directions of vertical flow velocities as shown in Figs. 4.8(a-e) can be justified. The magnitudes of the vertical flow velocities are found to increase as the width of the plates are increased. The magnitude observed in Figs. 4.8(a-e) is basically the addition of the wake vortex of the cylinder and the horseshoe vortex of the cylinder. The dominance of the wake vortex of the cylinder depends upon the strength of the horseshoe vortex. The justifications and the profiles suggest the existence of the external lift force acting on the cylinder up to e = 8 cm. From Fig. 4.8(a) the vertical velocity in between the gap of the cylinder and the plate was found to be -13, -30, -37 and -48 cm/s for plate widths b = 2, 4, 6 and 8 cm for e = 1 cm. Where the maximum vertical flow velocity were found to be -44, -44, -45 and -48 cm/s in the gap between cylinder and the plate for b = 2, 3, 4 and 5 cm respectively for e = 2 cm as seen from Fig. 4.8(b). As the e is increased from the vertical velocity in between the gaps also increase overall by 1.2 and 1.15 times the vertical velocity as found in Fig. 4.8(b) for each of the plates considered. At the upstream surface of the cylinder at all the considered e, the vertical velocity is near 35 cm/s. When the approaching flow of water strikes both the structures that are horizontal cylinder and the vertical plate then the vertical flow velocity is distributed in various forms. Firstly when the flow strikes the cylinder the water flow is distributed to both upwards and downward the cylinder. The vertical velocity here is been affected by the backflow of the longitudinal velocity coming from the vertical plate. The backflow

effect is more with the increase of the plate width. The vertical velocity formed by the upper side of the horizontal cylinder is been supplemented with the downflow of the plate and the magnitude of w is increased with the increase of the plate width. At the same time this vertical velocity is countered by the wake vortices aroused at the downstream of the cylinder which moves upwards. The vertical velocity in between the gap of cylinder and the plate is thus the resultant effect of the downflow due to vertical plate and the wake vortices formed in the upper side of the cylinder with the wake vortices developed from the down surface of the cylinder. The magnitude of w found at the turbulent outer layer at the region 12 to 22 cm upstream of the vertical plate. The positive magnitude of vertical flow velocity found near the flume bed at the downward rear side of the cylinder is very less in compared to the negative vertical flow velocity since the much of the energy of the wake vortex of the downside of the cylinder is exhausted by the downflow of water due to the vertical plate and the wake vortex occurring due to the upper portion of the cylinder. The positive vertical velocity contour at the upstream of the cylinder suggests the effect of the horseshoe vortex due to the vertical plates is dominant. The increase in the magnitude of the vertical velocity at the upward direction is observed for increased width of the plates. As e is increased the vertical flow velocity also decreases since the strength of the horseshoe vortex generated from the plates are reduced as it enter the turbulent outer boundary. Notably the magnitude of the vertical flow velocity also depends upon the stagnation point as created due to the horizontal cylinder. Since due to the geometry of the cylinder surface the area perpendicularly exposed to the longitudinal flow is very less. Due to this reason the strength of the downflow of water is very less in compared to the upward movement of water due to the horseshoe vortex generated by the plates.

Turbulence Intensities

From Figs. 4.10(a-e) the contours for turbulence intensities in around the plates and cylinder are represented. The turbulence intensities for longitudinal, transversal and vertical flow velocities were formulated respectively as $u^+ = \sqrt{\overline{u'u'}}$, $v^+ = \sqrt{\overline{v'v'}}$ and $w^+ = \sqrt{\overline{w'w'}}$ respectively where u', v' and w' are the fluctuations of u, v and w respectively. Fig 4.10(a-e) reveals that the distribution the turbulence intensities for all the experiments u^+, v^+ and w^+ are almost similar beyond the range of 12.5 cm upstream of the vertical plate. This reason is justified by the existence of the horseshoe vortex due to the vertical plates. The magnitude of the horseshoe at this region depends upon the vortex strength of the vertical plate. Interestingly the core of high turbulence intensities is mainly found in the gap between the cylinder and the plate. For b = 2, 3, 4 and 5 cm u^+ was found maximum of around the range of 85 cm/s at e = 1 cm. For e = 2 cm maximum u^+ values were found to be 43, 55, 57 and 60 cm/s for the plate widths b = 2, 3, 4 and 5 cm respectively. Same trend of increase in maximum u^+ is observed at e = 4 cm as 69, 73, 77 and 88 cm/s for b = 2, 3, 4 and 5 cm, respectively. But when e = 6 cm, the maximum values of u^+ were found to be decreasing as 41, 43, 69 and 70 cm/s

for considered plates b = 2, 3, 4, and 5 cm, respectively. At e = 8 cm again the increase in fluctuations in u is been observed but the position of the maximum fluctuations are changed and the maximum fluctuations were found to be 50, 52, 70 and 72 cm/s. From the above results it can be said that as the e is increased the fluctuations of u^+ mainly lies in the downside of the cylinder at the downstream of the cylinder. The justification for the fluctuations in u is due to the mixing of the horseshoe vortex arousing from the plate and the wake vortex in supplement to the mushroom shaped vortices of the cylinder. But as the cylinder is raised to e = 6 cm the effect of horseshoe vortex from the plates starts to decrease and the u is affected mainly by the downflow the plate and the wake vortex at the upper surface of the cylinder. At e = 8 cm when the horseshoe vortex form the plates are totally diminished then the maximum turbulence intensities are found near the upper surface of the cylinder. According to the limitations of the experiments, since the experiments were taken in x-z plane the v velocity component is supposed to be near to zero. But due to the immense turbulence effect as created by the approaching longitudinal there is always a fluctuation in the v component. The change in the magnitude of v^+ depicts the phenomenon as observed while discussing the u^+. While discussing w^+ it can be said that when e = 1 to 6 cm due to the horseshoe vortex effect maximum vertical fluctuations are observed near the down side of the cylinder but as it goes further up to e = 8 cm the horseshoe vortex effect is diminished then the downflow due vertical plate and tendency of the flow directed downward at the rear side of the cylinder due to adverse pressure gradient comes into existence. Hence maximum fluctuations of w at e = 8 cm is found to be at the upper side of the cylinder. In support to the phenomenon the maximum w^+ were found out as: for b = 2, 3, 4 and 5 cm w^+ values are 24, 32, 34 and 40 cm/s at e = 1 cm. At e = 2 cm the maximum intensity of w were found to be 29, 33, 39 and 44 cm/s for b = 2, 3, 4 and 5 cm respectively. For e = 4 cm all the intensities were increased by around 1.05 times the values as found for e = 2 cm. For e = 6 cm, the maximum values of turbulent intensity w^+ decreases to 23, 30, 37 and 40 cm/s respectively for plate widths b = 2, 3, 4 and 5 cm respectively. Again when e is increased to 8 cm the maximum w^+ at the upper side of the cylinder was found to be 29, 34, 39 and 44 cm/s respectively for b = 2, 3, 4 and 5 cm respectively. The magnitude of the turbulence intensities in the region of 12.5 cm and beyond upstream of the vertical plate increases with the increase in plate widths as considered. The magnitude of the intensities in between the vertical plates and cylinder are at least 10 times more than the rest of regions as depicted in Figs. 4.10(a-e). The reason is justified by the fact it happens due to the collision of the horseshoe vortex generated from the vertical plate, mushroom-shaped vortices and wake vortices generated by the cylinder. Hence for the above reason Figs. 4.10 - 4.12(a-e) reveals that the concentration of turbulence intensities are mainly found near the boundary layer region of the cylinder, as the cylinder moves away and towards the flume bed. Notably it is also revealed that the magnitude of the intensities at regions near the vertical plates beyond the range of boundary layer of the cylinder reflects the dominance of the horseshoe vortex of the vertical plate. Since the magnitude in this region is maximum of 13 cm/s for w^+.

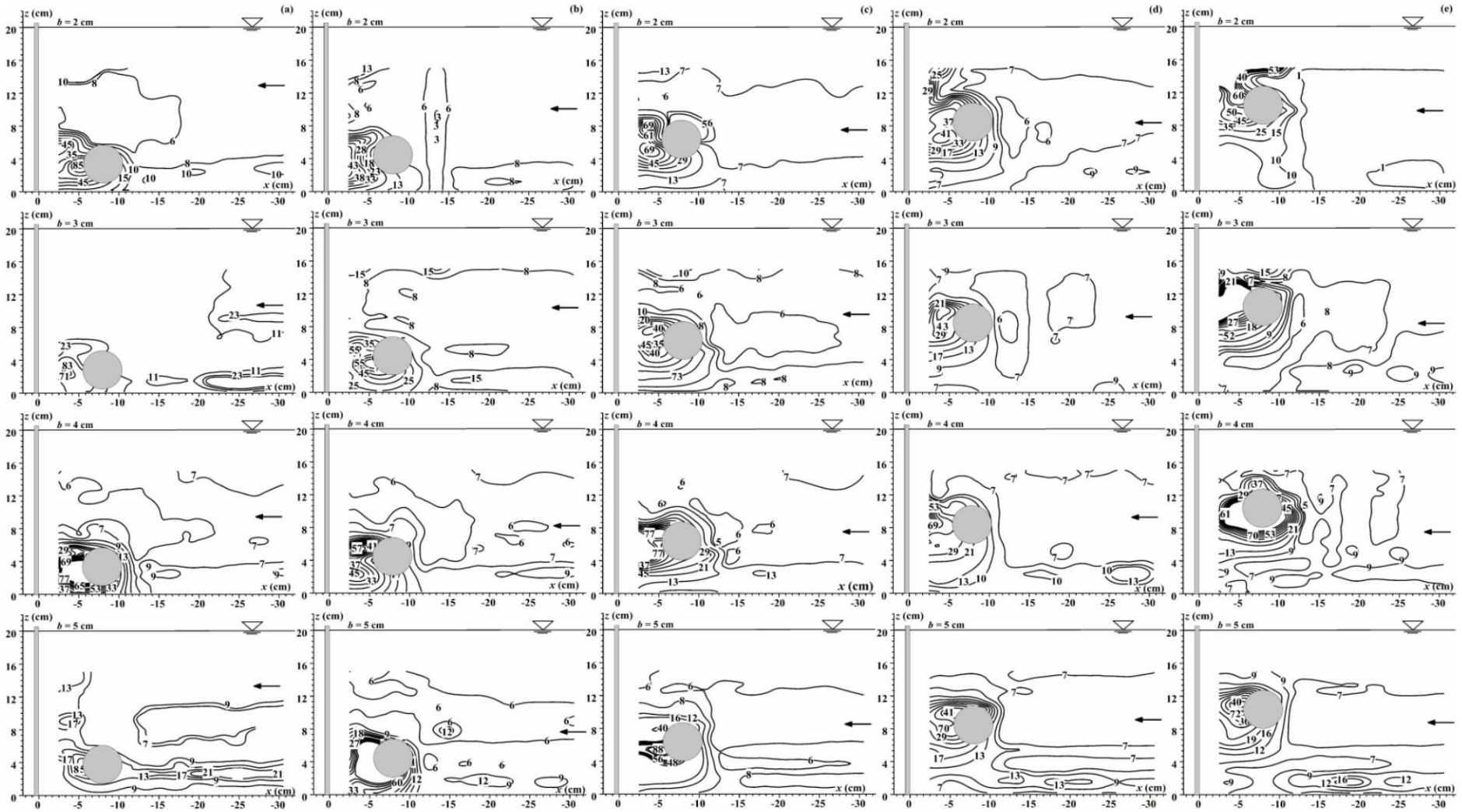

Fig. 4.10 Contours for longitudinal turbulence intensity u^+ (in cm/s) in and around the plate and cylinder, for cylinder and flume bed gap: (a) 1 cm; (b) 2 cm; (c) 4 cm; (d) 6 cm and (e) 8 cm

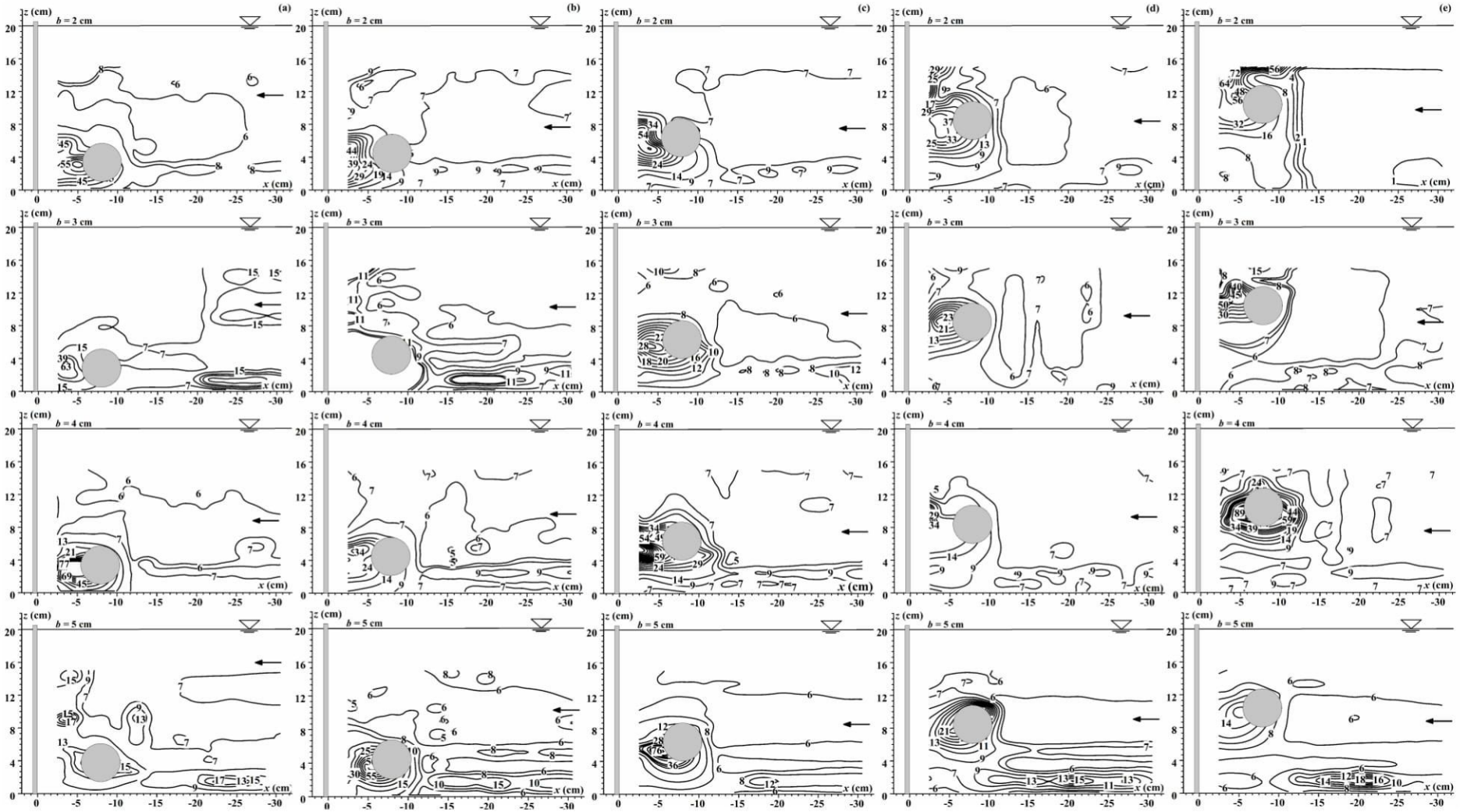

Fig. 4.11 Contours for transversal turbulence intensity v^+ (in cm/s) in and around the plate and cylinder, for cylinder and flume bed gap: (a) 1 cm; (b) 2 cm; (c) 4 cm; (d) 6 cm and (e) 8 cm

5.1 Introduction

A country's growth mainly depends upon the capacity of the electrical energy that can afford to run the wheels of technology. Natural energy in the whole world is found in a discrete manner as a result it becomes typical to harness electricity from every energy points. Today most challenging problem that a developing nation faces is low-cost sustainable energy generation. The crisis can be solved by finding out ways to harness electricity amongst the scattered energy points. Sustainable energy forms have become an important factor now-a-days, as when seen in environmental aspect. So efforts are being made to harness sustainable energy particularly in developing countries. Technologies relating to non-conventional energy sources like hydro energy, tidal energy, wind energy, bio-energy, geo-thermal energy and solar energy are basic resources which are collectively termed as sustainable energy sources.

Development is also required for every technology that can generate energy at a competitive cost. Many times as the availability of the energy points (sources of energy) are not feasible and the main source i.e. the fossil fuel has also its limitation, some ways are needed to be dug out. Technology development holds the main key in this juncture. Many non-conventional energy hydrokinetic devices have been discovered and have been mainly utilized in the marine region but if they could be modified according to the need at the normal river or canal areas the energy would not be wasted. An energy crisis becomes truly suffocating in the supply of energy resources to an economy of the state. In this juncture a device had to be developed at Fluvial Hydraulics Laboratory, School of Water Resources that basically runs on the concept of enhancing flow induced vibration over a cylindrical structure that harness electricity from very shallow streams. In this chapter research has been carried to visualize, in shallow depth of water flow how much power it is capable of harnessing. The device was found capable to grab the water energy at its maximum though amount of power generation in laboratory may be miniscule. After modification, same prototype in real life condition can be a very handy weapon to supply few lighting loads at remote places.

Keywords—*sustainable energy generation; flow induced vibration; shallow water depth; hydraulic structures; harness electricity*

5.2 Review of earlier works

Present scenario suggests that India is very much dependent on the conventional energy sources such as fossil fuel (coal and petroleum). Keeping in view to the limitations of the present conditions of the fossil fuels there are various other forms of renewable energy being started to be practiced in India such as solar energy, hydro power (including tidal power), bio-diesel, wind energy, bio-gas, etc. A continuous effort in developments in technology is under process to harness the non-conventional energy (Babu *et al.,* 2013). Leonardo da Vinci first observed vortex induced vibration (VIV), which is also been often termed as flow induced vibration approximate 1500 A.D. in the form of "Aeolian Tones". Engineers have been constantly trying to spoil vortex

shedding and suppress VIV to prevent the damage caused due to the Aeolian Tones to the very high head equipments and structures. Furthermore, it was von Karman at California Institute of Technology who proved that the Tacoma Narrows bridge collapse in 1940 was due to vortex induced vibration (VIV). The fluid-structure interaction phenomenon occurs due to the nonlinear resonance of cylinders (or spheres) through vortex shedding lock-in.

Bernitsas *et al.* (2006) first utilized the VIV rather enhanced the process of the vortex shedding to develop a new form of electrical energy generation technique. The VIV is also called synchronization between vortex shedding and cylinder (or sphere) oscillations. A bluff body, usually a cylinder, when introduced in a free stream features of boundary layer separation could be observed which results in unequal pressure distribution around the bluff body eventually leading to formation of vortices. The vortex shedding pattern is not symmetrical because of which there is a net force which results in the up and down motion of the bluff body. Conversion of up and down motion of the cylinder to useful electrical energy is the role of the power take-off mechanism which is a linear generator in this case. It had also been tested that this converter is capable of harnessing useful amount of electricity in the river flow velocity of about 0.25 m/s. The device had tried to harness the abundant clean and renewable energy from ocean and other water resources and claimed to have high energy density, with being robust and modest with low recurring expenditure and have 10–20 years of life. With the velocity of 0.84 m/s, VIV tests were carried out in the Low Turbulence Free Surface Water (LTFSW) channel of the University of Michigan, for Reynolds number in the range of 8×10^3–1.5×10^5, have shown undoubtedly a strong dependence of VIV of cylinders on proximity to a bottom boundary as depicted in (Bernitsas *et al.*, 2009 and Raghavan *et al.*, 2009). The range of synchronization of the upper branch increases with increase in Reynolds number. The amplitude ratio (*A/D* where *A* is the amplitude and *D* is the cylinder diameter) increases with Reynolds number within the upper branch. For high-Reynolds number, the magnitude of *A/D* is achieved as 1.9 routinely in-spite of high damping.

The lower branch disappears, overtaken by extended upper branch. High Reynolds number VIV enters into the two paired vortices per shed (2P) domain in the Williamson–Roshko (W–R) map beginning with the initial branch. Hysteresis was not observed in these experiments possibly because parameters remain in the 2P-domain. High Reynolds numbers have a stronger influence than mass ratio on *A/D*. High-damping high-Reynolds VIV amplitudes are double of those predicted by the modified Griffin plot by extrapolation as reflected in the works of Raghavan and Bernitsas (2010) . For large mass ratios, $m^* = O(100)$ the vibration frequency for synchronization lies close to the natural frequency ($f^* = f/f_N \approx 1.0$), but as mass ratio is reduced to $m^* = O(1)$, f^* can reach remarkably large values. An expression (Equation 5.1) for the frequency of the lower-branch vibration was deduced as follows (Govardhan and Williamson, 2000):

$$f^*_{lower} = \sqrt{\frac{(m^* + C_A)}{(m^* - 0.54)}} \tag{5.1}$$

f^*_{lower} is the lower branch frequency ratio as depicted in Fig. 5.1. Equation 5.1 agrees very well with a wide set of experimental data of Govardhan and Williamson (2000). This frequency equation uncovers the existence of a critical mass ratio, where the frequency f^* becomes large $m^*_{crit} = 0.54$, $m^* < m^*_{crit}$, the lower branch can never be reached and it ceases to exist. The upper-branch large-amplitude vibrations persist for all velocities, no matter how high, and the frequency increases indefinitely with flow velocity. Referring Table 5.1 the added mass, m_A is given by $m_A = C_A m_d$ where m_d is the displaced fluid mass and C_A is the potential added-mass coefficient. (C_A = 1.0 for a circular cylinder). In the above groups, D is the cylinder diameter, L is cylinder length, ρ is the fluid density, V is the free-stream velocity, μ is the viscosity of water, m is the mass of cylinder, f_N is the cylinder's natural frequency, k is the stiffness of supporting spring and A is the amplitude.

Table 5.1 Non-dimensional parameters in relation to frequency vibration

Description	**Notation**	**Formula**
Mass ratio	m^*	$\frac{m}{\pi\rho D^2 L/4}$
Damping ratio	ξ	$\frac{C}{2\sqrt{k(m+m_A)}}$
Velocity ratio	U^*	$\frac{V}{f_N D}$
Amplitude ratio	A^*	$\frac{A}{D}$
Frequency ratio	f^*	$\frac{f}{f_N}$
Transverse force coefficient	C_Y	$\frac{F}{\frac{1}{2}\rho V^2 DL}$
Reynolds Number	Re	$\frac{\rho VD}{\mu}$

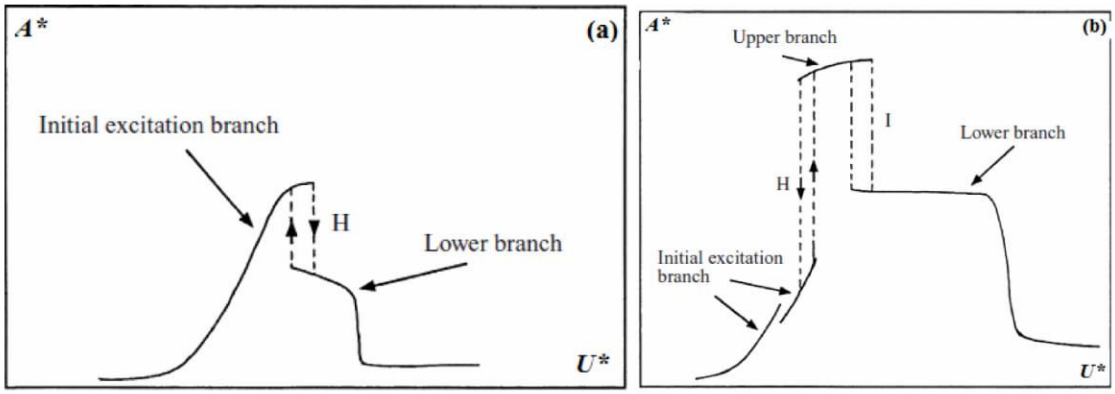

Fig 5.1 Two distinct types of amplitude response are shown schematically for (a) high mass damping ratio and (b) low mass damping ratio (Govardhan and Williamson, 2000)

From Fig. 5.1 it was depicted that the Feng-type of high mass damping ratio ($m^*\xi$) response exhibits only two branches (initial and lower), while the high mass damping ratio ($m^*\xi$) type of response (Khalak and Williamson 1999) exhibits three branches (initial, upper and lower). The mode transitions are either hysteretic (H) or involve intermittent switching (I). The range of synchronization is controlled primarily by m^* (when $m^*\xi$ is constant), whereas the peak amplitudes are controlled principally by the product of $m^*\xi$. By enhancing the nonlinear resonance of a new concept of vortex induced vibration aquatic clean energy (VIVACE) converter a notable change had been observed in shallow depth of water flow.

5.3 Need of the hydropower harnessing device

The coastal regions are been gifted with immense amount of marine energy. As a result variety of renewable energy generators have been discovered. The same, if could have been upgraded according to its usage in rivers and canals then more amount of energy could have been extracted. Since energy is the major part of the economy of a developing nation so the extraction of energy from rivers or canals becomes necessary. Earlier researches mainly deal with power generating potentiality of the converter that is regularly used to harness bulk electricity from large water bodies like sea or ocean. VIVACE as developed in Low Turbulence Free Surface Water channel (LTFSW), University of Michigan also could generate the electricity in the oceans and perennial rivers where the water depth is much higher. In India there are many dry and backward areas where there may be flowing rivers but with very low depths of water in the canals/rivers there conventional hydropower system cannot work there. Hence some other means of utilizing the water energy becomes necessary. The necessary check of the sustainability of such devices should also be done such as whether at all the devices are capable of producing the voltage for such shallow water channels / rivers of not. In this juncture VIVACE has been modified in the Fluvial Hydraulics Laboratory, School of Water Resources Engineering, Jadavpur University. Due to the modification the

same device was found to be capable of harnessing power from shallow water channels, where hardly any power generation could have been thought of.

5.4 Efforts in design of the energy generator

A prototype model had to be prepared in the existing laboratory set up before testing it in the field i.e. in any flowing water system such as rivers, canals or sea. A model of a structure consisting of a freely moving cylinder and supporting rods were first developed. The mass of the cylinder and its moving appendages (moving rods that are connected to cylinder) were considered by reference of equation 5.1 and shown in Fig. 5.2. The mass was considered for cylinder to be such that $m^* < m^*_{crit}$. Now since m^* is the addition of mass cylinder and the mass displaced by the cylinder including the mass of the floating appendages like mass of the rods and the magnets (with phantom load created due to the magnetic flux linkage). After much trial and error process the setup was created as shown in Fig. 5.1 and Fig. 5.2. The details of the parameters and design criteria considered are shown in Table 5.2.

Table 5.2 Lab based model details of the electro mechanical energy generator

Parameter considered	Value
Mass of the cylinder (1 piece)	0.236 kg
Mass of the moving rods (2 pieces)	0.144 kg
Mass of the magnets (38 pieces)	0.050 kg
Length of the cylinder	0.32 m
Diameter of the cylinder	0.05 m
Flume Length	3.96 m
Water Depth	0.20 m
Length of each of the moving rod	0.60 m
Velocity of flow in water channel	0.725 m/s
m^*	0.545
Cylinder material	Polyvinyl Chloride (PVC)
Moving rod and the fixed structure material	Aluminium

Basically the hydrokinetic energy converter consists of a rigid circular cylinder mounted with the help of two vibrating rods and connected to a power take-off system via a transmission mechanism. Whenever there is water flow over a blunt object like cylinder alternate vortices are been shed around the cylinder which creates asymmetry and oscillatory lift to the cylinder and as a result cylinder oscillates perpendicular to its axis and transversely to the water flow direction. Here in this case the body or the cylinder is said to be under resonance i.e. the cylinder's natural frequency equals with the vortex shedding frequency due to fluid flow. The body that undergoes resonance

due to flow induced vibration transmits the mechanical energy produced due to oscillations of the cylinder to a generator for conversion to electricity or directly to a mechanical or hydraulic form of usable energy via a transmission mechanism.

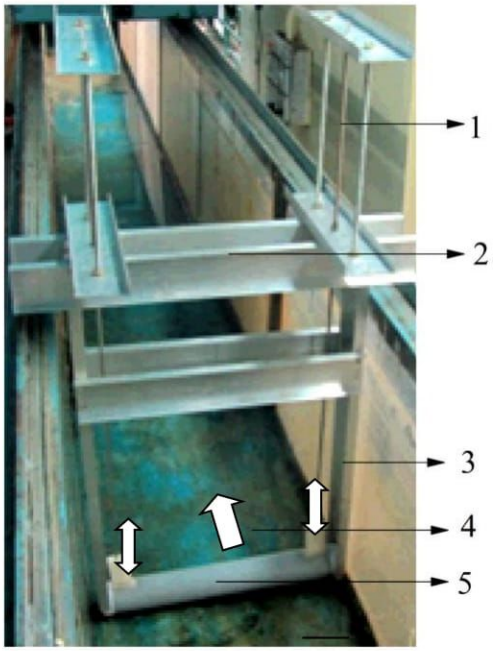

1. Moving rod connected to the moving cylinder
2. Fixed plate attached to the water channel/ flume
3. Linear directional motion of the moving rod and the cylinder
4. Water flow direction
5. Moving cylinder

Fig. 5.2 Lab model of the hydrokinetic energy converter as designed and developed in Fluvial Hydraulics Laboratory of School of Water Resources Engineering, Jadavpur University.

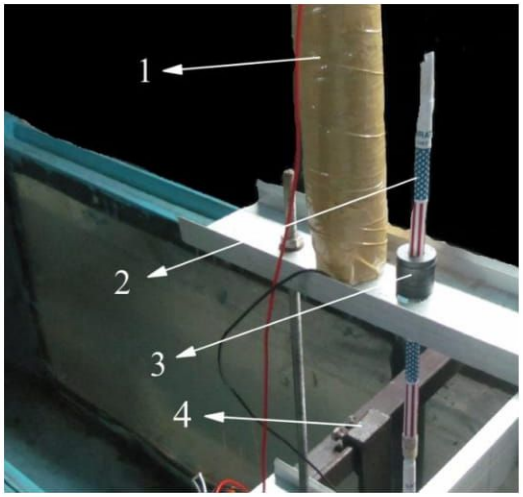

1. Fixed coil assembly
2. Moving rod attached with the moving cylinder
3. Annular ring magnets firmly fixed on moving rod
4. Hydraulic structure attached with the device.

Fig. 5.3 Power generating apparatus with introduction of the hydraulic structures.

The power that can be harnessed using the hydrokinetic energy converter is the power extracted by the generator, which is equal to the power from the vortex induced vibration of the fluid minus the power dissipated by the structural, transmission, and internal generator losses.

When a cylinder is transversely exposed to the water flow then mainly two types of forces come into act i.e. the lift force (F_L) and the drag force (F_D) as discussed in previous part of the research. The combined effect of the lift and drag force gives the resultant force (F_R). The lift, drag and resultant forces were mathematically shown in the works of Sumer and Fredsoe (2006) as:

$$F_D = \frac{1}{2}\rho D V^2 C_D \tag{5.2}$$

$$F_L = \frac{1}{2}\rho D V^2 C_L \tag{5.3}$$

$$F_R = F_L + F_D \tag{5.4}$$

where, C_D is the Drag coefficient and C_L is the Lift coefficient.

From the equations (5.2 to 5.4) the forces have been estimated at various water depth and been shown in Fig. 5.4. The values of C_D and C_L were referred from the researches of Kiya (1968) and Fredsoe *et al.* (1985) respectively for the achieved range of Reynolds Number (3.2×10^4 – 4.5×10^4). From Fig. 5.4, it is seen that the lift force is very low upto the water depth of 3 cm from the bed of the flume and estimated to be 25 N. This force is not sufficient to lift of the cylinder of the designed mass for the vortex induced vibration. Moreover above the water depth of 3 cm all the forces are increased as shown in Fig. 5.4. But at the same time to get amplitude of at least 0.1 m, the water depth is not sufficient. Hence to increase or to aid the lift force, some external forces are required to achieve the desired amplitude. In this juncture hydraulic structures (mainly vertical plates) have been introduced at the downstream of the cylinder.

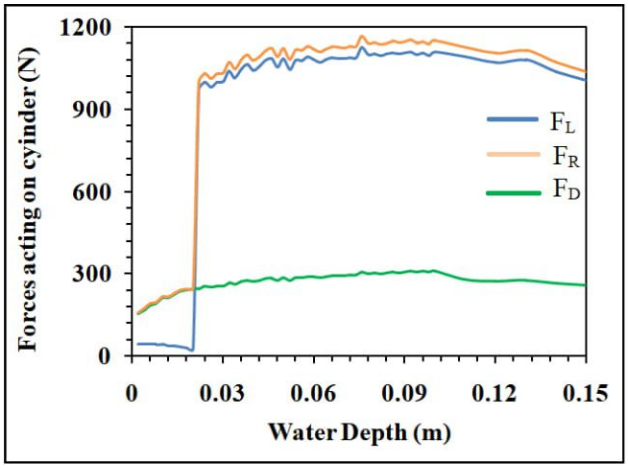

Fig. 5.4 Forces acting on the cylinder at various water depth

Accordingly maximum amplitude (cylinder movement) of 0.1 m is observed after the introduction of the plate. Notably in the same condition, no movement is seen when the plates are not there. The horseshoe vortex as generated from the plate aids or rather enhances the lift force. Tests were done by considering four sizes of flat plates of widths 2, 3, 4 and 5 cm. Various electrical parameters have been checked considering the various sizes of plates and varied flow of water.

A low voltage (minimum 30 mV required) that was generated has been step up with a special low coreless transformer circuit and a voltage is attained. This in turn had a voltage to glow a light emitting diode (LED) of 36 mW and 1.8 V rating in order to visualize the life of the power generating device as shown in Fig. 5.5. The circuit shown in Fig. 5.5 is the part of Linear Technology solution that had prepared a chip LTC 3109 and with the help of two transformers of 1:100 turns ratio each and is capable of stepping up the voltage from 30 mV to about 2.2 V details of which is provided in the report of LTC 3109 (2010). The output from the coil is been transferred to the circuit to get the requisite voltage to prove the existence of power (led will glow) though in a miniscule amount in laboratory level.

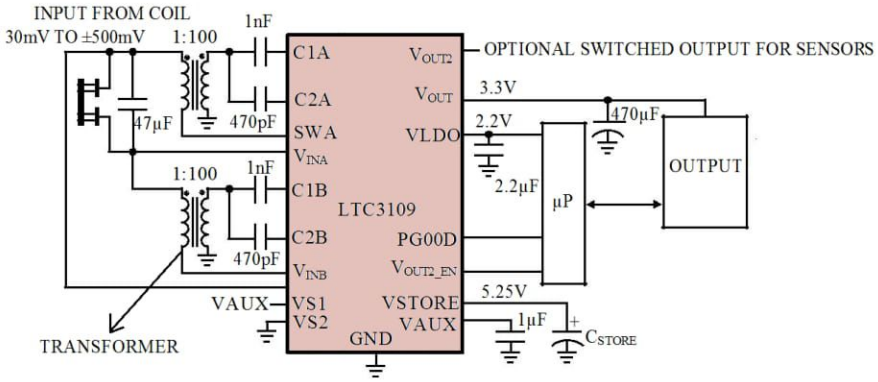

Fig. 5.5 Voltage step up process of the coil output through transformer and chip (LTC 3109) arrangement.

5.5 Outcome and Discussion

In order to visualize the results how the different electrical parameters vary at different course of time and various amplitude variation of the non-linear resonance of the cylinder. Here in order to generalize the conditions all parameters were non-dimensional zed. Here from Fig. 4 (a) and (b) Amplitude parameter $A^* = A/D$; Power parameter $(P^*) = P/P_l$ (P= power generated at every instant and P_l = power required light up the LED) and Voltage parameter $(V^*) = V/V_t$ (V = voltage generated at every instant and V_t = minimum voltage to be given to the transformer circuit in order to glow the bulb). From Fig. 5.6 it has become clear that as the amplitude increases there are also increments of power and voltage generation. Due to the non-linear resonance created due to the structures fitted along with the cylinder the increase of the electrical

parameters are not linear and normally it may happen in linear resonance but overall increase in the parameters is observed here in this case.

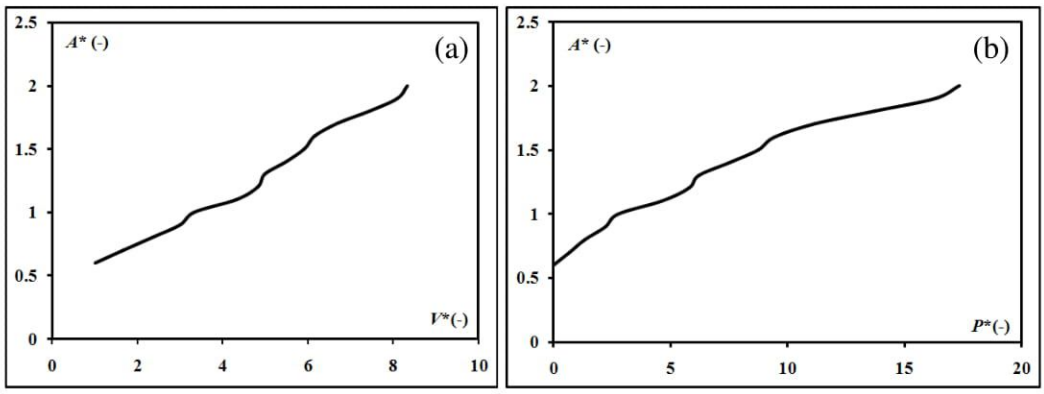

Fig. 5.6 Relation of amplitude with electrical parameters like (a) power and (b) voltage due to non-linear resonance at the time of flow induced vibration over the cylinder.

Due to the non-linear resonance the at some instance the current also shoots up to very high value though in the range of milliamps these fluctuations can be adjusted with the help of the filter circuits as shown in Fig.5.5. It was also noted that the generating apparatus could only generate electromotive force (emf) when the amplitude was found to be 2.5 cm. It was also calculated that overall efficiency of the hydrokinetic generator where input in the fluid energy provided to the cylinder due to vortex induced vibration and the output is the power obtained from each coil is 26.22%. Power in the hydrokinetic energy converter has been estimated as $P = 0.26 \times 0.5 \times \rho \times v^3 \times D \times L$ derived from the research of Raghavan and Bernitsas (2010) where L = length of the cylinder (in cm). Notably the fluid power is directly proportional to the cube of velocity of the water flow. In non-dimensional form, power parameter and varied flow depth parameter were transformed into $P^* = P_{max}/P$ where P_{max} is maximum power produced by a 5 cm vertical plate and P is instantaneous power produced by each plate at varied flow depth and $D^* = h/D$ where h is depth of water and D is diameter of cylinder, respectively. In the view point of comparison with all the plates tested in same flow conditions serially the common factor for power parameter and varied depth parameter were selected likewise.

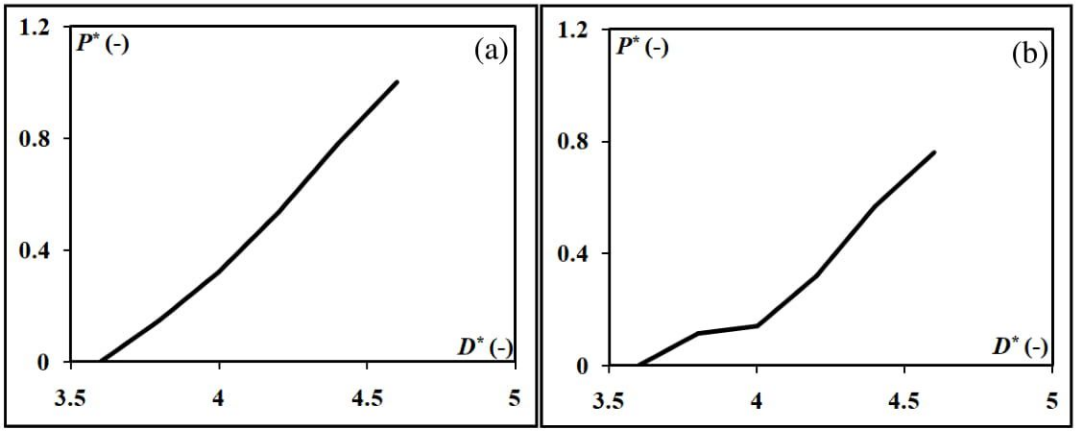

Fig. 5.7 Relation between generated power and varied flow depth for the resonance created by FIV around the cylinder alongwith (a) 5 cm and (b) 4 cm plate obstructions.

From Fig. 5.7, it is well observed that in low depth of water, the power could also be harnessed. The trendline relations for both 5 and 4 cm plates depict that though there is decrement of generation as the depth of water is lowered. But effectively the generating range is seen high in the view of greater prospect.

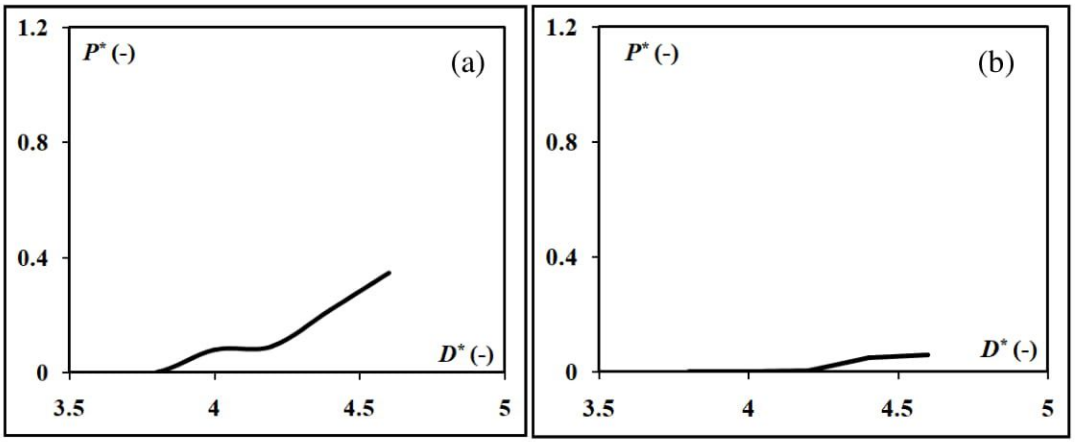

Fig. 5.8 Relation between generated power and varied flow depth for the resonance created by FIV around the cylinder and a obstruction of (a) 3 cm and (b) 2 cm plate.

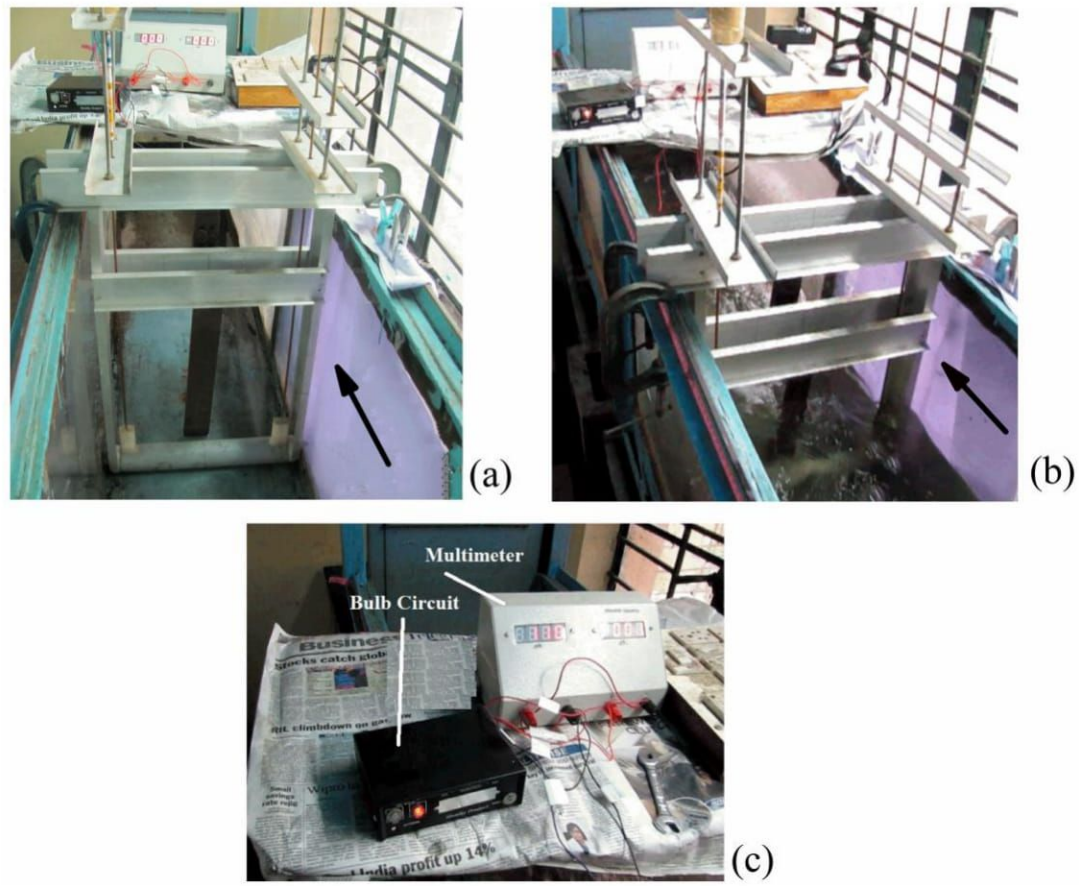

Fig. 5.9 Arrangements for the operation of modified VIVACE : (a) initial setup of the energy generator; (b) device in operation; (c) measurement of the electrical load

Same profile when observed for 3 and 2 cm vertical plates as shown in Fig. 5.8 - power generation occurs with a very low magnitude. The depth range of power generation becomes smaller in respect to the wider plates of 5 cm and 4 cm sizes. No voltage generation was observed when the hydraulic structure was not mounted at the downstream of the cylinder. The results clearly suggest that for shallow depth of water, the selection of the hydraulic structures plays a significant role for energy generation and its increase.

From the previous researches it was well recognized for the water power is directly proportional to velocity cube of the water. The change of efficiency for various depths is found insignificant in respect to changes of power. Finally the success comes when ultimately the power is generated. Fig. 5.9 shows finally how by use of the modified VIVACE a small bulb in the form of electrical load glows.

5.6 Conclusions

Main aspect of this research is to flourish this new environment friendly renewable form of energy device to mankind. The research undertaken would also open the possibilities of building up of cost effective device to serve the above purpose. In India this type of

modified practical device is first time thought of to build. Keeping in view of rural economic and energy status of India this device could be thought as a handy one. Moreover the trend shown in Fig. 5.6 clearly says that the device is capable of generating electricity even in turbulent flow condition by enhancing the flow induced vibration with the help of attached hydraulic structures to the device. There are numerous numbers of ways to harness electricity from the linear reciprocating motion but here it is harnessed by the use of the structures or constricting the water flow channel section. This type of green and clean energy with requiring very less constricting space could be very much competitive with respect to other renewable energy device. Since the research has been conducted in a laboratory flume with its own limitations the power generated is in miniscule amount but which each of the two coils having efficiency of about 26.22 % and it is hoped that in rivers or canals more number of modules could be developed for harnessing electrical energy in very higher range. For example for a cylinder of 1 m length and 15 cm diameter with velocity in tidal river upto 3 m/s, the estimated generated power from electric transmission system is 607 W. In a single module if ample amount of depth in the river is present, number of cylinders can be increased in order to get more power.

So here importance is also to be given to the modification in structure of the hydrokinetic energy converter. Plates of various widths have been utilized in this research which can be visualized in Figs. 5.7-5.8. The power generation capacity is remarkably increased for greater sized plates which is obvious. But notably the changes in the extraction of power in respect to the change of water depth are much minimal for combination of plates of 5 cm with 4 cm and 3 cm with 2 cm. The width of the water course also plays an important role in the selection of the plates. Bigger plates cannot be taken since this may lead to wall effect of the channel and disturb in the flow phenomenon over the cylinder. Smaller plates are also not suggestible since they don't have much surface area to provide the horseshoe vortex which would help in enhancing the VIV. From the above experimental results and the glimpses of which are shown in Figs. 5.7-5.8 plates of 5 and 4 cm would be more feasible in the type of water channel used here in the research. Moreover this device is more useful in the shallow water courses and the results observed in the research suggest that with proper selection of cylinder diameter and hydraulic structure sizes, a sustainable power could be generated. In India, there are many such shallow water courses like canals where this device could be utilized as a platform to get success towards producing green energy.

References

Babu P.R., Thej K.V., Nanda B.N., Singh S.P., Premlatha T., Deepak M.V. and Manisha J. (2013). Non conventional Micro level Electricity Generation. *IEEE GHTC-SAS*, Trivandrum, India. 102-105.

Bernitsas M.M., Raghavan K., Simon Y.B. and Garcia E.M.H. (2006). VIVACE (Vortex induced Vibration Aquatic Clean Energy): A New Concept in Generation of Clean and Renewable Energy from Fluid Flow. *Journal of Offshore Mechanics and Arctic Engineering*, 130(4), 041101-15.

Bernitsas M.M., Simon Y.B., Raghavan K. and Garcia E.M.H. (2009). The VIVACE Converter: Model Tests at Reynolds Number Around 10^5. *Journal of Offshore Mechanics and Arctic Engineering*, 131(1), 1-13.

Fredsoe J., Sumer B.M., Andersen J. and Hansen E.A. (1985). Transverse vibrations of a cylinder very close to a plane wall. Journal *of Offshore Mechanics and Arctic Engineering*, 109(1), 52-60.

Govardhan R. and Williamson C.H.K. (2000). Modes of vortex formation and frequency response of a freely vibrating cylinder. *Journal of Fluid Mechanics,* 420, 85-130.

Khalak A. and Williamson C.H.K. (1999). Motions, forces and mode transitions in vortex induced vibrations at low mass damping. *Journal of Fluids and Structures*, 13, 813-851.

Kiya M. (1968). Study on the turbulent shear flow past a circular cylinder. *Bulletin Faculty of Engineering*, Hokkaido University, 50, 1-100.

LTC 3109 (2010). Auto-Polarity, Ultra Low Voltage Step-Up Converter and Power Manager. *Linear Technology Corporation*, CA, USA.

Raghavan K. and Bernitsas M.M. (2010). Experimental Investigation of Reynolds Number Effect on Vortex Induced Vibration of Rigid Cylinder on Elastic Supports. *Journal of Ocean Engineering*, 38(5-6),719-731.

Raghavan K., Bernitsas M.M. and Maroulis D. (2009). Effect of Bottom Boundary on VIV for Energy Harnessing at $8\times10^3 <Re< 1.5\times10^5$. *Journal of Offshore Mechanics and Arctic Engineering*, 131(3), 031102-13.

Sumer M. and Fredsoe J. (2006). Hydrodynamics around cylindrical structures. *Advanced Series on Ocean Engineering,* 26, 36-75.

6.1 Synthesis of the present research

The research undertaken in the thesis consist the detailed analysis of both the hydraulics and electrical engineering aspects. Ever since Leonardo da Vinci first observed vortex induced vibration (VIV), circa 1500A.D. in the form of "Aeolian Tones" engineers have been trying to spoil vortex shedding and suppress VIV to prevent damage to equipment and structures. Furthermore, von Karman at California Institute of Technology proved that the Tacoma Narrows bridge collapse in 1940 was due to VIV. This fluid-structure interaction phenomenon occurs due to the nonlinear resonance of cylinders (or spheres) through vortex shedding lock-in. The VIV is also called synchronization between vortex shedding and cylinder (or sphere) oscillations. It was also tested that this converter is capable of harnessing useful amount of electricity in the river flow of about 0.25 m/s. **Related study of the device as made by Bernitsas *et al.* (2006) had been tested in American Scenario at a very high velocity and water depth above one meter**. Moreover the **structural details** of the above device is not **yet published** widely so by **designing with a new structural dimensions** the device's performance could be tested in Indian Scenario, then by analyzing its feasibility some new mechanism or thought can be introduced to harness more power from that device efficiently. India is in requirement of huge amount of energy for its development. In this juncture the VIVACE **was modified** at **Fluvial Hydraulics Laboratory of School of Water Resources Engineering, Jadavpur University**. In India, there are many such shallow water courses like canals where this device could be utilized as a platform to get success towards producing green energy. In view to the Design, Analysis and Development of an Electromechanical Hydropower Harnessing Model by Vortex Induced Vibration, the entire study in the thesis was divided into **three broad phases** in form of chapter. The classification of the study is justified by the fact that since the modified VIVACE consists of a hydraulic structure attached to it. So, at first the analysis of the **hydraulic structure** became important. Then the complex flow field analysis or the hydraulic engineering study had to be carried out combining both cylinder and the hydraulic structure **in the form of vertical plate**. Lastly the electrical design aspects were built and modeled which a premier resemblance with the chapters had been related to the hydraulic engineering.

In first phase the related chapter dealt with features of horseshoe vortex due to flat vertical plate, which is also a supportive hydraulic structure in the way of enhancing the vortex induced vibration. Four plates of widths 2, 3, 4 and 5 cm were considered for analysis. The same plates were used in the proceeding chapters in order to discuss about the complex field that aroused due to the introduction of horizontally laid cylinder. In the design of modified VIVACE, the selection of proper width of plate according to the availability of the working space became much important. The major outcomes of the chapter relating to the analysis of the associated hydraulic structure sums up as:

1. From the velocity vectors for different plate widths there a downflow of water been observed near to the plates which can be said as starting of the horseshoe vortex.

2. Longitudinal flow velocity as it approaches towards the plate decreases with the increase in the plate width. This happens due to the flow approaching towards the stagnation point at the obstruction plate. The magnitudes of the transverse and vertical flow velocity increases for each plate due to the effect of the horseshoe vortex and the flow striking obstruction plate.
3. Viewing the results from the contours of the turbulent intensities and shear stress it is clear except the plate width b = 2 cm the effect of horseshoe vortex generated from the plates are dominant.
4. The results of vorticity and turbulent kinetic energy depict that the core of the concentration of vorticity or turbulent kinetic energy mainly lies near the plate and the flume bed. The magnitude for both the aspects are highest for plate width b = 5 cm. From the summary of the points coming out of the study depicts that plate width b = 2 cm or less value in the present flow condition may not have sufficient vortex strength to lift the cylinder. So for selection of plates for the modification of the VIVACE the outcomes of this chapter will be very helpful.

Moving on to the second phase, the related chapter dealt with the flow fields between a vertical plate of different widths and a horizontal cylinder. The cylinder was placed at position away from the flume bed, e = 1, 2, 4, 6 and 8 cm away from the flume bed. Several experiments were carried out by considering a vertical plate and the cylinder positions at e = 1, 2, 4, 6 and 8 cm, respectively. Most importantly the cylinder was **placed 5.5 cm upstream of the vertical plate.** It is to be noted that the horizontal gap between the cylinder and the vertical plate **was selected 5.5 cm** because at this horizontal gap, the moving cylinder of the hydrokinetic generator gained **maximum amplitude of 10 cm and voltage of 1.05 Volt**. The results from the flow fields well explained in this chapter satisfies that at the gap of 5.5 cm the cylinder experiences the maximum power of horseshoe vortex from the vertical plate. With the collection of all the data, the chapter is summarized as:

1. The velocity vectors for different plates at different cylinder position it can be seen that there is a downflow of water near the plates which can be said as starting of horseshoe vortex.
2. A separation of the fluid is also observed near the upstream of the cylinder. The mixing of mushroom shaped vortices and wake vortex of the cylinder and the downflow due to the vertical plate, for which the magnitudes become nearly zero the directions are also reversed in the gap between cylinder and plate.
3. The changes in longitudinal flow velocities are observed in between the plate and cylinder states the dominance of the cylinder. When the width of the plate is more than the other widths considered, maximum amount of the longitudinal flow strikes the surface of the plate and the flow is exhausted and the approaching flow velocities are reduced. It was found for e = 1 cm that the longitudinal flow velocities near the flume bed and the vertical plates considered were found to 92, 75, 62 and 46 cm/s respectively for the plate widths b = 2, 3, 4 and 5 cm respectively. When e = 2 cm as shown in Fig.

4.5(b) the longitudinal velocities for different widths as considered revealed to 1.02, 1.25, 1.45 and 1.57 times of the velocities as observed when the cylinder was at e = 1 cm. At e = 4 cm the longitudinal velocities have started to reduce for the considered plate width at the upper side of the cylinder. The reason is justified by the fact; the supplementary effect of the horseshoe vortex developed by the plate reduces as the cylinder moves up. The longitudinal velocities in the lower part of the cylinder increases due to the fact the approaching flow gets more opening underneath the cylinder. Finally at e = 8 cm the longitudinal flow velocities were found to be near the depth averaged velocity at the upper surface of the cylinder which suggest that the effect of the horseshoe vortex had totally been diminished in that region. The same range of longitudinal velocities as found in the upper surface of the cylinder was observed underneath the cylinder for all the plate widths considered.

4. While dealing with the transverse flow velocity and vertical flow velocity, the knowledge of the turbulent mixing of the mushroom shaped vortices and alternate wake vortices from cylinder with downflow and the horseshoe vortex due to the vertical plate was gained.
5. The positive magnitude of vertical flow velocity found near the flume bed at the downward rear side of the cylinder is very less in compared to the negative vertical flow velocity. The reason can be justified by the fact that much of the energy of wake vortex from the downside of the cylinder is exhausted by the downflow of water due to the vertical plate and the wake vortex occurring due to the upper portion of the cylinder. The vertical velocity in between the gap of the cylinder and the plate was found to be -13, -30, -37 and -48 cm/s for plate widths b = 2, 4, 6 and 8 cm for e = 1 cm. Where the vertical velocity were found to be -44, -44, -45 and -48 cm/s in the gap between cylinder and the plate for b = 2, 3, 4 and 5 cm respectively for e = 2 cm. As the e is increased from the vertical velocity in between the gaps also increase overall by 1.2 and 1.15 times the vertical velocity as found for e = 2 cm for each of the plates considered. At the upstream surface of the cylinder at all the considered e, the vertical velocity is near 35 cm/s. At particular the increase in the magnitude of the vertical velocity at the upward direction is observed for increased width of the plates.
6. The magnitude of the turbulent intensities in between the vertical plate and cylinder are at least 10 times more than the rest of regions. The reason is justified by the fact that there is a mixing of the horseshoe vortex generated from the vertical plate with mushroom-shaped vortices and wake vortices generated by the cylinder. For b = 2, 3, 4 and 5 cm, u^+ was found maximum of around the range of 85 cm/s at e = 1 cm. For e = 2 cm maximum u^+ values were found to be 43, 55, 57 and 60 cm/s for the plate widths b = 2, 3, 4 and 5 cm respectively. Same trend of increase in maximum u^+ is observed at e = 4 cm as 69, 73, 77 and 88 cm/s for b = 2, 3, 4 and 5 cm, respectively. But when e = 6 cm, the maximum values of u^+ were found to be decreasing as 41, 43, 69 and 70 cm/s for considered plates b = 2, 3, 4, 6 and 8 cm, respectively. At e = 8 cm

again the increase in fluctuations in u is been observed but the position of the maximum fluctuations are changed and the maximum fluctuations were found to be 50, 52, 70 and 72 cm/s. From the above results it can be said that as the e is increased the fluctuations of u^+ mainly lies in the downside of the cylinder at the downstream of the cylinder. The justification for the fluctuations in u is due to the mixing of the horseshoe vortex arousing from the plate and the wake vortex in supplement to the mushroom shaped vortices of the cylinder.

7. The turbulence intensity profiles reveals that the concentration of turbulence intensities are mainly found near the boundary layer region of the cylinder, as the cylinder moves away and towards the flume bed. While discussing w^+ it can be said that when e = 1 to 6 cm due to the horseshoe vortex effect maximum vertical fluctuations are observed near the down side of the cylinder but as it goes further up to e = 8 cm the horseshoe vortex effect is diminished then the downflow due vertical plate and tendency of the flow directed downward at the rear side of the cylinder due to adverse pressure gradient comes into existence. Hence maximum fluctuations of w at e = 8 cm is found to be at the upper side of the cylinder. In support to the phenomenon the maximum w^+ were found out as: for b = 2, 3, 4 and 5 cm, w^+ values are 24, 32, 34 and 40 cm/s at e = 1 cm. At e = 2 cm the maximum intensity of w were found to be 29, 33, 39 and 44 cm/s for b = 2, 3, 4 and 5 cm respectively. For e = 4 cm all the intensities were increased by around 1.05 times the values as found for e = 2 cm. For e = 6 cm, the maximum values of turbulent intensity w^+ decreases to 23, 30, 37 and 40 cm/s respectively for plate widths b = 2, 3, 4 and 5 cm respectively. Again when e is increased to 8 cm the maximum w^+ at the upper side of the cylinder was found to 29, 34, 39 and 44 cm/s respectively for b = 2, 3, 4 and 5 cm respectively.
8. The magnitude of the turbulent stresses has been visualized as inversely proportional to e due to the reduction of the horseshoe vortex as generated by the plates. From Fig. 4.12 (a) the shear stresses in x-y plane where found for b = 2, 3, 4 and 5 cm for e = 1 cm. It was observed that in the gap between the cylinder and the plate the values of shear stresses to maximum of 25, 25, 43 and 50 cm^2/s^2 for b = 2, 3, 4 cm and 5 cm respectively. The rest of the region above and below the cylinder the values are -250, -200, -150 and -135 cm^2/s^2 for plate widths b = 2, 3, 4 and 5 cm respectively. As the e is increased to 2 - 6 cm the shear stresses also increase by atleast 1.3 times at e = 1 cm. This suggests that as the e is increased the development of the horseshoe vortex along with the development of the wake and mushroom shaped vortex also gain its fulfillment. When e = 8 cm then the horseshoe vortex effect arousing from the plate on the cylinder is diminished then the stresses depicts the dominance of the cylinder at the water level in range of 20 to 8 cm.
9. The magnitude of the shear stresses in between the vertical plate and the cylinder is the addition of wake vortex developed by the cylinder and the downflow of water due to the vertical plates. For e = 1 cm the maximum turbulent shear stress τ_{vw} was found -145 and 135 cm^2/s^2; -200 and 300 cm^2/s^2; -325 and 345 cm^2/s^2; -388 and 415 cm^2/s^2 for b = 2, 3, 4 and 5 cm respectively.

Interestingly from for e = 2, 4, 6 and 8 cm the maximum stresses where found for b = 2 cm as 265 and -120 cm^2/s^2; 145 and -105 cm^2/s^2; 125 and -135 cm^2/s^2; 125 and -200 cm^2/s^2 respectively. Considering for b = 3 cm, the maximum stresses were found to be 325 and -165 cm^2/s^2; 185 and -140 cm^2/s^2; 145 and -185 cm^2/s^2; 125 and -275 cm^2/s^2 for e = 2, 4, 6 and 8 cm respectively. For b = 4 cm the maximum stresses were found to be 375 and -275 cm^2/s^2; 225 and -230 cm^2/s^2; 185 and -310 cm^2/s^2; 115 and -450 cm^2/s^2 for e = 2, 4, 6 and 8 cm respectively. Viewing the results for b = 5 cm the maximum stresses were found as 465 and -330 cm^2/s^2; 325 and -275 cm^2/s^2; 150 and -360 cm^2/s^2; 66 and - 550 cm^2/s^2. The stresses are found to be negative in the region of upper side of the cylinder which is due to the downflow of the water. The downflow of water depends upon the wake vortex formed at the rear side due to the flow separation occurred at the upper side of the cylinder. The positive value thus depends upon the plate width as it is increased it should increase but at the same time it is countered by the vertical flow upward due to the horseshoe vortex of the plate and the wake vortex at the rear side of the cylinder due to the flow separation occurred at the lower side of the cylinder.

10. The magnitude of the shear stress at the bottom of the cylinder and the boundary layer region of the upstream of the cylinder happens due to the dominance of the horseshoe vortex as developed from the plates. For b = 2, 3, 4 and 5 cm at e = 1 positive values of τ_{wu} was found as 125, 180, 215 and 250 cm^2/s^2, respectively. The negative value of turbulent shear stresses in that region was found to be -750, -600, -450 and -375 for plate widths b = 2, 3, 4 and 5 cm respectively. The positive and negative values of τ_{wu} increases about 1.1, 1.8 and 2.1 times the stress values in each plates at e = 1 cm. At the e = 8 cm the stress values, both positive and negative each decreases to 0.8 times the shear stress as observed at e = 1 cm. The reason for justification of the values remains the same as τ_{vu} only difference lies in the magnitude as τ_{wu} is basically the product of the fluctuations of u and w. For the experiments in x-z plane the magnitudes of u and w are mainly found to be dominant.
11. The core of vorticity for all the plate width considered mainly lies at two places. Firstly in between the plate and the cylinder, secondly near the bottom and upstream part of the boundary layer of the cylinder.
12. From the magnitude of the vortex strength it is clear that a **minimum gap e = 2 cm** is required for the present scenario. **The minimum e would facilitate the formations of the horseshoe vortex to strike at the bottom of the cylinder.**
13. Finally when the cylinder reaches e = 8 cm, by the virtue of its weight and alternate vortex shedding the cylinder would come down to e = 1 cm.
14. After viewing the flow characteristics at the gap in between the cylinder and plates, the weight and diameter selection also becomes important. The material of the cylinder should be such that it should float in the water upto e = 2 cm.

The summary of the points from this chapter suggest that not only the **selection of the plate** widths becomes important for design purpose of the modified VIVACE. **Selection of the weight, diameter and material of the cylinder also become much more important.**

Finally from the third phase, the related chapter dealt with the design of the modified VIVACE. Here the design parameters as chosen a discussed in details and justified. The chapter could be summarized as follows:

1. The mass of the cylinder and its supporting appendages like moving rod and magnets were considered as $m^* < m^*_{crit}$,where $m^*_{crit} = 0.54.$
2. The material of the cylinder was selected to be polyvinyl chloride so that the cylinder can **initially float upto *e* = 2 cm.**
3. The **transversal movement of the** cylinder **was very low**, if the gap between the cylinder and the plate is above or less than 5.5 cm. This is justified by the fact that if the gap is more the strength of the horseshoe vortex generated from the vertical plates are exhausted before it reaches the bottom of the cylinder. **The formations of horseshoe vortex developed by the vertical plates are incomplete if the gap between the cylinder and the vertical plates is less than 5.5 cm in the present experimental conditions.**
4. The research has been conducted in a laboratory flume with its own limitations the power generated is in miniscule amount but which each of the two coils having efficiency of **about 26.22%** and it is expected that in rivers or canals more number of modules could be developed for harnessing electrical energy in very higher range.
5. Among the different plate widths considered during all the experiments, in respect to the generation of voltage and power the considered plates of ***b* = 4 cm and 5 cm** have been found more effective than other considered plates in this research. Maximum power and voltage obtained at an instant for considered plate widths ***b* = 2, 3, 4 and 5 cm as : 1.05 V and 1.25 W; 0.952 V and 0.952 W; 0.58 V and 0.435 W; 0.296 V and 0.074 W, respectively.**

Summarizing all the points as a whole it can be said that this device is more useful and efficient in the shallow water courses. The results observed in this research suggest that with proper selection of cylinder diameter and hydraulic structure that is among the width of vertical plates *b* = 2, 3, 4 and 5 cm a sustainable power could be generated. In India, there are many such shallow water courses like canals where this device could be utilized as a platform to get success towards producing green energy.

6.2 Future scope of similar research

After carrying out the total study on the design, analysis and development of an electro-mechanical hydropower harnessing model, few areas of the research could have been further developed:

1. Use of Particle Image Velocimeter (PIV) or Ultrasonic Doppler Velocimeter (UDV) for the flow visualizations would have been more perfect and much less time consuming. The flow fields right at the bottom of the cylinder could only be accessed by the viewing the upstream and downstream flow fields as measured by ADV. The PIV or UDV could easily visualize the flow what is happening just at the bottom of the cylinder due to the effect of horseshoe vortex generated by the vertical plates. For carrying out the experiments in immense turbulent zone instant visualization of the flow phenomenon is very much more important than viewing it in time averaged format. PIV can be the best option to get the accurate knowledge of the flow fields in between the cylinder and the vertical plate at a high velocity of 0.725 m/s.
2. The pressure measurements could also be done around the boundary layer to understand the adverse pressure gradient that can happen due to the introduction of the vertical plates.
3. Kolmogorov's hypothesis can be applied in order to minimize the spike of ADV data.
4. Numerical simulations could be carried out in order to get the flow characteristics in between the cylinder and plate. This will aid to quicker design of the modified VIVACE.
5. The use of neodymium magnets in place of the normal magnets as used here could increase the voltage upto 10 times.
6. To get the feasibility of the hydrokinetic device, the modified VIVACE should be tested in the natural water channels.

BIPRODIP MUKHERJEE
S/O Sh. Bibhas Kumar Mukherjee,
24, East Ghosh Para Road, Shyamnagar,
(N. 24 PGS). Pin - 743127.
Phone: 09474378690
e-mail: biprodip87@gmail.com

Objective

To seek a gainful position in an organization where my abilities will be utilized to the fullest, where my desire and drive to succeed will be an asset. I am seeking a position where I will be given an opportunity to work effectively and efficiently by enhancing organizations profitability.

Qualification

Ph.D. (Engineering)	**Pursuing (Registered: 15.01.2015)**
M.E. (Water Resources Engineering)	Jadavpur University with **85.94%**
B-Tech (Electrical Engineering)	West Bengal University of Technology with **75.1** %
Standard XII	I.S.C. board with **65.2 %** aggregate.
Standard X	I.C.S.E. board with **71.66 %** aggregate.

Industrial Experience

- Worked as GET (Electrical & Mechanical Maintenance Dept.) at Keventer Agro Limited, Barasat, India from 01.09.2009 to 04.03.2010.
- Helped as team member in various consultancy works in the subjects of Pipeline stress analysis, Transient analysis and related Hydraulic analysis on behalf of School of Water Resources Engineering, Jadavpur University from 2012 to present.

Research Experience

- Worked as Research Scholar in School of Water Resources Engineering, Jadavpur University, India in the projects of:
  (a) Effect of climate change on water resources of Damodar and Subarnarekha River Basin in Eastern India, Ministry of Water Resources, Govt. of India from 02/07/2012 to 18/09/2012.
  (b) Analysis of Sediment Transport mechanism in connection to reservoir life and dam safety, University of Potential and Excellence (UPE) Phase - II scheme, UGC, Govt. of India from 19/09/2012 to present.

Teaching Experience

- Worked as Guest Faculty of Power Engineering Department, Jadavpur University from 2013 to present.
- Delivered invited lectures at JIS Engineering College, Kalyani, India in the interest area of plumbing systems.

Software Knowledge

Designing Softwares – Bentley HAMMER, EPANET, CAESAR, LOOP, Water GEMS, Civil Storm, Sewer GEMS, AUTOCAD.

M.E. Thesis completed

Pipeline design and analysis of distribution network of Dhapa Water Treatment Plant, KMC by EPANET and HAMMER Software.

Ph.D Thesis Topic: (Under School of Water Resources Engineering, Jadavpur University)

A Study on the Design, Analysis and Development of an Electro-mechanical Hydropower Harnessing Model by Vortex Induced Vibration.

Strengths

- Good communication skills
- Comprehensive problem solving abilities.
- Adaptable
- Analytical

Personal Profile

Date of Birth: 21.09.1987
Sex: Male
Marital status: Married
Languages Known: English, Bengali and Hindi
Member of IEI: **AM138737-8**
Electrical Supervisor's Certificate of competency Registered No.: **29002**

Publication (in total)

Journal :	National: 4	International : 4
Conferences :	National : 3	International: 4

Declaration
I hereby declare that all the information provided by me is true & genuine as per the best of my knowledge and belief.

(BIPRODIP MUKHERJEE)

Complex Flow Phenomena of Horizontally Placed Underwater Cylinder above Water Bed

BIPRODIP MUKHERJEE *Research Scholar*
SUBHASISH DAS *Assistant Professor*
ASIS MAZUMDAR *Director & Professor*
School of Water Resources Engineering, Jadavpur University, India

ABSTRACT

This research is a presentation of complex flow phenomena in between the flow past a horizontally placed cylinder 8 cm above water channel bed and vertically placed plate placed at its downstream. Original experimental setup consists of a cylinder of 5 cm diameter placed about 5.5 cm horizontally away from a vertical plate having 5 cm width, where both causing hindrance to flow. Strict maintenance of 52 lps water flow and 20 cm flow depth for water recirculation in flume were followed. In such water flow, turbulence condition is obvious and the vortex formation is also in expectation as depicted in earlier researches. Acoustic Doppler Velocimeter (ADV) helped to determine the velocity and its direction while vortices were being created around the cylinder and in its wake, and also to record the velocity and observe its characteristics in the boundary layer.

With the determination of flow fields of the underwater composite hydrodynamic structures various other environmental issues come into play. These types of under-laying structures not only helps in dispersion of sediment decomposition in the river bed but also in this juncture help to get a free passage and movement area for aquatic fauna for a shallow type of water channel. Seeing so many advantages of this type of study could really boost to maintain aquatic ecological balance in addition to the territorial environment and socio-economic development. Vector plots of the flow fields at vertical plane reveal the complex characteristics of the horseshoe vortex flow and alternate vortex shedding by the cylinder. The circulation of the horseshoe vortex as created by the plate is determined by using Stokes theorem and forward difference technique.

Keywords *: flow fields, hydrokinectic energy generator, vortex induced vibration, submerged cylinder.*

1. INTRODUCTION

Investigation of flow fields around the underwater laid pipes are attaining curiosity in juncture to rapid increase in submerged pipes or cables. Such cylindrical cross-sectional structures faces wave-current climate of complex nature. Natural water channels containing erodible silts where there is high chance of scouring underneath such cylindrical structures due to the development of horseshoe vortex[1] along with transport of sediments due to equilibrium scour were depicted in the researches earlier[2,3] against the detrimental effects as seen in reservoir and river flow paths detailed in the researches of[4,5]. The aspects also become much important when the question arouse while assessing hydrological feasibility of an environment friendly mini hydro power plant which is known in the work of[6]. The phenomena of scour had proved to leave a cylindrical structure uncorroborated over a substantial distance resulting in fatigue failure due to flow-induced oscillation by wake-vortex shedding such types of works had been proven numerically[7,8] and experimentally[9-12] occurring at the base of the vertically mounted piers that are also related with the movements of sediments of the river beds from one locations to other locations in the exposure of the works of[13-16]. Additionally problem of vortex-induced vibration of structures is important in various fields of engineering, as it is also a cause for concern in the dynamics of riser tubes bringing oil from the seabed to the surface, in flow around heat exchanger tubes, in the dynamics of civil engineering structures such as bridges and chimneys, and also in many other situations of practical importance.

Therefore, one of the imperative aspects of pipeline design is the prediction of the extent of scour below pipelines. Thus the evaluation of forces on cylinders some distance away from the bottom becomes of interest. Recently, Acoustic Doppler Velocimeter (ADV) has become popular in the field of fluid dynamics. They are applied to study the three-dimensional flow field and turbulence in laboratory applications, as well as in rivers, lakes and the ocean. ADVs typically consist of one emitter surrounded by a number of receivers, each of them measuring one projection of the velocity vector as used in the studies of[1,17-18].

W & E INTERNATIONAL (WATER RESOURCES SECTION)

2016 2nd International Conference on Control, Instrumentation, Energy & Communication (CIEC)

Electrical Energy Generation by Enhancing Flow Induced Vibration

Biprodip Mukherjee, Subhasish Das and Asis Mazumdar
School of Water Resources Engineering
Jadavpur University
Kolkata, India
biprodip87@gmail.com, subhasishju@gmail.com, asismazumdar@yahoo.com

***Abstract*— A country's growth mainly depends upon the capacity of the electrical energy that it can afford to run the wheels of technology. Natural energy in the whole world is found in a discrete manner as a result it becomes typical to harness electricity from every energy points. Today most challenging problem that a developing nation face is low-cost sustainable energy generation and this can be solved by finding out ways to harness electricity amongst the scattered energy points. Development is also required for every technology that can generate energy at a competitive cost. In this juncture a device has been modified which basically runs on the concept of enhancing flow induced vibration over a cylindrical structure that might harness electricity from very shallow streams. Research has been carried to visualize in shallow depth of water flow how much power it is capable of harnessing and part of it is also reflected here. Power generating setup has been successful to grab the water energy at its maximum though in laboratory it may be miniscule but in real life condition it can be a very handy weapon to supply few lighting loads at remote places.**

Keywords*— *harness electricity; low-cost sustainable energy; flow induced vibration; shallow depth;development

I. INTRODUCTION

Today, India is the ninth largest economy in the world, driven by a real Gross Domestic Product (GDP) growth of 8.7% in the last 5 years (7.5% over the last 10 years). Present scenario suggests that country is very dependent on the fossil fuel that is coal and petroleum. These are conventional sources of energy and they also have a limitation. Keeping in view the limitations of the present conditions of the fossil fuels there are various other forms of renewable energy being started to be practiced in India such as Solar energy, Hydro Power (including Tidal ones), Bio-diesel, Wind energy, Bio-gas , etc. A continuous effort in developments in technology is under process to harness the non-conventional energy [1].

Leonardo da Vinci first observed vortex induced vibration (VIV) can also been often termed as flow induced vibration, circa 1500 A.D. in the form of "Aeolian Tones". Engineers have been constantly trying to spoil vortex shedding and suppress VIV to prevent the damage caused due to the Aeolian Tones to the very high head equipments and structures. Furthermore, it was von Karman at California Institute of Technology who proved that the Tacoma Narrows bridge collapse in 1940 was due to VIV. This fluid-structure interaction phenomenon occurs due to the nonlinear resonance of cylinders (or spheres) through vortex shedding lock-in. The VIV is also called synchronization between vortex shedding and cylinder (or sphere) oscillations. It was also tested that this converter is capable of harnessing useful amount of electricity in the river flow of about 0.25 m/s. The device explained in the research aims to harness the abundant clean and renewable energy from ocean and other water resources and have high energy density, with being robust and modest with low recurring expenditure and have a 10–20 years life [2]. With the test velocity 0.84 m/s, VIV tests were carried out in the Low Turbulence Free Surface Water (LTFSW) channel of the University of Michigan, for Reynolds number in the range of 8×10^3–1.5×10^5, have shown undoubtably a strong dependence of VIV of cylinders on proximity to a bottom boundary [3,4]. The range of synchronization of the upper branch increases with increase in Reynolds number. Amplitude ratio (A/D where A is amplitude and D is cylinder diameter) increases with Reynolds number within the upper branch. For high-Reynolds number, the magnitude of A/D is achieved as 1.9 routinely in-spite of high damping. The lower branch disappears, overtaken by extended upper branch. High Reynolds number VIV enters into the two paired vortices per shed 2P domain in the Williamson–Roshko (W–R) map beginning with the initial branch. Hysteresis was not observed in these experiments possibly because parameters remain in the 2P-domain. High Reynolds numbers have a stronger influence than mass ratio on A/D. High-damping high-Reynolds VIV amplitudes are double of those predicted by the modified Griffin plot by extrapolation [5].

System identification (SI), in air, reveals nonlinear viscous damping, static and dynamic friction. Hysteresis is a phenomenon which occurs in the zero velocity limits, has been modeled by a nonlinear dynamic damping model Linear Auto Regression with Nonlinear Static model (LARNOS). A bluff body, usually a cylinder, when introduced in a free stream features of boundary layer separation could be observed which results in unequal pressure distribution around the bluff body eventually leading to formation of vortices. The vortex shedding pattern is not symmetrical because of which there is a net force which results in the up and down motion of the bluff body. To convert this up and down motion of the cylinder to useful electrical energy is the role of the power take-off mechanism which is a linear generator in this case. By enhancing the nonlinear resonance of a new concept of vortex

978-1-5090-0035-7/16/$31.00©2016IEEE

Proceedings of the 2016 IEEE Students' Technology Symposium

Sustainable Electrical Energy Generation Technique in Shallow Water Channels

Biprodip Mukherjee, Subhasish Das and Asis Mazumdar
School of Water Resources Engineering
Jadavpur University
Kolkata, India
biprodip87@gmail.com, subhasishju@gmail.com, asismazumdar@yahoo.com

Abstract— **Without electrical energy, technology is nothing other than a playing toy. So, efforts always need to harness electricity from almost every plausible energy points which are discrete or continuous in nature. In true sense, a developing country's most challenging problem is low-cost sustainable energy generation. Efforts are being made to develop technologies which would lead to sustainable energy generation. The present research deals with a new environment friendly hydrokinetic device producing energy using a technique of vibration induced by vortex (VIV) which may be sometimes called as technique of vibration induced by flow (FIV) via a linear generator shall be of useful impact. In this research a modified device was tested in various types of flow depths basically approaching towards shallow water depth in water-channels and observed the voltage and power correlations for various modified structures used in an effort to enhance the VIV. This type sustainable generation techniques would be very much useful to various parts of rural areas where there is limited amount of available electricity.**

Keywords—sustainable energy generation; VIV; shallow water depth; hydraulic structures; harness electricity

I. INTRODUCTION

Sustainable energy forms have become an important factor now-a-days, as when seen in environmental aspect. So efforts are being made to harness sustainable energy particularly in developing countries. The present research deals with the development of a hydrokinetic energy device which can harness sustainable energy in shallow water channels or courses. Commonly, sustainable energy is also a defined energy system that is used to serve the present needs without hampering future generations keeping in view to their own demand. Four unified domains such as ecology, economics, politics and culture plays a role as organizing principle for sustainable energy development. Technologies relating to non-conventional energy sources like hydel power, tidal power generation, wind energy, bio-energy, geo-thermal energy and solar energy are basics resources which are collectively termed as sustainable energy sources.

As the days past by the world economy, the cost of producing such technologies leading to renewable sustainable energy are falling day by day. This supports the investors' confidence in these technologies and hence the markets are also expanding with effective government policies. A lucrative 100% confident encouragement of renewable energy is pointed out in studies where a considerable progress all over the world is being followed in the process of transition of energy from fossil fuels to not wastefully sustainable systems. A few developmental works had been carried in the step to find the sustainable energy resources [1].

Hydropower is termed as one of the best sustainable clean energy in relation to the renewable energy resources. Since many years, the study of the harnessing electricity from the hydropower is actually concentrated to the usage of various types of fan like structures i.e. turbines. But this turbines operated hydropower systems has its own limitations such as inflow velocity of water in the hilly areas would only be the most suitable where the slope is very high and accordingly the gravitational flow of water is also very high, reclamation of huge amount of land which is very difficult in today's arena - keeping in view to imbalances to ecology and also disturbances to aquatic environment. So, in the process of harnessing energy from water, many other developments took place. Various types of marine energy harnessing devices had come like floating buoys, Pelamis wave energy converter etc. These devices are fit to harness power from immense amount of energy that the oceans or sea have. In relation to the study regarding low discharge and low head (slope of head not the depth of water) a hydel power generating system of reciprocating nature was produced from the concept of Magnus effect which is claimed to generate electrical power from low head water courses and squat discharge [2]. Likewise another concept of harnessing power came where a lock-in phenomenon of the vortices are utilized to give a linear reciprocal motion. In 1500 A.D. Leonardo da Vinci first thought about the VIV. In 1940 Tacoma Narrows Bridge was collapsed due to FIV, the report of which came out in the research of von Karman. Splitting the vortex shedding had been a general practice in order save the high rise structures where the damage could be easily done by the FIV of the normal wind. A water-cylinder interconnection phenomenon due to FIV give rise to nonlinear resonance in cylinders or FIV will help to a reciprocating motion of a moving cylinder and this motion would be converted to electrical energy. From previous researches, it was observed that such type of electrical power harnessing structures can generate electricity from a river water velocity around 0.25 m/s which is of very lower range. Such type of devices aimed to harness the non-conventional energy from various types of water resources

978-1-5090-5163-2/16/$31.00 ©2016 IEEE

BIPRODIP MUKHERJEE
Research Scholar
School of Water Resources Engineering
Jadavpur University
Kolkata – 700 032, West Bengal, India